March 12, 2015

NRC 2015-0017
10 CFR 50.54(f)

U.S. Nuclear Regulatory Commission
ATTN: Document Control Desk
Washington, DC 20555-0001

Point Beach Nuclear Plant, Units 1 and 2
Docket 50-266 and 50-301
Renewed License Nos. DPR-24 and DPR-27

NextEra Energy Point Beach, LLC, Response to NRC 10 CFR 50.54(f) Request for Information Regarding Near-Term Task Force Recommendation 2.1, Flooding – Submittal of Flooding Hazards Revaluation Report

References:

1. U.S. Nuclear Regulatory Commission, Request for Information Pursuant to Title 10 of the Code of Federal Regulations 50.54(f) Regarding Recommendations 2.1, 2.3 and 9.3 of the Near-Term Task Force Review of Insights from the Fukushima Dai-ichi Accident, dated March 12, 2012 (ML12073A348), and letter Enclosure 2 (ML12056A048)

2. U.S. Nuclear Regulatory Commission, Prioritization of Response Due Dates for Request for Information Pursuant to Title 10 of the Code of Federal Regulations 50.54(f) Regarding Flooding Hazard Reevaluations for Recommendation 2.1 of the Near-Term Task Force Review of Insights from the Fukushima Dai-ichi Accident, dated May 11, 2012 (ML12097A509)

3. David L. Skeen, U.S. Nuclear Regulatory Commission, to Mr. Joseph E. Pollock, Nuclear Energy Institute, Trigger Conditions for Performing an Integrated Assessment and Due Date for Response, dated December 3, 2012 (ML12326A912)

4. NextEra Energy, Inc., 60-Day Response to NRC 10 CFR 50.54(f) Request for Information Regarding Near-Term Task Force Recommendation 2.1, Flooding, dated January 24, 2013 (ML13028A473)

On March 12, 2012, the NRC staff issued a Request for Information pursuant to Title 10 of the Code of Federal Regulations 50.54(f) regarding Recommendations 2.1, 2.3 and 9.3 of the Near-Term Task Force Review of insights from the Fukushima Dai-ichi accident (Reference 1). Enclosure 2 of that letter requested submittal of a flooding hazards reevaluation report. By letter dated May 11, 2012 (Reference 2), Point Beach Nuclear Plant, Units 1 & 2, was prioritized as Category 3, requiring submittal of the flooding hazards reevaluation by March 12, 2015. The enclosure to this letter provides the requested report.

The enclosed flooding hazards reevaluation (FHR) report demonstrates that one hazard, Local Intense Precipitation, exceeds the current design basis for Point Beach Nuclear Plant, Units 1 and 2. The results of all other hazards evaluated are bounded by the current licensing basis. An Integrated Assessment will be performed for the Local Intense Precipitation event and will be submitted by March 12, 2017 (Reference 3). Interim actions are not required as the existing station design and procedure actions are adequate to implement the Flexible Coping Capability (FLEX) strategies during a Local Intense Precipitation event.

It should be noted that the FHR report indicates that the station is protected from a current licensing basis maximum precipitation event by natural site drainage. The station is currently implementing modifications to provide additional protection for the Primary Auxiliary Building and Containment facades due to a maximum precipitation event caused by the current licensing basis combination of snowmelt and precipitation. These modifications have not yet been included in the Updated Final Safety Analysis Report (UFSAR). Consequently, the modifications are not reflected in the FHR report.

This letter contains one new regulatory commitment:

1. An Integrated Assessment will be performed for the Local Intense Precipitation event and will be submitted by March 12, 2017.

If you have any questions, please contact Mr. Michael Millen, Licensing Manager, at (920) 755-7845.

I declare under penalty of perjury that the foregoing is true and correct. Executed on March 12, 2015.

Sincerely,

Dan DeBoer for E. McCartney

Eric McCartney
Site Vice President
NextEra Energy Point Beach, LLC

Enclosure

cc: Administrator, Region III, USNRC
Resident Inspector, Point Beach Nuclear Plant, USNRC
Project Manager, Point Beach Nuclear Plant, USNRC

ENCLOSURE

NEXTERA ENERGY POINT BEACH, LLC
POINT BEACH NUCLEAR PLANT, UNITS 1 AND 2

FLOODING HAZARDS REEVALUATION REPORT
FPL-076-FHRPR-002, REVISION 2

127 pages follow

FLOODING HAZARDS REEVALUATION REPORT
FPL-076-FHRPR-002, REVISION 2

IN RESPONSE TO THE 10 CFR 50.54(f) INFORMATION REQUEST REGARDING NEAR-TERM TASK FORCE RECOMMENDATION 2.1: FLOODING
for the

Point Beach Nuclear Plant
Units 1 & 2

6610 Nuclear Road
Two Rivers, Wisconsin 54241-9516
Facility Operating License Nos. DPR-24 and DPR-27

NEXTera ENERGY RESOURCES

Presented to:
NextEra Energy Resources
700 Universe Boulevard
Juno Beach, Florida 33408-2683

Prepared by:
Enercon Services, Inc.
1501 Ardmore Boulevard, Suite 200
Pittsburgh, Pennsylvania 15221-4451

March 6, 2015

	Printed Name/Title	Affiliation	Signature	Date
Preparer:	Shaun W. Kline, Ph.D. / LRE	ENERCON	Shaun W. Kline	3/6/2015
Reviewer:	Sandra C. Dinzeo, P.E. / MGR	ENERCON	Sandra C. Dinzeo	3/6/2015
Approver:	Gerald E. Williams, P.E. / MGR	ENERCON	Gerald E. Williams	3/6/2015
Site Sponsor:	Wayne B. Fromm	NEE	W B Fromm	3/6/15

Table of Contents

List of Tables

List of Figures

Acronyms and Abbreviations

AFW	Auxiliary Feedwater
ANSI/ANS	American National Standards Institute and American Nuclear Society
AOP	Abnormal Operating Procedure
ASCE	American Society of Civil Engineers
CDF	Cumulative Distribution Function
CEM	Coastal Engineering Manual
CFL	Courant-Friedrichs-Lewy
CFR	Code of Federal Regulations

CLB	Current License Basis
COLA	Combined License Application
CWPH	Circulating Water Pump House
DTM	Digital Terrain Model
DIAC	Daily Ice Analysis Charts
ESP	Early Site Permits
ESRI	Environmental Systems Research Institute
FHR(R)	Flooding Hazards Reevaluation (Report)
FLEX	Flexible Coping Capability
GCS	Geographic Coordinate System
HMR	Hydrometeorological Report
IA	Integrated Assessment
IGLD55	International Great Lakes Datum of 1955
IGLD85	International Great Lakes Datum of 1985
ISG	Interim Staff Guidance
JLD	Japan Lessons-Learned Project Directorate
JONSWAP	JOint North Sea WAve Project
LIP	Local Intense Precipitation
NAD27	North American Datum of 1927
NAD83	North American Datum of 1983
NAVD88	North American Vertical Datum of 1988
NED	National Elevation Dataset
NEE	NextEra Energy
NEI	National Energy Institute
NGDC	National Geophysical Data Center
NOAA	National Oceanographic and Atmospheric Administration
NRC	Nuclear Regulatory Commission
NSE	Nash-Sutcliffe (Model Quotient) Efficiency
NTTF	Near-Term Task Force
NWS	National Weather Service
PAB	Primary Auxiliary Building
PBNP	Point Beach Nuclear Plant Units 1 & 2
PMF	Probable Maximum Flood

PMP	Probable Maximum Precipitation
PMSS	Probable Maximum Storm Surge
PMT	Probable Maximum Tsunami
PMWS	Probable Maximum Windstorm
POI	Point of Interest
RFI	Request for Information
RMP	Routine Maintenance Procedure
RMSE	Root Mean Square Error
SCO	(Wisconsin) State Cartographer's Office
SSCs	Structures, Systems and Components
SWAN	Simulating WAves Nearshore
SWL	Still Water Level
TB	Turbine Building (Hall)
The Lake	Lake Michigan
UFSAR	Updated Final Safety Analysis Report
UHS	Ultimate Heat Sink
USACE	U.S. Army Corps of Engineers
USGS	U.S. Geological Survey
USNIC	U.S. National Ice Center
WISCRS	Wisconsin Coordinate Reference Systems
WSEL	Water Surface Elevation

Units of Measure

°F	Degrees Fahrenheit
ac-ft	Acre-feet
ac	Acres
ft	Feet
ft/s	Feet per second
hr	Hours
in.	Inches
in. Hg	Inches of Mercury
kg	Kilogram
knots	Nautical miles per hour
kWe	Kilowatt-electric

MW	Megawatt
MWe	Megawatt-electric
m	Meters
m/s	Meters per second
mbar	Millibars (of pressure)
mi	Miles
min	Minutes
mph	Miles per hour
lbs	Pounds
pcf	Pounds per cubic foot
psf	Pounds per square foot
s	Seconds
yr	Years

1.0 PURPOSE

This report provides the NextEra Energy (NEE) Point Beach Nuclear Plant Units 1 and 2 (PBNP) response to the U.S. Nuclear Regulatory Commission's (NRC's) March 12, 2012 Request for Information (RFI) pursuant to the post-Fukushima Near-Term Task Force (NTTF) Recommendation 2.1 Flooding Hazards Reevaluation (FHR) of PBNP.

1.1 Background

In response to the Fukushima Dai-ichi nuclear facility accident resulting from the March 11, 2011 earthquake and subsequent tsunami, the NRC established the NTTF to conduct a systematic review of NRC processes and regulations, and to make recommendations to the NRC for its policy direction. The NTTF reported a set of recommendations that were intended to clarify and strengthen the regulatory framework for protection against natural phenomena.

On March 12, 2012, the NRC issued an information request pursuant to Title 10 of the Code of Federal Regulations (CFR) Part 50, Section 50.54(f) (NRC, 2012) which included Enclosures 1 through 6, inclusive:

1. NTTF Recommendation 2.1: Seismic;
2. NTTF Recommendation 2.1: Flooding;
3. NTTF Recommendation 2.3: Seismic;
4. NTTF Recommendation 2.3: Flooding;
5. NTTF Recommendation 9.3: Emergency Preparedness; and
6. Licensees and Holders of Construction Permits.

In accordance with Enclosure 2 of the NRC 10 CFR 50.54(f) letter request (NRC, 2012), licensees are required to reevaluate the flooding hazards at their sites against present-day regulatory guidance and methodologies being used for early site permits (ESP) and combined license applications (COLA).

1.2 Requested Actions

Per Enclosure 2 of the NRC 10 CFR 50.54(f) letter request (NRC, 2012):

> *"Addressees are requested to perform a reevaluation of all appropriate external flooding sources, including the effects from local intense precipitation on the site, probable maximum flood (PMF) on stream and rivers, storm surges, seiches, tsunami, and dam failures. It is requested that the reevaluation apply present-day regulatory guidance and methodologies being used for ESP and COL reviews including current techniques, software, and methods used in present-day standard engineering practice to develop the flood hazard. The requested information will be gathered in Phase 1 of the NRC staff's two phase process to implement Recommendation 2.1, and will be used to identify potential vulnerabilities.*

For the sites where the reevaluated flood exceeds the design basis, addressees are requested to submit an interim action plan that documents actions planned or taken to address the reevaluated hazard with the hazard evaluation.

Subsequently, addressees should perform an integrated assessment of the plant to identify vulnerabilities and actions to address them. The scope of the integrated assessment report will include full power operations and other plant configurations that could be susceptible due to the status of the flood protection features. The scope also includes those features of the ultimate heat sinks (UHS) that could be adversely affected by the flood conditions and lead to degradation of the flood protection (the loss of UHS from non-flood associated causes are not included). It is also requested that the integrated assessment address the entire duration of the flood conditions."

NEE PBNP submitted a 60-day response letter (Letter NRC-2012-0027) to the NRC titled, "NextEra Energy Point Beach, LLC's 60-Day Response to NRC Letter, Request for Information Pursuant to Title 10 of the Code of Federal Regulations 50.54(f) Regarding Recommendations 2.1.2.3, and 9.3, of the Near-Term Task Force Review of Insights from the Fukushima Dai-ichi Accident: dated March 12, 2012," dated May 10, 2012 (NEE, 2012a). In the letter, NEE PBNP stated intentions regarding the RFI.

1.3 Requested Information

This report provides the following requested information for PBNP, in accordance with Enclosure 2 of the NRC 10 CFR 50.54(f) letter request (NRC, 2012):

a. Site information related to the flood hazards. Relevant structures, systems and components (SSCs) important to safety and the UHS are included in the scope of this reevaluation, and pertinent data concerning these SSCs are also included. Other relevant site data include the following:
   i. Detailed site information (both designed and as-built), including present-day site layout, elevation of pertinent SSCs important to safety, site topography, as well as pertinent spatial and temporal datasets (Section 2.0);
   ii. Current design basis flood elevations for all flood-causing mechanisms (Section 2.3.2);
   iii. Flood-related changes to the licensing basis and any flood protection changes (including mitigation) since license issuance (Section 2.3);
   iv. Changes to the watershed and local area since license issuance (Section 2.4);
   v. Current license basis (CLB) flood elevations for all flood-causing mechanisms (Section 3.0); and
   vi. Additional site details, as necessary, to assess the flood hazards (i.e., bathymetry, walkdown results, and other pertinent data).

b. Evaluations of the flood hazards for each flood-causing mechanism, based on present-day methodologies and regulatory guidance. Analyses are provided for each flood-causing mechanism that may impact the site, including local intense precipitation (LIP) and site drainage, flooding in streams and rivers, dam breaches and failures, storm surge and seiche, tsunami, channel migration or diversion, and combined effects. Mechanisms that are not applicable at the site may be screened

out; however, justification should be provided. A basis will be provided for inputs and assumptions, methodologies and models used including input and output files, and other pertinent data (Section 4.0).

c. Comparison of current and reevaluated flood-causing mechanisms at the site. An assessment of the current design basis flood elevation to the reevaluated flood elevation for each flood-causing mechanism will be provided. This will include how the findings from Enclosure 2 of the 10 CFR 50.54(f) letter (i.e., NTTF Recommendation 2.1 FHR) support this determination. If the current design basis flood bounds the reevaluated hazard for all flood-causing mechanisms, how this finding was determined will be included (Section 5.0).

d. Interim evaluation and actions taken or planned to address any higher flooding hazards relative to the design basis, prior to completion of the integrated assessment described below, if necessary (Section 6.0).

e. Additional actions beyond Requested Information Item 1.d taken or planned to address flooding hazards, if any (Section 7.0).

1.4 Applicable Guidance Documents

The following documents were used as guidance in performing the FHR analyses:

1. ANSI/ANS (1992), American National Standards Institute and American Nuclear Society (ANSI/ANS), "Determining Design Basis Flooding at Power Reactor Sites," ANSI/ANS-2.8-1992, La Grange Park, Illinois, July 28, 1992;
2. NRC (1977), "Design Basis Floods for Nuclear Power Plants," Regulatory Guide 1.59, Revision 2, Washington, D.C., August 1977, with errata dated June 30, 1980;
3. NRC (1978), "Standard Format and Content of Safety Analysis Reports for Nuclear Power Plants," Regulatory Guide 1.70, Revision 3, Washington, D.C., 1978;
4. NRC (2007), "Standard Review Plan for the Review of Safety Analysis Reports for Nuclear Power Plants: LWR Edition," NUREG-0800, Washington, D.C., March 2007;
5. NRC (2009), "Tsunami Hazard Assessment at Nuclear Power Plant Sites in the United States of America Final Report," NUREG/CR-6966, PNNL-17397, Washington, D.C., March 2009;
6. NRC (2011), "Design-Basis Flood Estimation for Site Characterization at Nuclear Power Plants in the United States of America," NUREG/CR-7046, Washington, D.C., November 2011;
7. NRC (2013a), "Guidance for Performing a Tsunami, Surge and Seiche Hazard Assessment," Japan Lessons-Learned Project Directorate (JLD), Interim Staff Guidance (ISG), JLD-ISG-2012-06, Revision 0, January 4, 2013; and
8. NRC (2013b), "Guidance for Assessment of Flooding Hazards Due to Dam Failure," JLD-ISG-2013-01, Revision 0, July 29, 2013.

2.0 SITE INFORMATION

PBNP is located in Manitowoc County in east-central Wisconsin on the western shore of Lake Michigan (the Lake), approximately 30 mi southeast of Green Bay and about 90 mi north-northeast of Milwaukee. The site comprises approximately 1,260 ac owned by NEE. Farming is the predominant activity in this sparsely populated area of the state. The plant is situated in a productive dairy farming and vegetable canning region; however, heavy industry occurs to the south in Two Rivers and Manitowoc, and to the west in the Fox River Valley. Cooling water is drawn from an intake crib located 1,750 ft offshore in the Lake. Figure 2.1 depicts the site location (NEE, 2012c).

2.1 Datums and Projections

Various horizontal and vertical datums and mapping projections are referenced throughout this report. This section describes the horizontal and vertical datums and mapping projections used, their definitions and relationships, and the methods used to convert from one datum or projection to another.

2.1.1 Horizontal Datums and Projections

A horizontal datum is a system which defines an idealized surface of the earth for positional referencing. Two North American horizontal datums are used currently: the North American Datum of 1927 (NAD27) and the North American Datum of 1983 (NAD83). Latitude and longitude are typically used to identify location in spherical units.

A map projection is a mathematical transformation that converts a three-dimensional (spherical) surface onto a flat, planar surface. Each projection produces a distortion. Depending on their intended use, projections are chosen to preserve different relationships of characteristics between features. Projections in the United States are typically defined as State Plane coordinate systems with units of Northing and Easting. The United States is divided into many State Plane maps, and large states can be defined by several maps. PBNP is within the extents of the Wisconsin South State Plane projection.

The PBNP site topographic and bathymetric surveys were performed in 2013 and 2014, respectively (NEE, 2014a). Both surveys use the Wisconsin Coordinate Reference Systems (WISCRS) of Manitowoc County horizontal projection (NEE, 2014a). The de facto horizontal geodetic datum and adjustment for WISCRS is NAD83 (SCO, 2012).

2.1.2 Vertical Datums

There are two types of vertical datums: tidal and fixed. Fixed datums are reference level surfaces that have a constant elevation over a large geographical area. Tidal datums are standard elevations that are used as references to measure local water levels. Because of the negligible tidal oscillations in the Great Lakes, fixed datums are used near PBNP. The following is a list of datums referenced in this report:

- International Great Lakes Datum of 1955 (IGLD55) – Fixed datum specific to the Great Lakes, referenced to mean water level at Pointe-au-Pere (Father Point), Rimouski, Quebec, Canada, over the period 1941 to 1956 (USACE, 1991).

- International Great Lake Datum of 1985 (IGLD85) – Fixed datum specific to the Great Lakes, also referenced to the tide station and benchmark at Pointe-au-Pere (Father Point), Rimouski, Quebec, Canada over the period 1982 to 1988. IGLD85 replaced IGLD55 in January 1992 (USACE, 1991).
- North American Vertical Datum of 1988 (NAVD88) – Fixed vertical control datum determined by geodetic leveling, referenced to the tide station and benchmark at Pointe-au-Pere (Father Point), Rimouski, Quebec, Canada (NOAA, 2013).
- PBNP Plant Datum (Plant Datum) – Fixed vertical datum where zero elevation is equivalent to +580.2 ft-IGLD55 and +580.9 ft-IGLD85 (NEE, 2012c). The CLB, historical site survey drawings, and PBNP building structural elevations typically refer to this datum.

2.1.3 Vertical Datum Conversions

Where required, vertical transformations were performed using the conversions shown in Table 2.1 (NEE, 2012c). Elevations throughout this report will be reported in both ft-NAVD88 and ft-Plant Datum.[1] Based on Table 2.1, 0.0 ft-Plant Datum is equivalent to +581.3 ft-NAVD88.

2.2 PBNP Plant Description

The reactors at PBNP are Westinghouse-designed, pressurized light-water moderated and cooled systems. Unit 1 commenced commercial operation in December 1970; Unit 2 began commercial operation in October 1972. Each unit was originally licensed at a maximum core thermal power output of 1,518.5 MW. Each steam and power conversion system, including its turbine generator, was originally designed to permit generation of 523.8 MW of gross electrical power. Each unit underwent a low pressure turbine retrofit modification which increased the unit design output to 537,960 kWe. In 2003, a measurement uncertainty recapture power uprate was performed increasing each unit's rated thermal power level to 1,540 MW. In 2010, an extended power uprate resulted in Units 1 and 2 increasing their output to 1,800 MW and approximately 640 MWe (NEE, 2012c).

2.2.1 PBNP Topography

The ground surface at PBNP is gently rolling to flat with elevations varying from +584.3 to +639.3 ft-NAVD88 (+3 to +58 ft-Plant Datum). In the area around the plant, the land surface either slopes from west to east towards the Lake or to the north and south to divert runoff away from the plant. A topographic high point just to the west of the switchyard prevents any runoff inland of the plant from affecting plant operations (NEE, 2012c).

In relation to the Lake, a majority of the plant grounds are located at +607.3 ft-NAVD88 (+26 ft-Plant Datum). The only exception to this is the area near the Circulating Water Pump House (CWPH) where the plant draws its circulating water from the Lake and has a ground floor elevation of +588.3 ft-NAVD88 (+7 ft-Plant Datum). On the east side of PBNP, the service roads slope down from +607.3 ft-NAVD88 (+26 ft-Plant Datum) to around +588.3 ft-NAVD88 (+7 ft-Plant Datum) near the

[1]Note that the storm surge and seiche numerical model (Section 4.4) is set in a metric model datum, such that 0 m-Model Datum is equivalent to the 100-yr maximum Lake Michigan water level (Section 4.4.6). Results from the storm surge model were then converted to ft-NAVD88 and ft-Plant Datum for reporting purposes.

CWPH. The next closest structure to the Lake is the Units 1 and 2 Turbine Building (TB), approximately 100 ft inland from the CWPH. The ground floor elevation of the TB is +589.3 ft-NAVD88 (+8 ft-Plant Datum) (NEE, 2012b).

2.3 Flood-Related and Flood Protection Changes to the Licensing Basis since License Issuance

Since the initial license, there have been many changes made to the barriers and to the administrative protections for the postulated floods. This section begins with the 2012 Flooding Walkdown Report, its findings and the changes since that time. These changes reflect a fundamental change to the protection strategy for the wave runup.

2.3.1 2012 Flooding Walkdown Summary

NEE submitted a Flooding Walkdown Report, dated November 14, 2012, in response to the 50.54(f) information request regarding NTTF Recommendation 2.3: Flooding for PBNP (NEE, 2012b). The walkdowns were performed in accordance with National Energy Institute (NEI) 12-07 (Revision 0-A), "Guidelines for Performing Verification of Plant Flood Protection Features," dated May 2012 and endorsed by NRC on May 31, 2012 (NEI, 2012).

Configuration and procedures were compared to the flood protection features credited in the CLB documents for external flooding events. Site-specific features credited for protection and mitigation against external flooding events were identified and evaluated. The results of the walkdown are summarized below.

2.3.1.1 Reasonable Simulations

The only reasonable simulation conducted during the 2012 Flooding Walkdown was the installation of the temporary concrete jersey barriers as directed by a now-obsolete site procedure. Six barriers were installed on the south side to demonstrate the arrangement; only three barriers were installed on the north side due to constraints from construction occurring in the area at the time. No challenges to the time window or site resources needed for completion of the task were noted (NEE, 2012b).

2.3.1.2 Inspection Deficiencies and Corrective Actions

The flooding walkdown resulted in the following inspection deficiencies and resulting corrective actions (NEE, 2012b):

- The concrete jersey barriers installed at the CWPH did not extend far enough to the north and south to provide a barrier up to +590.3 ft-NAVD88 (+9.0 ft-Plant Datum). Also due to uneven ground and features on the barriers, some gaps existed in the installed configuration. Work requests were written to add additional barriers and pour a concrete pad to correct these issues. This strategy was subsequently revised in October 2014 as discussed in Section 2.3.2.
- The site procedure for the installation of the concrete jersey barriers was found to be deficient. It did not identify that the barriers were being installed in a B.5.b staging area and also did not provide pertinent information for the support equipment that would be needed. Procedure changes were made to address these issues as well as institute a regular check on the staging condition of the barriers. This strategy was subsequently revised in October 2014 as discussed in Section 2.3.2.

- The control panel and battery for the diesel fire pump in the CWPH were below +590.3 ft-NAVD88 (+9.0 ft-Plant Datum). The control panel, which also has circuitry for the battery, contains electrical components at +589.68 ft-NAVD88 (+8.375 ft-Plant Datum) which is below the flood height of +589.72 ft NAVD88 (+8.42 ft-Plant Datum). The Updated Final Safety Analysis Report (UFSAR) was updated to credit installed floor dampers for external as well as internal flooding. This reduced the flood height within the CWPH to +589.05 ft-NAVD88 (+7.75 ft-Plant Datum).
- A catch basin in the plant yard near the northwest corner of the Unit 2 Façade Building was covered with a metal plate. This plate was removed, and procedural controls to prevent this condition from reoccurring were evaluated.
- The UFSAR states that PBNP has north and west interceptor ditches outside of the plant yard to divert runoff to the Lake. The west side interceptor ditch runs between the plant yard and switchyard, but is obstructed by newly installed equipment and is not continuous. The north side ditch was not found. The UFSAR was updated to replace the northern interceptor ditch with the storm drain system, and to contain a reevaluation of the drainage near the western interceptor ditch. The UFSAR was subsequently revised to remove credit for the storm drain system and west interceptor ditch as these features were conservatively not credited in the design basis maximum precipitation analysis.
- There were several instances of inadequate drainage ditch maintenance, including partially obstructed culverts and some cases of drainage ditches needing to be cleared out or regraded. The maintenance program and supporting documentation have been updated to accurately reflect the drainage ditch configuration on site and ensure its functionality. The ditches and culverts have been cleaned under the Work Order process where the inspection criteria were not met. Ditches and culverts were conservatively not credited in the design basis maximum precipitation analysis.

2.3.1.3 Flood Protection Compliance

PBNP was found to be in compliance with its flood protection requirements per the CLB upon completion of corrective actions for the above deficiencies (NEE, 2012b). However, an improved flood protection strategy was adopted in October 2014 (NEE, 2015a; NEE, 2014b; NEE, 2014c) which is outlined in Section 2.3.2 below.

2.3.2 Flood Protection Features and Protected Equipment

The changes to the external flood strategy in October 2014 began with a clear definition of the CLB flood. The licensing basis at PBNP requires mitigation of design basis floods in rooms with SSCs important to safety.

2.3.2.1 Protection against Wave Runup

The CLB maximum wave runup elevation on a vertical structure is +589.72 ft-NAVD88 (+8.42 ft-Plant Datum). A duration for this CLB flood is not defined (NEE, 2014b). Protection to +590.3 ft-NAVD88 (+9.0 ft-Plant Datum) is provided by temporary barriers installed at the entrances to the CWPH and TB.

The site layout, consisting of the intake structure and rip-rap bank topography, are credited in the flooding evaluations, which demonstrate that the calculated flood level is bounded by the license basis flood level of +9.0 feet. Protection to +9.0 feet is provided by procedurally driven installation of temporary barriers at entrances to the CWPH and TB. When the Lake level exceeds administratively controlled limits, both units are brought to cold shutdown and barriers are installed. The Circulating Water, Condensate and Feedwater Systems are secured prior to installation of barriers at the TB doors/flood dampers in order to eliminate the major sources of internal flooding while the TB relief paths are blocked.

There are no openings in the CWPH walls, other than tight fitting doors, that have a bottom elevation less than +9.0 feet. In addition, storm drains are provided outside each of the CWPH doors. The TB, which is the structure next closest to the Lake, is more than 100 ft from the top of the bank. The combination of this distance, the shoreline riprap and the storm drains mitigate Lake effect flooding.

2.3.2.2 Protection against Maximum Precipitation Flood

The CLB maximum precipitation flood event is defined as the combined volume of water from the water content of snow in late March with a 50-yr recurrence frequency and the volume of water from a 6-hr rainfall with a 50-yr recurrence frequency. The topography of the site allows for the adequate natural drainage to remove the runoff and limit ponding near external access points to safety-related equipment (NEE, 2014b).

2.4 Hydrosphere

2.4.1 Climate

The continental climate at PBNP is influenced by the storms which move eastward along the northern tier of the United States and by those that move northeastward from the southwestern part of the country to the Great Lakes. However, the climate is modified by the Lake. During the spring, summer, and fall months, the Lake temperature differs greatly from the air temperature. In the spring and summer, cool daytime temperatures persist due to wind shifts from westerly to easterly directions. In autumn, the relatively warm water of the Lake prevents nighttime temperatures from falling as low as they do further inland. Summer temperatures exceed 90°F for six days on average. Freezing temperatures occur 147 days in a year on average, and temperatures are below 0°F for 14 days of the winter on average (NEE, 2014b).

2.4.2 Rainfall

Rainfall averages about 28 in./yr, with 55 percent falling in the months of May through September. The maximum rainfall of 6.17 in. over a 24-hr period occurred in September 1931. Snowfall averages about 45 in./yr; the maximum snowfall occurred in January 1947 and was 15 in. over a 24-hr period (NEE, 2014b).

2.4.3 Severe Weather

Tornadoes are relatively rare in the region north of Sheboygan, Wisconsin along the Lake shoreline. Tornadoes occur in Wisconsin but only one has been reported causing major property damage and injury to people in this region. This tornado occurred in Green Bay in 1959, 30 mi northwest of the site. Tornadoes appear to advance from the west with most of the tracks from the southwest. Maximum occurrence during

the year is in June, with 90 percent reported in May through September. Extreme winds are not expected to exceed 108 mph more than once in 100 yr (NEE, 2014b).

2.4.4 Wind

On an annual basis, the winds blow onshore (i.e., from the Lake towards the western shore) an average of 33.8 percent of the time. Onshore winds are defined as those which blow from the north through the south-southeast. Annually, winds blow offshore (i.e., from the western shore towards the Lake) an average of 63.5 percent of the time. Calm conditions are experienced the remaining 2.7 percent of the time (i.e., 100 percent – 33.8 percent – 63.5 percent = 2.7 percent) (NEE, 2014b).

During the spring season, the predominant wind directions during the period of record were northeasterly and south-southwesterly. Wind speeds tended to be above 10 mph from all directions but east. A very predominant south-southwest wind direction was noted over the summer. Again, wind speeds averaged near 10 mph, with the exception of southeasterly quadrant winds. The lowest average wind speed was 4.4 mph from the east (NEE, 2014b).

During autumn, average wind speeds from the west ranged from 10 to 14+ mph. There were relatively frequent occurrences of winds approximately parallel to the shoreline in both the northerly and southerly directions. The lowest wind speeds were again from the east (NEE, 2014b).

The onset of cold weather is evidenced by the increased frequencies of winds from the northwesterly quadrant. The winter season is characterized by a preponderance of winds from the northwest quadrant, observed to occur over 60 percent of the time. During the winter months, no average wind speed from any direction was below 10 mph. The average wind speed from the north-northeast was over 20 mph (NEE, 2014b).

On an annual basis, PBNP experiences predominating spikes of higher frequency winds from the west-northwest and the south-southwest. Average wind speeds are generally quite high from all directions from south-southeast clockwise through northeast. All average values are in excess of 10 mph. Significantly lower frequencies and lower wind speeds are observed with easterly winds, partially due to the Lake's influence on winds traveling against the normal gradient flow (NEE, 2014b).

2.4.5 Ice Storms

Ice storms are infrequent in this region of Wisconsin. Only a single transmission line extending from Green Bay to Kewaunee to Sturgeon Bay has experienced outages due to ice storms since 1940. Since rebuilding that line with improved conductors in 1956, only one outage has occurred (NEE, 2014b).

2.4.6 General Lake Michigan Hydrology

Lake Michigan and Lake Huron are considered at unity with respect to drainage and water level since the two lakes are connected via the Mackinac Straits. The drainage basin for the two lakes comprises 115,700 mi^2 and has an average annual rainfall of 31 in. (NEE, 2014b).

Lake Michigan is the third largest of the Great Lakes. The Lake is 307 mi long from north to south and has an average east-to-west width of 70 mi. It has a maximum depth of 923 ft, an average depth of 325 ft, and covers an area of 22,400 mi^2. The total volume of water in the Lake is approximately 1,400 mi^3. In the

general vicinity of PBNP, the 30-ft depth contour of the Lake is between 1.0 and 1.5 mi offshore, and the 60-ft depth contour is between 3.0 and 3.5 mi offshore (NEE, 2014b).

The water level in the Lake depends primarily on the runoff from the surrounding drainage basin. The nominal water level in the Lake at the time of the original license submittal was +579.3 ft-NAVD88 (-2.0 ft-Plant Datum). A maximum water level was recorded in 1886 at +583.0 ft-NAVD88 (+1.7 ft-Plant Datum) and the minimum recorded to date occurred in 1964 at +576.5 ft-NAVD88 (-4.8 ft-Plant Datum) (NEE, 2014b). The temperature stratification and circulation patterns of water in the Lake have very distinct characteristics, as described in the following sections.

2.4.6.1 Thermal Stratification

At the beginning of March, a warming trend starts in the Lake and, at the end of May, all of the water in the Lake has reached approximately 40°F, which is the temperature of maximum water density. Until the temperature reaches this point, the surface water is colder than the deeper water in the Lake; the colder surface water, which remains at approximately 34°F, is lighter than the 40°F deeper water. This layer of colder water circulates on the surface of the warmer deep water, reaching depths of 25 to 30 ft from the surface (NEE, 2014b).

When all of the water in the Lake reaches approximately 40°F, the thermocline layer disappears and complete mixing of all the water in the Lake occurs. However, when the ambient air temperature warms up the surface water, a thermocline layer is formed again at depths of 30 to 50 ft from the surface. This occurs from May to July and, at this time, parts of the water in the Lake reach 65°F to 70°F. Consequently, the warmer and lighter surface water circulates above the denser and relatively stagnant 40°F water at the bottom of the Lake. This condition continues until a cooling trend starts in September, reaching a peak about the last part of January, at which time the water in the Lake again reaches an overall temperature of 40°F. At this time, complete mixing of the waters in the Lake takes place until a colder and lighter layer of surface water starts to build up (NEE, 2014b).

2.4.6.2 Currents, Tides, and Littoral Drift

Surface currents in the Lake are generated primarily by wind stress on the water surface. The Lake surface wind-driven currents have speeds averaging 1 to 2 percent of the wind speeds. Thus, an average wind speed of 15 mph over the Lake would generate an average surface current of about 0.15 to 0.3 mph (0.22 to 0.44 ft/s). Such currents may persist for several days after the wind has ceased. On large water surfaces, the wind-driven current is theoretically 45 degrees to the right of the wind vector (e.g., the current would be to the east for a northward wind) due to the rotation of the earth (i.e., the Coriolis effect). On the western side of the Lake, the current is largely parallel to the shore and more nearly 22 degrees to the right of the prevailing wind (e.g., the current would be to the north-northeast for a northward wind). The predominant current direction near the western shore during the period of greatest stratification is in the northerly direction. However, temporary reversals of the general trend may take place (NEE, 2014b).

Tides on the Lake created by the gravitational attraction of the moon and sun are insignificant. The total tidal range of oscillation does not exceed 0.17 ft (2 in.) (NEE, 2014b).

Waves are responsible for most of the littoral drift on the Lake. In this specific area, the predominant drift appears to be to the north. Under unfavorable conditions, littoral drift may have a pronounced effect on the advance or retreat of certain shorelines. At PBNP, the beach is narrow, ranging from 20 to 50 ft. The shoreline recession rates range from 2.5 to 5 ft/yr. Special protection is provided to control further recession of the shoreline at PBNP (NEE, 2014b).

3.0 CURRENT LICENSE BASIS FOR FLOODING HAZARDS

This section describes the primary flooding mechanisms and their associated water surface elevations (WSELs) and effects at PBNP based on information contained in UFSAR Chapters 2 and 5 and Appendix A.7 (NEE, 2010; NEE, 2014b; NEE, 2014c). This section also summarizes PBNP's current flood protection features and procedures.

3.1 CLB – Maximum Precipitation Flood

The CLB precipitation event for PBNP is the combination of the 6-hr rainfall with a 50-yr recurrence frequency and the water content of snow in late March with a 50-yr recurrence frequency. This combined volume of water is equivalent to 4.90 in. over the 6-hr duration. The topography of the site results in adequate natural drainage to remove this amount of water and limit ponding depth to prevent adversely affecting safety-related equipment (NEE, 2014b). Maximum WSELs at PBNP points of interest (POIs) are shown in Table 3.1.

3.2 CLB – Riverine (Streams and Rivers) Flooding

No significant streams flow by or near the site. Two small creeks drain to the north and south. One creek discharges into the Lake about 1,500 ft north of the northern corner of PBNP property and the other near the center of PBNP property. Therefore, a PMF runoff analysis was not performed for the CLB (NEE, 2014b).

3.3 CLB – Dam Breaches and Failure Flooding

There are no dams, area reservoirs, plant cooling water canals, or plant cooling water reservoirs planned for or located upstream from the site. Cooling water is supplied by the Lake as the primary source and UHS. In view of the topography and characteristics of the local streams, it seems unlikely that reservoirs of any substantial size will be built in the future. Dam failures were not considered a meaningful hazard at PBNP (NEE, 2014b).

3.4 CLB – Lake Michigan Flooding

The CLB Lake flood level, +589.72 ft-NAVD88 (+8.42 ft-Plant Datum), is a combination of the historical maximum Lake elevation of +583.0 ft-NAVD88 (+1.7 ft-Plant Datum) coincident with +0.17 ft wind setup and +6.55 ft wave runup on a vertical surface. Bank protection is based on riprapping the slope adjacent to the beach. The wave runup will encounter this slope or the vertical faces formed by the front of the intake structure or adjacent sheet piling walls (NEE, 2014b).

3.4.1 Storm Surge Background

The water level of the Lake is a function of a number of factors: the amount of snowmelt and runoff, long-term variation in the Lake level due to variations in water supply, storm surge, seiche, and wind setup. The frequency that the Lake rises to a particular level is a function of the frequency of the individual independent contributing primary causes.

At any given time, the Lake level is a function of the still water level (SWL) plus wind-generated waves. Breaking waves also produce runup onshore. Therefore, the resultant final water elevation is equal to the level of the Lake due to a storm surge, seiche, or other flooding mechanism plus the amount of runup due to breaking waves near the shore.

The maximum water surface level at PBNP is defined as the SWL produced by storm surge, seiche, wind setup, and wave runup at the shore.

Flooding on the Lake shoreline can occur due to storm surge produced by moving squall lines, seiche, and wave setup. In addition to these effects, wave runup could result in somewhat higher elevations at the Lake shore due to waves breaking on or near sloped or vertical surfaces.

3.4.2 Astronomical Tides

Tides on the Lake created by the attraction of the moon and sun are quite small; the total range of oscillation does not exceed 0.17 ft (2 in.). The CLB does not use a tidal component in determining the maximum Lake flooding (NEE, 2014b).

3.4.3 Maximum Historical Lake Michigan Water Level

The maximum Lake level of +582.0 ft-NAVD88 (+1.7 ft-Plant Datum) was recorded in 1886. This maximum Lake level was used to determine maximum Lake flooding (NEE, 2014b).

3.4.4 Probable Maximum Windstorm

A sustained easterly wind velocity of 40 mph over a fetch length of 70 mi and average depth of 465 ft was used to determine the CLB wind setup component coincident with the maximum wave runup (Section 3.4.6). The maximum storm surge was calculated based on a squall line with a pressure rise of 8 mbar (0.236 in. Hg) traveling at 65 knots (NEE, 2014b).

3.4.5 Wave Action

The 500-yr frequency maximum, deep water wave height in the Lake was defined as 23.5 ft for a full-yr period and 18.0 ft for the ice-free period. Due to the extremely flat slopes of the beach near PBNP (1:100 in the first 1,000 ft into the Lake and 1:200 for the next 4,000 ft into the Lake[2]), such large waves would break far offshore and do not need to be considered for runup at PBNP. In this case, only waves of lesser height actually need to be evaluated for the runup on the beach (NEE, 2014b).

3.4.6 Wave Runup

Two methods of wave runup analysis were followed in the CLB. In the first case, the 500-yr maximum full-yr, deep water wave was treated as impinging upon a breakwater with very flat slopes, with the toe of

[2]Slopes are reported as vertical (V) to horizontal (H), V:H.

the slope located in a water depth of 12 ft. The computed vertical height above normal water level for this case was 1.4 ft (NEE, 2014b).

In the second case, an estimate of the probable maximum secondary wave, a wave height of 4.68 ft, was determined from the average depth (6 ft) prevailing after the larger deep water wave has broken and reformed (S&L, 1967). The runup on the beach above the water level was computed for a wave period of 8 s as 7.72 ft on a 1:1.5 smooth slope,[3] 5.38 ft on a 1:1.5 riprap slope, and 6.55 ft on a vertical structure (Table 3.2) (NEE, 2014b).

Prolonged winds of high velocity tend to form a wind tide setup. Accordingly, a conservative wind setup of 0.17 ft was used, based on a sustained easterly wind velocity of 40 mph over a fetch length of 70 mi and average depth of 465 ft. Thus, the maximum expected runup on a vertical structure would be 6.72 ft above the antecedent water level (i.e., 6.55 ft + 0.17 ft = 6.72 ft) (NEE, 2014b).

The maximum recorded water level in the Lake was +583.0 ft-NAVD88 (+1.7 ft-Plant Datum). Assuming conservatively that the maximum wave runup occurs simultaneously with the maximum level, the runup would reach to +589.72 ft-NAVD88 (+8.42 ft-Plant Datum) on a vertical structure (i.e., +580 ft-NAVD88 + 6.72 ft = 586.72 ft-NAVD88) (NEE, 2014b).

3.4.7 Maximum Storm Surge

The CLB storm surge was calculated to be 4.14 ft due to the passage of a squall line with a pressure increase of 8 mbar (0.236 in. Hg) and a simultaneous speed of movement of 65 knots with a shoaling factor of 3.5. Adding this 4.14 ft of storm surge to the maximum recorded Lake level of +583.0 ft-NAVD88 (+1.7 ft-Plant Datum) results in an elevation of +587.14 ft-NAVD88 (+5.84 ft-Plant Datum), which is considerably lower than the TB grade floor elevation of +589.3 ft-NAVD88 (+8.0 ft-Plant Datum) or the CWPH operating floor elevation of +588.3 ft-NAVD88 (+7.0 ft-Plant Datum) (NEE, 2014b).

The value of 4.14 ft was developed using Platzman's contours of amplitude for pressure. There are no contours for the Lake in the area near PBNP, so the reflected surge values for Waukegan, Illinois were used for a squall line moving east (i.e., 90 degrees) with a speed of 65 knots (75 mph). The resulting pressure rise was 0.05 ft. Using 8 mbar (0.236 in. Hg) and applying a 3.5 shoaling factor, the maximum surge due to pressure is

$$0.05\,ft \times \frac{0.236\,in\,Hg}{0.01\,in\,Hg} \times 3.5 = 4.14\,ft.$$

This amplitude was adjusted further based upon the wind velocity. For velocities greater than or equal to 70 knots (81 mph), a surge increase of 1 ft over the computed value is applied, so that the maximum storm surge becomes 5.14 ft (i.e., 4.14 ft + 1 ft = 5.14 ft), which is bounded by the maximum wave runup on a vertical structure. If the maximum surge occurs coincident with the maximum historical Lake level, the

[3]Slopes are reported as vertical (V) to horizontal (H), V:H.

maximum storm surge elevation will be +588.14 ft-NAVD88 (+6.84 ft-Plant Datum) (i.e., +583.0 ft-NAVD88 + 5.14 ft = +588.14 ft-NAVD88), which is still below the TB floor level (NEE, 2014b).

3.4.8 Seiche

Seiches are caused by a frontal squall line defining an abrupt change in atmospheric pressure in the range of 3.4 mbar (0.1 in. Hg) moving across the Lake at a high velocity. An average of 20 seiches/yr occur near Chicago, but the rise in Lake level is often insignificant (NEE, 2014b).

The open shoreline at PBNP will not be subject to reflection and should not produce any amplification of the seiche height. It appears logical to consider that the rise in water level due to the seiche would be a maximum of 1 to 2 ft. Historical records show that the peak rise in water level associated with a seiche can be achieved very quickly. The record seiche in Chicago on June 26, 1954 lasted about 0.5 hr. The historical records did not reveal the coincident occurrence of a major seiche with a major high wave condition. Winds of high velocity have been recorded before or after seiches for relatively short periods of time, but there is no basis to superimpose the conditions of the maximum wave upon the maximum seiche. Thus, a maximum seiche is not combined with the maximum Lake level, maximum wind setup and maximum wave runup in the combined effects analysis (NEE, 2014b).

3.5 CLB – Tsunami Flooding

A tsunami was not considered a meaningful hazard to PBNP (NEE, 2014b).

3.6 CLB – Ice-Induced Flooding

No specific ice flooding design criteria are proposed for safety-related facilities since the facilities are located at an elevation which makes them invulnerable to any local ice activity. Local flooding due to ice formation is considerably below maximum surge conditions (NEE, 2014b).

Ice flooding and associated effects were not considered meaningful hazards at PBNP. The U.S. Coast Guard reported pile up of ice in the form of frozen spray and ice floes to a height of 30 to 40 ft at the shore and extending about 100 ft into the Lake. These observations were made at Rawley Point Lighthouse 5 mi south of the site. Similar conditions have been experienced at many power stations along the Lake (NEE, 2014b).

The primary reason for the buildup seems to be the formation of ice which is driven out to deep water by offshore winds and collected until a change in wind drives these ice floes towards the shore. As they approach shallow water, they ground and the offshore floes are driven up and over the grounded floes. The peak point in height of this buildup does not occur at the shoreline on extremely flat beaches, but some distance offshore. This action has given rise to reports of "ice shoves" which have damaged fish shanties on a beach or light wharf structures projecting into the water (NEE, 2014b).

Beach structures for power stations represent a massive installation and the history of such structures has shown no major damage from ice shoves even where these have been located next to the shoreline on shallow beaches. The outer wall of the intake forebay, the only structure on the beach, is designed with

3-ft-thick reinforced concrete. This is considered adequate to withstand any pressure from the ice. The water intake is located 1,750 ft offshore in a water depth of 18 ft, measured from the lowest recorded Lake level of +576.5 ft-NAVD88 (-4.8 ft-Plant Datum). Water is drawn from the intake crib through two 14-ft-diameter pipes buried below the Lake bed and will not be affected by ice. The cooling water is discharged through two flumes consisting of well-braced steel sheet piling driven 40 ft into the Lake bed and protected by riprap. This is considered adequate to withstand any pressure from the ice. Other structures are located approximately 190 ft from the beach line and are further protected by the low bluff along the shoreline (NEE, 2014b).

3.7 CLB – Channel Migration or Diversion Flooding

No significant streams flow by or near the site. Channel migrations or diversions of the small creeks were not considered meaningful hazards at PBNP (NEE, 2014b).

3.8 CLB – Combined Events Flooding

The combined CLB precipitation-snowmelt event is discussed in Section 3.1. The resulting maximum WSELs are listed in Table 3.1. The maximum storm surge was considered coincident with the maximum historical Lake level. The maximum flood level was the maximum wave runup on a vertical structure occurring during the maximum historical Lake level with wind setup from a sustained 40 mph easterly wind. No other combination events were considered in the CLB (NEE, 2014b).

3.9 CLB – Flooding Protection

The external CLB protection at PBNP provides for the mitigation of CLB floods to prevent ingress of water from occurring in rooms with SSCs important to safety with the exception of possible water intrusion to the service and fire water pump rooms in the CWPH during a wave runup event. The CLB does not specify which plant configurations are considered (NEE, 2014b).

The CLB maximum probable wave runup from the Lake is +589.72 ft-NAVD88 (+8.42 ft-Plant Datum). The CLB requires the installation of concrete barriers and sandbags to provide a flooding barrier at the CWPH that would protect equipment in the CWPH and TB from the flood waters up to +590.3 ft-NAVD88 (+9.0 ft-Plant Datum) (NEE, 2014b).

The following strategies are used to protect the CWPH from wave runup (NEE, 2014c):

- Monitoring of Lake level;
- Combining shore riprap with intake structure to reduce the total wave runup height;
- Constructing temporary barriers (i.e., concrete blocks and sandbags on the outside and sandbags on the inside) at CWPH rollup Door 336 and Door 340 (shown on Figure 4.5);
- Crediting sufficient frames at tight-fitting CWPH personnel Door 338 and Door 339 (shown on Figure 4.5) to protect against wave runup forces; and

- Placing sandbags inside of tight-fitting CWPH personnel Door 338 and Door 339 (shown on Figure 4.5) to protect from water ingress.

Further, the CWPH service water pump motors, at +590.63 ft-NAVD88 (+9.33 ft-Plant Datum), are the lowest safety-related component in the CWPH. All flooding-susceptible, safety-related equipment in the CWPH is mounted above the external CLB flood level and would not be subject to flooding, irrespective of other protection features. The augmented quality diesel fire pump control panel is mounted at +589.675 ft-NAVD88 (+8.375 ft-Plant Datum), which exceeds the calculated levels inside the CWPH from the CLB external flood when crediting the floor flood relief dampers (NEE, 2014c).

The forebay portion of the intake structure extends 65 ft from the shoreline back to the CWPH and has vertical walls extending to elevation +596.7 ft-NAVD88 (+15.4 ft-Plant Datum) parallel to the shoreline (i.e., east side of the CWPH) and to elevation +593.3 ft-NAVD88 (+12.0 ft-Plant Datum) perpendicular to the shoreline (i.e., north and south sides of the CWPH). These walls protect the CWPH portion of the intake structure from the runup due to a wave impinging on a vertical structure. The bank adjacent to the intake structure has riprap placed on a 1:2 slope, and the runup portion will be somewhat less than the maximum of +589.72 ft-NAVD88 (+8.42 ft-Plant Datum) indicated above. If the waves break over the bank around the CWPH, storm drains are provided outside each of the doors of the CWPH and there are no openings in the walls, other than tight-fitting doors that have a bottom elevation less than +590.3 ft-NAVD88 (+9.0 ft-Plant Datum). In addition, storm drains are provided outside of the CWPH doors (NEE, 2014b; NEE, 2014c).

The following strategies are used to protect the TB, Control Building, and PAB (which are separate structures approximately 100 ft inland from the CWPH) from wave runup (NEE, 2014c):

- Monitoring of Lake level.
- Combining shore riprap with intake structure to reduce the total wave runup height.
- Crediting the distance from the Lake to the TB to reduce the total wave runup height.
- Protecting from wave impact forces with the concrete and steel missile barriers for the diesel air intake louvers.
- Crediting sufficient frames at TB personnel Door 2 and Door 11 (shown on Figure 4.5) to protect against wave runup forces.
- Sealing covers on Manhole Z-66A and Manhole Z-67A to block conveyance into the Control Building.
- Operator-directed action to shut down operating reactors and secure secondary systems (i.e., cooling water, condensate, and feedwater) prior to the Lake reaching a critical level.
- Operator-directed action to detect and mitigate a leak from other non-Category I (seismic) sources.
- Procedurally installing temporary barriers at +589.3 ft-NAVD88 (+8.0 ft-Plant Datum) exterior doors and openings of the TB prior to the Lake reaching a critical level. These barriers and strategies include:

- Station a dedicated flood watch any time the external flooding barriers are in place;
- Open Auxiliary Feedwater Tunnel Door 6 and Door 19 prior to installation of turbine hall exterior barriers to protect against non-Category I (seismic) component rupture;
- Install steel stop logs outside of TB rollup Door 4 and Door 13 (shown on Figure 4.5), TB Flood Dampers 1 and 2Z-329, and Maintenance Shop rollup Door 76 (shown on Figure 4.5) to protect from wave forces;
- Procedurally install Presray devices inside TB access Door 2 and Door 11 (shown on Figure 4.5) to limit water ingress;
- Place sandbags inside TB rollup doors, TB flood dampers, the Maintenance Shop rollup door, and Maintenance Shop access Door 1 (shown on Figure 4.5) to limit flood water ingress into the structures; and
- Install stackable, water-resistant stop logs on the inside of the air intake louvers to Rooms G-01 and G-02 to limit water ingress.

The installation of turbine hall external flooding barriers requires both units to be in Operation Mode 5, which is outside the mode of applicability for auxiliary feedwater operability. The Diesel Generator G-03/04 Building slab is at +609.3 ft-NAVD88 (+28.0 ft-Plant Datum), well exceeding the +590.3 ft-NAVD88 (+9.0 ft-Plant Datum) CLB flood level.

3.10 CLB – Low Water Effects

The lowest recorded Lake water level was +576.5 ft-NAVD88 (-4.8 ft-Plant Datum). The intake structure is 18 ft below this level and sufficient water is still available to meet PBNP requirements. Low water levels related to surges, seiches, or tsunamis were not evaluated in the CLB (NEE, 2014b).

3.11 CLB – Hydrostatic, Hydrodynamic, Sediment, and Debris Loading

Hydrostatic, hydrodynamic, sediment, and debris loading on permanent PBNP structures were not evaluated in the CLB. The wave barriers to be deployed during elevated Lake levels were designed to prevent sliding or overturning from hydrostatic and hydrodynamic forces associated with CLB maximum wave runup elevations (NEE, 2014b).

3.12 CLB – Waterborne Projectiles

Waterborne projectiles were not considered in the CLB; however, tornado missiles were analyzed. The following tornado missiles were considered (NEE, 2010; Bechtel, 1970):

1. A wood plank measuring 4 in. x 12 in. x 12 ft, weighing 200 lbs, traveling at a velocity of 440 ft/s (300 mph) and
2. An automobile with a cross-sectional area of 20 ft^2, weighing 4,000 lbs, traveling at a velocity of 74 ft/s (50 mph).

All Class I structures were designed to withstand tornado missiles. None of the analyzed missiles would penetrate the containment (NEE, 2010). From the above tornado missiles, the maximum design impact pressure is for the wood plank: 149,068 psf.

4.0 FLOODING HAZARDS REEVALUATION

The following sections discuss the flood-causing mechanisms, associated WSELs and related effects that were considered in the PBNP FHR. Selected PBNP site features are shown on Figure 4.1 for reference throughout Section 4.0.

4.1 Local Intense Precipitation

LIP is a measure of high intensity, short duration precipitation at a given location. Generally, for smaller basin areas (up to 10 mi^2), shorter storm durations produce the most critical runoff scenario. High intensity rainfall in a small area has a short concentration time and, therefore, a high intensity runoff. Thus, the shorter storm occurring over a small watershed will result in higher flow rates and depths at PBNP. As defined in NUREG/CR-7046 (NRC, 2011), the LIP event will be the 1-hr, 1-mi^2 probable maximum precipitation (PMP) at PBNP.

The sections below describe the LIP evaluation process for PBNP:

- LIP intensity and temporal distribution development (Section 4.1.1);
- Runoff and routing model overview (Section 4.1.2);
- Surface topography generation (Section 4.1.3);
- Impediments and obstructions to flow (Section 4.1.4);
- Selection of surface infiltration and roughness characteristics (Section 4.1.5);
- Incorporation of yard drain network (Section 4.1.6);
- Runoff model scenarios evaluated (Section 4.1.7);
- Runoff transformation, translation, and conveyance processes (Section 4.1.8); and
- Model results (maximum water depths and flow velocities) (Section 4.1.9).

4.1.1 Local Intense Precipitation Intensity and Distribution

A site-specific LIP evaluation was used for PBNP, following a recommended storm-based approach (ANS/ANSI, 1992; WMO, 2009; NRC, 2011). The storm-based approach is detailed in Hydrometeorological Report (HMR) 33 (Riedel et al., 1956) and HMR 51 (Schreiner and Riedel, 1978). The storm-based approach uses historical, regional rainfall data, which are maximized and transpositioned to occur at PBNP. The initial step in the storm-based approach was to identify a set of storms which represent extreme precipitation events, such that high rainfall totals occurred over short durations and small area sizes. Storm types included thunderstorms and intense rainfall associated with Mesoscale Convective Complexes. This procedure is similar to what is described in HMR 52, Section 6 (Hansen et al., 1982). A total of 21 historical events from a similar meteorological and topographic setting were selected for detailed evaluation of LIP totals at PBNP. Thirteen of these storms were previously analyzed in HMR 33 and HMR 51 by the National Weather Service (NWS) and U.S. Army Corps of Engineers (USACE).

Each historical storm event was modified by a transpositioning algorithm. The adjustment factor is a combination of the atmospheric moisture and terrain influences (e.g., elevation, temperature) on rainfall,

maximized and transpositioned to PBNP. The result is the rainfall total volume to be expected at PBNP if all contributing factors were maximized and occurred simultaneously. After adjustments were applied, the maximized and transpositioned May 1943 Mounds, Oklahoma storm event had the highest 1-hr rainfall; several other storms provided slightly smaller total rainfall amounts. The 1-hr, 1-mi^2 total precipitation depth is 12.8 in.

To fully develop the temporal rainfall distributions (i.e., hyetographs), the hourly rainfall total was disaggregated into subhourly increments of 5, 15, and 30 min. A lack of subhourly PMP-type storm data prevented an updated evaluation from being completed; therefore, the ratios derived in HMR 52 Figures 36 and 38 (Hansen et al., 1982) were applied to PBNP for the subhourly precipitation intensities. The site-specific 5-min, 15-min, 30-min, and 60-min LIP intensities are shown in Table 4.1. The peak LIP rainfall intensity is 4.4 in. over 5 min.

The total precipitation depths were applied to four hyetographs: (1) first quartile, (2) second quartile, (3) third quartile, and (4) fourth quartile (Figure 4.2). Each hyetograph is distinct based on the time to peak rainfall intensity. For example, the first quartile hyetograph has the most intense precipitation at the beginning of the event, whereas the fourth quartile hyetograph has the most intense precipitation at the end of the event. All four hyetographs have the same total rainfall (i.e., 12.8 in. over 1 hr). The hyetographs were used to determine the sensitivity of the temporal rainfall distribution and bounding maximum flow depths in Section 4.1.9.

4.1.2 Runoff and Routing Model Overview

FLO-2D PRO (Build 14.08.09) software by FLO-2D Software, Inc. (FLO-2D, 2014) was used to evaluate the LIP runoff event at PBNP. FLO-2D PRO has a number of components to simulate street flow, building and obstructions, sediment transport, spatially variable rainfall and infiltration, floodways, and other flooding effects. Predicted flow depths and velocities between the grid elements are average hydraulic flow conditions computed for small time steps (on the order of seconds). Typical applications of FLO-2D PRO have grid element resolution that ranges from 5 to 500 ft. The number of grid elements is theoretically unlimited but is confined practically by processing capability. The output files provide time-dependent WSELs, flow velocities, and other hydraulic parameters at each computational element (FLO-2D, 2014).

4.1.3 Surface Topography Generation

A digital terrain model (DTM), derived primarily from a recent site topographic survey (NEE, 2014a), shown on Figure 4.3, was imported into FLO-2D PRO and a 5-ft resolution grid domain was developed because the typical flow pathways on the site are of that width or wider. The boundary elements were prescribed as outflow points with no hydrograph, allowing runoff to freely leave the domain.

4.1.4 Obstructions and Flow Impediments

Obstructions and surface flow impediments include permanent buildings, temporary structures (e.g., storage containers), (wave) barriers, and topographic features. Buildings, temporary structures and barriers were entered explicitly into the DTM (Figure 4.3).

Runoff from the permanent building and temporary structure areas is a hydrologic feature of the model. Permanent building roofs were incorporated as flat surfaces (Figure 4.3). This approach prevents rooftop

water storage and assumes roof drains are nonfunctional; runoff from building rooftops is routed directly to the ground adjacent to the building. The model layout captures building heights relative to each other to preserve anticipated runoff routing. Further, the building heights used in the DTM were set higher than expected maximum runoff flow depths to prevent flow into buildings or roofs. Temporary structures were modeled as flat, raised surfaces with heights typical of storage containers. All rainfall in these areas was routed to adjacent ground cells.

The elevations of the model cells chosen to represent POIs on the east side of the TB were set at +589.3 ft-NAVD88 (+8.0 ft-Plant Datum) to accurately determine the flood elevations at TB east doors. To ensure model stability, all elevations directly east of the TB were adjusted to +589.3 ft-NAVD88 (+8.0 ft-Plant Datum) (Figure 4.3).

4.1.5 Surface Infiltration and Roughness Characteristics

Because of the large percentage of impervious, paved area across the model domain, the relatively short duration of the storm (i.e., 1 hr), and the extreme rainfall total (i.e., 12.8 in.), the antecedent conditions are assumed to be full ground saturation. Accordingly, zero infiltration was credited in the runoff model. This assumption is consistent with NUREG/CR-7046 (NRC, 2011).

Manning's equation, based on uniform, fully developed turbulent runoff flow, was used to determine hydraulic roughness. The assignment of overland flow roughness accounts for vegetation and surface irregularities. The following Manning's roughness coefficients (dimensionless) were selected:

- 0.02 for asphalt or concrete;
- 0.20 for open ground with debris; and
- 0.40 for shrubs and forest litter and/or pasture.

The spatial distribution of the designated Manning's roughness coefficients at PBNP is provided on Figure 4.4.

4.1.6 Storm Drain Network

The yard drain system was considered nonfunctioning (i.e., 100 percent blocked) in the runoff results presented in Section 4.1.9.

4.1.7 Runoff Model Scenarios

Two LIP scenarios were evaluated:

- Scenario A, which considered the temporary laydown areas (Figure 4.5) completely occupied with equipment/containers.
- Scenario B, which had the same occupied temporary laydown areas as Scenario A in addition to the temporary wave barriers installed adjacent to the CWPH (Section 3.9 contains details regarding temporary wave barrier deployment and positioning). In the FLO-2D model, the cells adjacent to the CWPH where the wave barriers would be installed were manually adjusted to be 3.5 ft higher for Scenario B.

Assuming the temporary laydown areas are completely occupied removes the storage area and/or flow paths available if equipment, containers or barriers are not present there. Thus, Scenario A and Scenario B should be considered bounding if temporary structures are removed from the areas shown on Figure 4.5. Each scenario was evaluated for the four hyetographs detailed in Section 4.1.1, such that eight total model simulations were completed (i.e., two scenarios times four hyetographs equals eight model simulations).

Thirty-three doors were identified as POIs for the LIP evaluation (Figure 4.5). Time-dependent flow depths, velocity time series, maximum flow depths, and maximum WSELs were reported at each POI. The simulations were allowed to run for 10 hr to allow for flood recession and adequately capture the total duration of the LIP flood event at each POI.

4.1.8 Runoff Model Processes and Successful Application Criteria

FLO-2D PRO is a simple, two-dimensional, physical process model based on a volume conservation model. The general governing equations are the continuity equation (i.e., conservation of mass/volume) and dynamic wave momentum equation (i.e., conservation of motion). These equations are solved to route rainfall-runoff and flood hydrographs over unconfined surfaces or in channels (FLO-2D, 2013).

A set of partial differential equations (St. Venant or shallow water equations, which are derived from the conservation of mass and motion criteria described above) is solved using the second-order Newton-Raphson tangent finite difference method. The computational domain in the FLO-2D PRO model is discretized into uniform, square grid elements. The discharge is computed in eight different directions across the grid element boundary (FLO-2D, 2013).

The full dynamic wave equation is a second-order, nonlinear, hyperbolic differential equation. To solve the equation for flow velocity at a grid element boundary, the flow velocity is calculated initially with the diffusive wave equation using the average water surface slope (i.e., bed slope plus pressure head gradient). This velocity is then used as a first estimate in the second-order Newton-Raphson tangent method to determine the roots of the full dynamic equation. Then, Manning's equation is applied to compute the friction slope. If the solution fails to converge after three iterations, the algorithm defaults to the diffusive wave solution (FLO-2D, 2013).

Successful FLO-2D PRO model applications meet the following criteria:

- A small volume conservation error;
- No invalid areas of inundation introduced by one-dimensional channel elements; and
- No numerical surging resulting from mismatched flow area, slope, and roughness.

The maximum mass balance error in the runs (volume conservation error) was less than 0.001 percent (6.1×10^{-4} ac-ft), which is within the acceptable continuity error range (FLO-2D, 2013). Further, since the PBNP runoff model does not contain one-dimensional channel elements, there are no invalid areas of inundation.

The maximum velocity and numerical surging are related to the area of inundation. Numerical surging is the result of a mismatch between flow areas, slope, and roughness and can cause an over-steepening of the flood wave. To avoid numerical surging, the FLO-2D PRO model is subject to the Courant-Friedrichs-

Lewy (CFL) condition used for the explicit solution scheme. The CFL condition states that the numerical solution remains stable only for Courant numbers (C) less than or equal to 1.0, defined as:

$$C = \frac{|V|+c}{\frac{\Delta x}{\Delta t}} \qquad \text{Equation 4.1}$$

where:

C = Courant number (dimensionless);
V = flow velocity (ft/s);
c = wave celerity (ft/s);
Δx = grid size resolution (ft); and
Δt = time step (s).

To preserve stability, a conservative maximum Courant number (C_{max}) less than or equal to 0.6 is imposed on the floodplain cell solution. This setting forces a reduction in time step if the stability threshold is approached as the solution progresses. A 5-ft grid resolution (Δx) is used to describe the surface topography of PBNP (Section 4.1.3). The default time step (Δt) of FLO-2D PRO is 30 s (FLO-2D, 2013). Violation of the CFL condition was a consideration for the PBNP FLO-2D PRO model. FLO-2D PRO internally modified the time step until the specified CFL condition (i.e., Equation 4.1) was met. The typical minimum time step during peak LIP runoff flows at PBNP was on the order of 0.01 s.

A minimum depth of flow of 0.01 ft was imposed across the computational elements to prevent small flow oscillations from unnecessarily increasing the computational time. As the PBNP LIP runoff model is primarily concerned with maximum flooding and therefore water depths greater than 0.01 ft, this modification was assumed to be valid.

A nonzero storage volume must be applied to each grid cell for FLO-2D PRO to compute a solution. A storage depth of 0.01 ft was applied to all grid cells since 0.01 ft is small in comparison to the LIP rainfall of 12.8 in. over 1 hr. This artificial abstraction was assumed to have a negligible effect on the final results.

Artificial viscosity and change of flow depth tolerance were not required to preserve numerical stability of the solution. Coefficients for these terms were set to zero.

The CFL condition was satisfied for all model simulations. Thus, all criteria were met for a successful FLO-2D PRO model application.

4.1.9 Model Results

The direct drainage area for PBNP is mapped on Figure 4.6. The drainage area includes the power block and extends north and west, extending across the northern portion of the switchyard. In general, runoff is directed west to east, around the PAB and TB. Surface runoff ultimately flows around the north and south sides of the CWPH and exits the site to the Lake.

Two scenarios were considered (A and B), as defined in Section 4.1.7. The maximum flow depths and peak WSELs (in ft-Plant Datum and ft-NAVD88) for Scenario A and Scenario B at the 33 POIs are listed in Table 4.2. Maximum flow depths are mapped for the PBNP power block on Figure 4.7 (Scenario A) and Figure 4.8 (Scenario B). Since the CWPH wave barriers partially obstruct the flood relief pathways to the Lake, the runoff takes longer to exit the site during Scenario B. Accordingly, the maximum ponded levels

at the east TB and CWPH are higher in Scenario B than Scenario A. Scenario A and Scenario B produced similar maximum flood levels for POIs at other locations. In general, the third quartile and fourth quartile hyetographs resulted in the maximum flood elevations, with maximum flow depths up to +2.1 ft at the CWPH for the fourth quartile LIP event. A flow depth time series at TB Door 13 (see Figure 4.5 for location) for LIP Scenario B, typical of the TB and CWPH POIs, is shown on Figure 4.9. The peak flow depth (i.e., 2.6 ft) is reached near the end of the 1-hr event; the flow depth drops to less than 1 in. after an additional 2 hr (i.e., approximately 3 hr from the beginning of the LIP event).

4.2 Riverine Flooding

PBNP is located on Lake Michigan and there are no major streams or rivers that contribute to flooding at the site. The only contributing runoff drainage area to PBNP is less than 1 mi^2; there are no adjacent surface water run-ons to the site. Thus, the riverine PMF is not applicable to PBNP.

4.3 Dam Breaches and Failures

There are no dams located upstream or downstream of PBNP; therefore, there is no potential for dam breach-related flooding.

4.4 Probable Maximum Storm Surge

A computer-based numerical model is used to estimate the probable maximum storm surge (PMSS) and associated wave effects from a suite of theoretical design storms. The numerical model is developed using the Delft3D Version 4.00.01 software package (Deltares, 2011). The synthetic probable maximum windstorm (PMWS) events are developed in accordance with applicable guidance documents (e.g., ANSI/ANS, 1992; NRC, 2011; NRC, 2013a), which provide the basis for the site-specific storm methodology.

The sections below describe the PMSS evaluation process at PBNP:

- Description of the Delft3D modeling system and processes (Sections 4.4.1, Section 4.4.2 and Section 4.4.3);
- Development of the numerical surge model and physical parameters (Section 4.4.4);
- Selection of numerical parameters (Section 4.4.5);
- Determination of antecedent Lake levels (Section 4.4.6);
- Development of design synoptic PMWS events suite (Section 4.4.7);
- Calibration and validation of the numerical surge model (Section 4.4.8);
- Description of PMSS methodology (Section 4.4.9); and
- PMSS and wave runup maximum WSEL results (Section 4.4.10).

4.4.1 Methodology Overview

The PMSS is simulated with a two-dimensional, depth-averaged unsteady flow characterizing storm surge and lake currents with Delft3D-FLOW Version 4.00.04.757 (Deltares, 2011). The Navier-Stokes equations for incompressible flow are solved under the shallow water and Boussinesq assumptions. These equations

are reduced to an implicit finite difference approximation through the Crank-Nicholson numerical scheme (Deltares, 2014a). The simplifications incorporated into Delft3D-FLOW allow for shoaling within shallow water. A detailed review of Delft3D benchmarking test cases is presented in Walstra and Koster (2006).

Wave transformation in Delft3D-WAVE is performed using Simulating WAves Nearshore (SWAN). SWAN is a spectral wave model that evaluates the refracted wave height and wave angle based on a spectrum of waves using linear wave theory (Booij et al., 1999; Deltares, 2014b). The SWAN model accounts for (refractive) wave propagation due to current and depth and represents the physical processes of wave generation by wind, dissipation due to whitecapping, bottom friction, depth-induced wave breaking, and nonlinear wave-wave interactions (both quadruplets and triads) explicitly with state-of-the-art formulations (Booij et al., 1999; Deltares, 2014b). Wave blocking by currents is also explicitly represented in the model. The SWAN model is based on the discrete spectral action balance equation and is fully spectral (across all directions and frequencies). The latter implies that short-crested random wave fields propagating simultaneously from widely different directions can be accommodated (e.g., a wind sea with superimposed swell). SWAN computes the evolution of random, short-crested waves in coastal regions with deep, intermediate, and shallow water depths and ambient currents.

For these analyses, the Delft3D-FLOW and Delft3D-WAVE modules were used to simulate the coupled effects of flow movement (i.e., storm surge) and wave propagation (i.e., wave spectra, height, period, and setup) through a water body (i.e., Lake Michigan and Lake Huron) when acted upon by external forcing functions (i.e., wind and atmospheric pressure fields). The physical features of the numerical model were created from regional and local bathymetry and topography. The model was calibrated and validated to observed historical windstorms (December 1, 1985; December 2, 1990; and October 25, 2010). The antecedent Lake level (i.e., 100-yr high Lake level) is included in the numerical model.

For these analyses, the design synoptic windstorm event is selected in accordance with applicable guidance documents (e.g., ANSI/ANS, 1992; NRC, 2011; NRC, 2013a). ANSI/ANS (1992) and NRC (2011) state the following storm surge combination applies to coastal locations:

- PMSS with wind-wave activity and
- Lesser of the 100-yr or the maximum controlled water level in the enclosed body of water.

This combination event was evaluated for the PMWS occurring coincident with the 100-yr recurrence monthly average Lake level to determine the peak PMSS WSEL at PBNP.

4.4.2 Development of Model Domain

The numerical model used a Cartesian coordinate system (Geographic Coordinate System [GCS] NAD27 Albers projection). The vertical datum of the model was set so that the 0 m-Model Datum was equivalent to the 100-yr high Lake level (Section 4.4.6).

A detailed numerical model was created from local and regional bathymetric and topographic data sources:

- Lake Michigan and Lake Huron bathymetry (NOAA, 1999a; NOAA, 1999b) was obtained from the National Oceanic and Atmospheric Administration (NOAA) National Geophysical Data Center (NGDC) website with an approximate resolution of 90 m (NOAA, 2014a). The horizontal datum is referenced to the World Geodetic System of 1984, and the vertical datum is referenced to the IGLD85 with a low water datum of +176.0 m.
- The 1/3-Arc Second (approximately 10 m) National Elevation Dataset (NED) was obtained from the U.S. Geological Survey (USGS) National Map Viewer (USGS, 2011). One NED (n45w88_13) covers the PBNP site area. It is referenced to GCS m-NAD83 (horizontal datum) and m-NAVD88 (vertical datum).
- Recent site topographic and bathymetric surveys were conducted (NEE, 2014a). Horizontal coordinates reference WISCRS of Manitowoc County (in ft) and elevations are referenced to ft-Plant Datum.

These data required conversion to consistent horizontal (GCS NAD27 Albers projection) and vertical (100-yr high Lake level) datums and units for use as the base geometry for the numerical model.

Due to the size, bathymetry and geometry of the Great Lakes, six Delft3D-FLOW domains were necessary. The coarsest grids represent conditions over Lake Michigan and Lake Huron. The extents of the domains were chosen to include the surrounding coast up to approximately 66 ft (20 m) above the 100-yr Lake level. A horizontal resolution of 6,562 ft (2,000 m) was chosen to accurately represent the bathymetric contours of Lake Michigan and Lake Huron away from PBNP (Figure 4.10).

Near PBNP, a grid resolution of 19.0 ft (5.8 m) was determined to be acceptable to represent PBNP's coastline and nearshore bathymetry (Figure 4.11). In order to resolve the Delft3D-FLOW computations from the coarse grids to the PBNP nearshore grid, refinements of 1 to 7 were applied. A total of three grids were used to pass boundary conditions from the coarser lake grids to the PBNP nearshore grid.

As discussed in Deltares (2014a), orthogonality, aspect ratio, M (horizontal) smoothness, and N (vertical) smoothness limitations cannot be violated by grids using Cartesian coordinates. An evaluation of the estimated Courant number was calculated for each grid to determine the appropriate numerical time step to be used in Delft3D-FLOW simulations. Based on the resolution of the finest grid, a time step of 0.05 min (3 s) was chosen to meet Delft3D-FLOW Courant number (Equation 4.1) limitations (Deltares, 2014a).

The entire spatial domain of Lake Michigan and Lake Huron was enclosed within the coarse Delft3D-FLOW and Delft3D-WAVE grids. Open model boundaries, called "water-water" boundaries (Deltares, 2014a), are created when the simulation domain covers only a portion of an open body of water. Boundary condition forcing and reflectivity must be considered when a model domain includes open boundaries. As no open boundaries exist in the Delft3D model, there was no need to specify open water boundary conditions. Delft3D-FLOW grids were joined along each boundary through domain decomposition (Deltares, 2014a). A total of 12 domain decomposition boundaries were created. Delft3D-WAVE domain resolutions and extents were identical to the Delft3D-FLOW domains. Delft3D-WAVE requires nested grids; therefore, each grid covers the extents of the finer, nested grids.

4.4.3 Model Processes

4.4.3.1 Delft3D-FLOW Processes

In Delft3D-FLOW, the hydrodynamics of storm surge conditions are simulated by solving the Navier-Stokes equations for incompressible free surface flow. The Navier-Stokes equations are reduced to two-dimensional, depth-averaged unsteady flow characterizing storm surge and ocean currents with Delft3D-FLOW Version 4.00.04.757 (Deltares, 2011). The Navier-Stokes equations for incompressible flow are solved under the shallow water and Boussinesq assumptions. These equations are reduced to an implicit finite difference approximation through the Crank-Nicholson numerical scheme (Deltares, 2014a). The simplifications incorporated in Delft3D-FLOW allow shallow water shoaling and inundation to be explicitly simulated. A detailed review of Delft3D benchmarking test cases is presented in Walstra and Koster (2006).

Delft3D-FLOW can be used to explicitly simulate open water boundary forcing, bed roughness boundary conditions, air-water boundary forcing through atmospheric inputs (wind and pressure), astronomic forcing on the water column, and direct flow inputs or outputs (inflows from streams, rivers, etc.).

4.4.3.2 Delft3D-WAVE Processes

There are three generations of wave models available to compute the sea surface state in Delft3D-WAVE (i.e., SWAN) (Deltares, 2014b). First generation wave models do not consider nonlinear wave interactions. Second generation models parameterized these interactions and include the coupled hybrid and coupled discrete formulations. Third generation models explicitly represent all the physics relevant for the development of the sea state in two dimensions, without assumptions regarding the spectral space. Further, energy terms are described explicitly with the addition of bottom dissipation and reflection, diffraction, and refraction terms. For PBNP, the model computes the sea state from the hurricane using the third generation mode of physics.

The Delft3D-WAVE computations accounted for the following processes (Deltares, 2014b): depth-induced breaking, nonlinear triad interactions, bottom friction, wind growth, whitecapping, refraction, and frequency shift.

4.4.3.3 Coupled Delft3D-FLOW and Delft3D-WAVE Model

To account for the effect of flow on the waves (via setup, current refraction, and enhanced bottom friction) and the effect of waves on current (via forcing, enhanced turbulence, and enhanced bed shear stress), an online coupling of Delft3D-WAVE with Delft3D-FLOW was performed. The Delft3D-WAVE model has a dynamic interaction with the Delft3D-FLOW module (i.e., two-way wave-current interaction). Through this dynamic coupling, both the effect of waves on current and the effect of flow on waves were modeled. The Delft3D-FLOW and Delft3D-WAVE models were coupled every 30 min throughout the simulation.

4.4.4 Physical Parameters and Model Constants

The following physical parameters are values associated with the conditions and properties of the physical world used to represent surge and wave processes in the numerical model.

4.4.4.1 Delft3D-FLOW Physical Parameters and Model Constants

The physical parameters and constants of the model were selected as follows:

Gravitational Acceleration – A constant gravitational acceleration of 32.2 ft/s^2 (9.81 m/s^2) was used. The National Geodetic Survey, Office of Charting and Geodetic Services, establishes and maintains the basic national horizontal, vertical, and gravity networks of geodetic control (NOAA, 1986). The gravitational constant varies slightly across the study area; however, a constant value of 32.2 ft/s^2 (9.81 m/s^2) was selected for the model.

Water Density – A freshwater density of 62.4 pcf (1,000 kg/m^3) was used (Street et al., 1996).

Air Density – An air density of 0.08 pcf (1.28 kg/m^3) was used (Street et al., 1996).

Wind Drag Coefficient – The wind drag coefficient is dependent on the wind speed, since the roughness of the water surface varies directly with wind speed. Previous formulations for wind drag were evaluated (Liu, 1965; Wuest and Lorke, 2003; Jensen et al., 2012; Deltares, 2014a). The wind drag formulation was evaluated as a calibration parameter so that the best fit was selected.

Bottom Roughness – Calibrated, uniform Manning's roughness values were supplied to the Delft3D-FLOW model.

Wall Roughness – Due to the large size of the four coarsest Delft3D-FLOW domains, the free slip condition was used; in other words, zero tangential shear stress was applied at the model walls. In very large-scale hydrodynamic simulations, the tangential shear stress for all lateral boundaries or vertical walls can be safely neglected (Deltares, 2011).

Horizontal Eddy Viscosity and Diffusivity – In Delft3D-FLOW, for the Reynolds-averaged Navier-Stokes equations, the Reynolds stresses are modeled using the eddy viscosity concept. The horizontal eddy viscosity is mostly associated with the contribution of horizontal turbulent motions and forcing that are not resolved (sub-grid scale turbulence) either by the horizontal grid or a priori removed by solving the Reynolds-averaged shallow water equations (Deltares, 2011). The value for both horizontal eddy viscosity and horizontal eddy diffusivity depends on the flow and the grid size of the simulation. For large tidal areas with a grid that is hundreds of meters or more, the values for eddy viscosity and eddy diffusivity typically range from 0 ft^2/s to 1,076 ft^2/s (0 m^2/s to 100 m^2/s). Herbert (1987) found that horizontal eddy viscosity is approximately 538 ft^2/s (50 m^2/s) for the Gulf Stream due to internal waves. Therefore, 538 ft^2/s (50 m^2/s) was used in the overall model domain for horizontal eddy viscosity and 538 ft^2/s (50 m^2/s) was used for horizontal eddy diffusivity. For the fine grid model domains, a horizontal eddy viscosity of 54 ft^2/s (5 m^2/s) was used. Deltares (2014a) recommends a typical value of 11 ft^2/s to 108 ft^2/s (1 m^2/s to 10 m^2/s) for grid sizes on the order of 10 m. Secondary flow, which adds the influence of helical flow to the momentum transport, was ignored due to the large size of the domain area as these flows are insignificant.

4.4.4.2 Delft3D-WAVE Physical Parameters and Model Constants

The physical parameters and constants of the model were selected as follows:

North Convention – The direction of north with respect to the x-axis (i.e., Cartesian convention). The default value of 90 degrees (i.e., x-axis pointing east) was selected for the model (Deltares, 2014b).

Wind and Wave Convention – The nautical convention for wind and wave direction was used, which measures the wind vector, so that the angle is the direction from which the waves are coming or from where the wind is blowing (Deltares, 2014b).

Gravitational Acceleration – A constant gravitational acceleration of 32.2 ft/s^2 (9.81 m/s^2) was used, consistent with the value selected for the Delft3D-FLOW model.

Water Density – A freshwater density of 62.4 pcf (1,000 kg/m^3) was used, consistent with the value selected for the Delft3D-FLOW model.

Wave Forces – With the integration of the fully spectral SWAN model within the Delft3D model, it is possible to compute the wave forces on the basis of the energy wave dissipation rate or on the gradient of the radiation stress tensor (Deltares, 2014b). The radiation stress tensor describes the additional forcing due to the presence of the waves, which changes the mean depth-integrated horizontal momentum in the fluid layer. As a result, varying radiation stresses induce changes in the mean surface elevation (wave setup) and the mean flow (wave-induced currents) (Deltares, 2014b). The wave forces were computed by the radiation stress tensor to account for wave setup in the model.

Depth-Induced Breaking – The process of depth-induced breaking is an improved version of the model proposed by Battjes and Janssen (1978). The model for the rate of dissipation is defined by the alpha and gamma parameters. These physically based values were treated as calibration parameters.

Nonlinear Triad Interactions – In Delft3D-WAVE nonlinear wave-wave interaction computations are carried out with the Discrete Interaction Approximation of Hasselmann et al. (1985). The model is defined by the alpha and beta parameters. These physically based values were treated as calibration parameters. Similar to results presented in Alkyon (2003), these parameters showed no sensitivity to the model calibration.

Bottom Friction – The JOint North Sea WAve Project (JONSWAP) bottom friction formulation was used to represent the bottom friction for wave computations. The JONSWAP method is a semi-empirical methodology developed by Hasselmann et al. (1973) which uses the C_{JON} parameter to define the bottom roughness. This value was considered a calibration parameter.

4.4.5 Numerical Parameters

4.4.5.1 Delft3D-FLOW Numerical Parameters

Advection Scheme for Momentum – In Delft3D-FLOW, three primary algorithms are available: Cyclic, Waqua, and Flooding schemes. In the Lake Michigan and Lake Huron storm surge model, the Cyclic method was used.

Threshold Depth – The threshold depth is the depth above a grid cell which is considered to be wet. The threshold depth must be defined in relation to the change of the water depth per time step in order to prevent the water depth from becoming negative in just one simulation time step (Deltares, 2014a). In order to prevent this, the threshold depth is calculated in such a way that it is larger than the maximum distance the water level can fall over a half time step (the time which the flooding and drying algorithm uses). A threshold depth of 0.03 ft (0.1 m) was chosen based on numerical stability tests.

4.4.5.2 Delft3D-WAVE Numerical Parameters

Spectral Space – The amount of diffusion of the implicit scheme in the directional space through the Directional space (CDD) parameter and frequency space through the Frequency space (CSS) parameter (Deltares, 2014b).

Directional Space – A value of CDD = 0 corresponds to a central scheme and has the largest accuracy (diffusion ≈ 0), but the computation may more easily generate spurious fluctuations. A value of CDD = 1 corresponds to an upwind scheme and it is more diffusive and therefore preferable if (strong) gradients in depth or current are present (Deltares, 2014b). The default value of CDD = 0.5 was used in the model.

Frequency Space – A value of CSS = 0 corresponds to a central scheme and has the largest accuracy (diffusion ≈ 0), but the computation may more easily generate spurious fluctuations. A value of CSS = 1 corresponds to an upwind scheme and it is more diffusive and therefore preferable if (strong) gradients in current are present (Deltares, 2014b). The default value of CSS = 0.5 was used in the model.

Accuracy Criteria – These options influence the criteria for terminating the iterative procedure in the Delft3D-WAVE computation (for numerical convergence criteria). In the PBNP storm surge model, Deltares (2014b) recommended numerical accuracy criteria were sufficient for maintaining numerical stability.

Temporal Computation Mode – Delft3D-WAVE allows for wave computations to be performed in stationary mode, which conservatively assumes infinite time for development of wave fields from a static constant wind distribution and nonstationary mode, which explicitly accounts for time allowed for development of wave fields (Deltares, 2014b). Numerical tests run on the Delft3D-WAVE model for Lake Michigan and Lake Huron indicated that the stationary computational method reproduced observed wave distributions with greater accuracy than the nonstationary method. The stationary mode is valid in a case of waves with a relatively short residence time in the computational area under consideration (i.e., the travel time of the waves through the region should be small compared to the time scale of the geophysical conditions, such as the wave boundary conditions, wind, tides, and storm surge) (Deltares, 2014b).

4.4.6 Antecedent Lake Level

Delft3D-FLOW and Delft3D-WAVE simulations of PMSS at PBNP used the 100-yr high Lake level as the antecedent condition. Simulations of the low water effects at PBNP used the 100-yr low Lake level as the antecedent water level.

The 100-yr recurrence monthly average high and low water levels near PBNP were derived using a log-Pearson Type III statistical analysis. The estimated water levels were determined from two NOAA water level recording stations near PBNP: Kewaunee, Wisconsin (Station ID 9087068) (NOAA, 2014c) and Milwaukee, Wisconsin (Station ID 9087057) (NOAA, 2014h). Table 4.3 summarizes the results of the frequency analysis.

The most conservative high and low 100-yr Lake levels from Table 4.3 were used in subsequent analyses: a 100-yr recurrence monthly average high water level of +583.1 ft-NAVD88 (+1.8 ft-Plant Datum) was used in the PMSS and seiche evaluations[4] and a 100-yr recurrence monthly average low water level of +575.6 ft-NAVD88 (-5.7 ft-Plant Datum) was used in the low water effects evaluation.

4.4.7 Probable Maximum Windstorm Development

The synthetic probable maximum synoptic events are developed in accordance with applicable guidance documents (ANSI/ANS, 1992; NRC, 2011), which provide the basis for the site-specific storm methodology.

The spatially and temporally variable wind and pressure fields for each simulation were created using historically extreme storm events. The wind and pressure data for the probable maximum synoptic events were provided in 3-hr and 6-hr average intervals utilizing the NWS model reanalysis data (NOAA, 2014jj; NOAA, 2014kk; NOAA, 2014ll) and in 1-hr increments based on manual analysis for synthetic squall line events.

Most of the historical instances of sustained winds over 50 mph (22 m/s) in the Great Lakes region are associated with deep low pressure areas which move through the region from the southwest to the northeast. The general synoptic pattern is one in which the deep low pressure area results in a strong pressure gradient between the storm's center and the high pressure region to the north or west. Strong winds result from strong gradients. When the gradient is extreme and lasts for days, very strong winds can persist for an extended period. Due to the preferred track directions, the vast majority of the strongest sustained winds occur from the south or southwest. Low pressure centers as low as 955 mbar (equivalent to a Category 3 hurricane) have occurred near PBNP.

In other cases, tropical systems making landfall along the Gulf of Mexico coast or U.S. east coast move inland (e.g., Hurricane Hazel in 1954, Hurricane Sandy in 2012). By the time these storms reach the Great Lakes region, they have transitioned into extratropical cyclones; however, the general circulation and deep low pressure center persist. Thus, strong winds can remain. The preferred track direction of these storms is to the northwest, north, or northeast.

Three-hr or 6-hr wind and pressure data for 31 historical synoptic events from 1907 to 2012 were evaluated, which produced 45 maximized, potential synoptic PMWS scenarios (Table 4.4). Each scenario was maximized and transposed to occur directly over PBNP. Since pressure gradients are directly linked to strong winds, the analysis inherently captured the worst-case wind and pressure patterns that could reasonably be expected at PBNP. A comparison to regional weather station data revealed that the storms listed in Table 4.4 significantly exceeded a 100,000-yr return period (i.e., 10^{-5} annual frequency). When

[4]The antecedent water level for all calibration and validation simulations was the present-day Lake level.

combined independently with the 100-yr recurrence monthly average Lake level (i.e., less than 10^{-2} annual frequency), the combined PMSS event will have an annual frequency less than 10^{-6}.

4.4.8 Storm Surge Model Calibration

4.4.8.1.1 Calibration Overview

Calibration and validation of a storm surge model are critical to the success of PMSS modeling, the defensibility of the technical approach, and ultimately to acceptance of PMSS results. As required by NRC (2011), the parameters of a given model may be calibrated using data of relatively large historical storm events and then validated on comparable storm events not used in the calibration. To verify the prediction capability of the coupled Delft3D-FLOW and Delft3D-WAVE model, calibration and validation are performed by comparing the model water level and wave outputs with measured historical storm surges and significant wave heights (H_S) for three independent storm events.

4.4.8.1.2 Historical Synoptic Events

The model is calibrated and validated with observed historical storms (December 1, 1985; December 2, 1990; and October 25, 2010). The October 25, 2010 event was constructed at a 3-hr temporal resolution. The December 1, 1985 and December 2, 1990 events were constructed at a 6-hr temporal resolution based on availability of historical meteorological observations.

4.4.8.1.3 Historical Surge and Wave Observations

Observed storm surge time series recorded at NOAA tide stations (NOAA, 2014b through NOAA, 2014r) were used to calibrate the simulated storm surges (Table 4.5; Figure 4.12). The observed wave characteristics time series recorded at NOAA buoy stations (NOAA, 2014s through NOAA, 2014gg) were used to calibrate the simulated wave fields (Table 4.6; Figure 4.13).

4.4.8.1.4 Selection of Calibration / Validation Events

The October 25, 2010 storm was selected as the calibration event due to the finer temporal resolution of the atmospheric wind and pressure data (i.e., 3 hr versus 6 hr), as well as the availability of observed storm surge and wave characteristics (Table 4.5; Table 4.6). The remaining historical storms discussed above were used as model validation.

4.4.8.1.5 Calibration Methodology

A typical calibration procedure consists of three steps that are repeated until the simulation results are deemed accurate enough for the desired application: (1) running the model; (2) crosschecking the results against actual measured data; and, if necessary, (3) adjusting the model parameters. In each case, simulation results are compared with measured (historical) observations obtained with other parameter values. Knowledge is gained about the sensitivity of the different parameters in the model.

The objective functions Root Mean Square Error (RMSE) and Nash-Sutcliffe model quotient efficiency (NSE) were used to maintain an objective view of model calibration adjustments (i.e., Step (3) described above).

$$RMSE = \sqrt{\frac{\sum_{t=1}^{n}(y_0^t - y_m^t)^2}{n}} \qquad \text{Equation 4.2}$$

$$NSE = 1 - \sum_{t=1}^{n}\frac{(y_0^t - y_m^t)^2}{(y_0^t - y_{bar_0})^2} \qquad \text{Equation 4.3}$$

where:

t = time step;
n = total number of time steps;
y_0 = observed value;
y_m = simulated value; and
y_{barO} = average of all observed values.

The NSE provides a quantitative measure of model performance on the interval (-∞, 1) (Nash and Sutcliffe, 1970). Values closer to 1 suggest better model performance, whereas values closer to -∞ indicate poor model performance. An NSE value of 0 suggests the model's predictive power is equal to a model that simply reproduces the average of the observed time series. Numerical models producing an NSE value of 0 or less add no additional value. An NSE value of 1 suggests an ideal model that has no error in reproduction of observed data. Values between 0 and 1 suggest that use of the model adds value to the prediction; however, the transformation is not ideal. The RMSE represents the sample standard deviation between simulated and observed values.

The calibration and validation of the PBNP Delft3D-FLOW and Delft3D-WAVE model were completed as follows:

- Selected an historical calibration event based on availability of observed storm surge data, the available resolution of the wind and pressure forcing data, and the magnitude of the event.
- Performed a series of sensitivity simulations of the wind drag coefficient for the calibration event. Calculated the objective functions RMSE and NSE of the WSEL time series to determine the calibration value for Delft3D-FLOW.
- Performed a series of sensitivity simulations of the Manning's roughness for the calibration event. Calculated the objective functions RMSE and NSE of the WSEL time series to determine the calibration value for Delft3D-FLOW.
- Performed a series of sensitivity simulations of the Delft3D-WAVE solution technique to determine if a stationary or nonstationary solution produces more ideal results. Calculated the objective functions RMSE and NSE of H_S time series to determine the appropriate solution for Delft3D-WAVE. Reviewed peak wave period (T) and wave direction to verify model predictions.
- Performed a series of sensitivity simulations on the C_{JON} bottom friction coefficient. Calculated the objective functions RMSE and NSE of H_S time series to determine the calibration value for Delft3D-WAVE. Reviewed T and wave direction to verify model predictions.

- Performed a series of sensitivity simulations of the depth-induced breaking γ parameter. Calculated the objective functions RMSE and NSE of H_S time series to determine the calibration value for Delft3D-WAVE. Reviewed T and wave direction to verify model predictions.
- Ran the remaining events as validation to determine if the final calibration parameter values are acceptable for storm surge modeling. Observed wave data exist only for the 2010 event; therefore, only WSEL (i.e., Delft3D-FLOW) validation was performed.

4.4.8.1.6 Calibration Results

Wind Drag Formulation – Several formulations for the wind drag coefficient over enclosed bodies of water have been proposed throughout the scientific literature. Liu (1965) studied wind waves generated over the Lake and proposed an empirical wind drag relationship. Jensen et al. (2012) similarly developed a wind drag relationship for the Lake through model calibration. Wuest and Lorke (2003) performed experiments on enclosed bodies of water and proposed an empirical wind drag relationship. For comparison, the default wind drag relationship proposed in Deltares (2014a) was also evaluated.

Documentation of all model calibration iterations is presented in Table 4.7. Final calibration results are presented for NOAA Station ID 9087068 (Figure 4.14) and NOAA Buoy 45022 (Figure 4.15). Storm surge validation results are presented on Figure 4.16 and Figure 4.17, respectively. The following sections discuss the selection of final model calibration parameter values.

The ambient ice cover of the Great Lakes was evaluated for each calibration and validation event. Wang et al. (2012) demonstrate that ice cover was minimal for the 2010 calibration event. Assel (2014) demonstrates that ice cover for the 1985 and 1990 validation events was also minimal. The presence of some ice cover may have a conservative effect on the wind drag coefficient (Jensen et al., 2012).

Through calibration to observed WSEL data for the 2010 event, it was determined that the relationship proposed in Liu (1965) best reproduced the observed WSELs (Table 4.7).

Bed Roughness – Bed roughness in the Manning's roughness formulation was treated as a calibration parameter; therefore, the final accepted value was determined through calibration. An initial value of 0.02 was selected based on discussion in Deltares (2014a). The roughness value was increased in each run. The RMSE and NSE objective function values did not significantly change between 0.03 and 0.04; therefore, a final value of 0.04 was selected.

JONSWAP Bottom Friction Coefficient (C_{JON}) – The bottom friction model selected for Delft3D-WAVE is the empirical model of JONSWAP. The Delft3D-WAVE User Manual suggests $C_{BOTTOM} = C_{JON} = 0.410$ ft^{2}s^{-3} (0.038 m^{2}s^{-3}) for swell conditions and $C_{JON} = 0.721$ ft^{2}s^{-3} (0.067 m^{2}s^{-3}) for fully developed wave conditions in shallow water. For the computational wave grid in this calculation, the bottom friction parameter (C_{JON}) is determined using model calibration, using $C_{JON} = 0.721$ ft^{2}s^{-3} (0.067 m^{2}s^{-3}) for the initial trial run.

The JONSWAP bottom friction coefficient was varied within the acceptable parameter range (0.06 to 0.075) (Deltares, 2014b). The results show no sensitivity to the C_{JON} parameter (Figure 4.18). Alkyon (2003) similarly performed sensitivity analysis of C_{JON} over several case studies and reached the same conclusion.

Depth-Induced Breaking α Parameter – The depth-induced breaking α parameter was found to be not sensitive to the prediction of wave characteristics. This conclusion is similar to that presented in Alkyon (2003). This parameter was left at the default Delft3D-WAVE parameter value (Deltares, 2014b).

Depth-Induced Breaking γ Parameter – The depth-induced breaking γ parameter was varied within the acceptable parameter range (0.55 to 1.2) (Deltares, 2014b). As the depth-induced breaking only affects waves in shallow water, only results from Buoy 45022 were evaluated. The lower limit of the depth-induced breaking parameter (0.55) produced the most statistically significant calibration results (Table 4.8 for overall results and Figure 4.19 and Figure 4.20 for results at Buoy 45022).

Nonlinear Triad Interactions – Similar to results presented in Alkyon (2003), the parameters controlling the simulation of nonlinear triad interaction were not sensitive in the prediction of wave fields. These parameters were left at the default Delft3D-WAVE parameter values (Deltares, 2014b).

4.4.8.1.7 Summary of Final Calibrated Model Parameters

A summary of all the parameters used in the Delft3D-FLOW and Delft3D-WAVE models is presented in Table 4.9 and Table 4.10.

4.4.9 Probable Maximum Storm Surge Methodology

4.4.9.1 Overview of Probable Maximum Storm Surge Methodology

The following steps were followed to evaluate the PMSS at PBNP:

- Simulated each hypothetical maximized and transposed synoptic event with the calibrated Delft3D-FLOW and Delft3D-WAVE model discussed in Section 4.4.8.
- Post-processed model results of each scenario to determine the time series of the PMSS SWL, H_S, and T.
- Calculated the runup for each scenario using an empirical formulation for wave runup on a gently-sloping impermeable surface (USACE, 2008). The scenario that produced the peak WSEL (i.e., PMSS SWL plus coincident wave runup) was determined to be the bounding PMWS scenario.
- Simulated the critical PMWS event(s) with the critical peak wind location while applying the overland to overlake and averaging duration adjustments to the PMWS meteorological forcing data to determine the PMSS.
- Calculated the wave runup on near vertical slope to determine the peak WSEL.
- Estimated the durations of flooding for which the peak WSEL was above +588.3 ft-NAVD88 (+7.0 ft-Plant Datum), +589.3 ft-NAVD88 (+8.0 ft-Plant Datum), and +590.3 ft-NAVD88 (+9.0 ft-Plant Datum) from the bounding synoptic PMWS event.

4.4.9.2 Simulation of Maximized Synoptic Events

Each hypothetical maximized and transposed synoptic event was simulated with the calibrated Delft3D-FLOW and Delft3D-WAVE models discussed in Section 4.4.8. The results of the Delft3D

simulations were evaluated to the north and south of the CWPH to determine the bounding event and location (Figure 4.21).

4.4.9.3 Calculation of Runup on an Impermeable Gently-Sloping Surface

Runup was calculated for wave characteristics simulated at Observation Points 1 and 2 (Figure 4.21). Figure 4.22 demonstrates the PMWS-induced waves break completely along the beach and discharge flumes east of the CWPH and TB.

Wave runup was calculated for all potential PMSS scenarios using the empirical formula for runup on a smooth, impermeable slope as presented in USACE (2008). The equations for the calculation of runup are as follows:

$$\zeta = \frac{\tan(\phi)}{\sqrt{\frac{H_0}{L_0}}} \qquad \text{Equation 4.4}$$

$$\frac{R_{u\,2\%}}{H_s} = (A\zeta + B)\gamma_r\gamma_b\gamma_h\gamma_\beta \qquad \text{Equation 4.5}$$

where:

ζ = breaker number or Iribarren number (dimensionless);
ϕ = beach slope (radians);
H_0 = deep water wave height (m);
L_0 = deep water wave length (m);
$R_{u\,2\%}$ = runup level (m) exceeded by 2 percent of breaking waves;
H_s = significant wave height (m);
A, B = coefficients dependent on ζ (dimensionless);
γ_r = surface roughness reduction factor (dimensionless);
γ_b = berm influence reduction factor (dimensionless);
γ_h = non-Rayleigh distribution reduction factor (dimensionless); and
γ_β = angle of incidence reduction factor (dimensionless).

Coefficients A and B in Equation 4.5 are dependent on wave steepness (ζ). The base equation is presented for runup on a smooth surface. The coefficient γ_r accounts for wave runup reductions due to the presence of riprap (i.e., rough surface), such as that present at PBNP. The total combined reduction factor (i.e., the product of $\gamma_r\gamma_b\gamma_h\gamma_\beta$) was set to be greater than or equal to 0.5. Calculated wave runup is added to the simulated PMSS SWL to determine the peak WSEL resulting from each scenario.

4.4.9.4 Sensitivity of Maximum Wind Location

An additional sensitivity of the PMWS scenario was conducted by shifting the PMWS wind and pressure fields one and two meteorological grid cells (horizontal resolution: approximately 20 mi [32 km]) east of PBNP to determine if peak winds further over the Lake (rather than directly over PBNP) would produce a higher storm surge.

4.4.9.5 Overwater Wind Speed Adjustment

The bounding synoptic event wind speeds developed were representative of overland wind speeds. As events observed occurring overland are transposed over Lake Michigan and Lake Huron, an adjustment is applied to account for the estimated overwater wind speeds of the same event.

As discussed in Schwab and Morton (1984), the wind speed developed over open water often differs from that developed overland. Four relationships between overland and overwater wind speeds are proposed in Schwab and Morton (1984) (Figure 4.23). The relationship in Equation 4.6 was determined to be the most appropriate by the authors when evaluated against observed wind speed data:

$$U_W = C_{ij} U_L \qquad \text{Equation 4.6}$$

where:
U_W = overwater wind speed (m/s);
U_L = overland wind speed (m/s); and
C_{ij} = constant (dimensionless) that is a function of the air-water temperature difference (ΔT) and U_L.

NOAA Buoy 45007 was used to compile 10 yr (2004 to 2013) of observed air and water temperature observations. The distribution of ΔT was calculated (Figure 4.24). The 95 percent exceedance value of -6° Celsius was conservatively used to determine C_{ij} (Figure 4.23).

A U_L value of 33 ft/s (10 m/s) was assumed as these coefficients are applied to potential PMWS events. A value of 1.42 for C_{ij} was determined from Figure 4.23 and Figure 4.24. The entire PMWS wind field was modified by this constant.

4.4.9.6 Wind Speed Averaging Duration Adjustment

When evaluating wave generation in water bodies of different sizes, different wind speed averaging intervals are appropriate. The USACE Coastal Engineering Manual (CEM) notes that if extreme wind speeds are being considered, wind speeds should be adjusted from the averaging interval of the observation to an averaging time appropriate for wave prediction (USACE, 2008). As per ANSI/ANS (1992), Section 7.2.2.3.4, hourly values of pressure and wind fields should be used for each grid point of the water body. Additionally, the USACE Great Lakes Coastal Flood Study (USACE, 2012) notes that if measured wind data are averaged at different time intervals (U_i) than a 1-hr average (U_{3600}), adjustment to a 1-hr averaging interval is recommended for the wave modeling application. CEM Figure II-2-1 (USACE, 2008, page II-2-4), which also includes the best-fit equations, was used for the wind speed averaging duration adjustment:

$$\frac{U_i}{U_{3600}} = -0.15 \log(t_i) + 1.5334, \; where: 3{,}600 < t_i < 36{,}000 \; seconds \qquad \text{Equation 4.7}$$

where:
U_i = i s wind speed (m/s);
U_{3600} = 1-hr wind speed (i.e., 3600 s wind speed) (m/s); and
t_i = duration of i (s).

For all wind forcing data developed with a 3-hr time step, a constant velocity adjustment for the 3-hr (i.e., t_i=10,800 s) averaging interval was developed as follows:

$$\frac{U_i}{U_{3600}} = -0.15\log(t_i) + 1.5334 = 0.928386 \qquad \text{Equation 4.8}$$

$$\frac{U_{3600}}{U_i} = \left(\frac{U_i}{U_{3600}}\right)^{-1} = 1.077 \qquad \text{Equation 4.9}$$

4.4.10 Storm Surge Results

4.4.10.1 Synoptic Event Screening

Table 4.11 presents the peak WSEL for each synoptic event and the coincident breaking water depth (h), H_S, T, and wave runup (R) calculated for a smooth impermeable sloped surface, based on the methodology described in Section 4.4.9.3. Scenario 13 (i.e., the January 10-12, 1975 event from the southeast direction) produced the highest peak WSEL and was concluded to be the bounding PMWS case (Table 4.11).

4.4.10.2 Probable Maximum Storm Surge Maximum Water Surface Elevations

The overwater wind adjustments and sampling interval adjustments described in Section 4.4.9.5 and Section 4.4.9.6, respectively, were applied to the bounding PMWS synoptic event (i.e., Scenario 13) to determine the PMSS and peak WSEL at PBNP. The results of the PMSS are presented in Table 4.12 and Figure 4.25.

The WSEL at the maximum SWL, shown on Figure 4.25, is lower than plant grade at the CWPH and TB. Thus, no standing water is present at any PBNP POIs during the PMSS event. The location of 100 percent PMSS wave breaking occurred approximately 50 ft (15 m) east of the closest POI, Door 336 on the southern side of the CWPH (Figure 4.22). Therefore, wave runup on a vertical structure was not applicable for PBNP. Rather, the wave runup was calculated using Equation 4.5, as discussed in Section 4.4.9.3. Results of the PMSS and runup calculation are presented in Table 4.12. The runup on a gently-sloping impermeable surface reached a maximum WSEL of +589.7 ft-NAVD88 (+8.4 ft-Plant Datum) (Figure 4.26). The formulation accounted for the effects of surface roughness, berm elevation, and wave refraction on wave runup height; however, the maximum combined reduction factor was limited conservatively to 0.5. However, the lateral landward extent of overtopping is limited by the transfer of kinetic to potential energy as overtopping runup flows over a berm/riprap crest.

Since the PMSS SWL, +585.8 ft-NAVD88 (+4.5 ft-Plant Datum), at the time of maximum PMSS WSEL is slightly below the top of the riprap slope (approximately +586.3 ft-NAVD88 [+5.0 ft-Plant Datum]) on the south side of the CWPH/forebay, the wave runup will overtop the berm and flow towards the CWPH. Additional frictional losses and flow expansion between the riprap slope and CWPH were not considered. Accordingly, the actual maximum WSEL at the wave barrier installed adjacent to CWPH rollup Door 336 is expected to be slightly less than that calculated (+589.7 ft-NAVD88 [+8.4 ft-Plant Datum]). Figure 4.27 shows a map view of the maximum PMSS inundation, including the estimated lateral extent of wave runup overtopping the riprap slope protecting the beach.

The duration of inundation is estimated to be 1020 min, 120 min, and 0 min for +588.3 ft-NAVD88 (+7.0 ft-Plant Datum), +589.3 ft-NAVD88 (+8.0 ft-Plant Datum), and +590.3 ft-NAVD88

(+9.0 ft-Plant Datum), respectively (Figure 4.26). These durations are provided conservatively at the landward edge of the riprap slope and do not consider frictional losses or flow expansion as the overtopped water travels towards the CWPH.

4.5 Seiche

The same computer-based numerical model used in the PMSS evaluation (developed using the Delft3D Version 4.00.01 software package [Deltares, 2011]) was used to estimate the maximum seiche from a suite of theoretical design storms. Synthetic squall line (derecho) events were developed in accordance with applicable guidance documents (e.g., ANSI/ANS, 1992; NRC, 2011; NRC, 2013a), which provide the basis for the site-specific storm methodology.

The maximum seiche at PBNP was evaluated from site-specific maximized squall line (derecho) events moving across the Lake. ANSI/ANS (1992) and NRC (2011) state the following storm surge combination applies to coastal locations:

- Maximum seiche with wind-wave activity and
- Lesser of the 100-yr or the maximum controlled water level in the enclosed body of water.

This combination was evaluated to determine the peak seiche SWL occurring coincident to the 100-yr recurrence monthly average high Lake level at PBNP.

4.5.1 Squall Line Event Development

Historical squall lines (or derechos), which are widespread straight-line windstorms associated with fast-moving bands of severe thunderstorms, were analyzed. The winds in these storms can produce some of the highest instantaneous recorded wind gusts, but last only for a short time (i.e., less than 30 min) at a given location. A squall line can advance hundreds of miles during its lifetime; some squall lines have formed over the U.S. upper Midwest and advanced across the Great Lakes to the U.S. east coast. Squall lines occur exclusively during the warm season, generally from April through August.

Squall lines have multiple characteristics that eliminate them from PMWS consideration (with respect to PMSS):

- Short durations at particular locations due to fast forward speeds;
- It is physically impossible to have two consecutive squall lines over the same region due to the significant time required to recharge the required atmospheric parameters (i.e., at least 12 hr); and
- Squall line events do not occur within low pressure systems or remnant tropical storms (i.e., synoptic events) and would not be considered coincident with those discussed in Section 4.4.7.

Seventeen historical squall lines between 1909 and 2012 were analyzed to develop maximized, transposed squall lines (derechos). These synthetic storms were evaluated for potential seiches independent of the PMSS. Since the squall lines initially move offshore at PBNP, the flooding impact at PBNP will be indirect: the primary storm surge will occur along the eastern and/or southern shorelines of the Lake. The seiche will

then propagate to the west and/or north after the squall line has passed completely over the Lake, due to the water surface gradient induced by pressure and winds of the squall line.

4.5.2 Model Development

The calibrated numerical model developed to evaluate the PMSS was used for the seiche analysis. Refer to Section 4.4.2 through Section 4.4.6 and Section 4.4.8 for details of the numerical model. The same antecedent Lake level (i.e., 0 m-Model Datum) was used for the seiche simulations. A validation run of an historical squall line event was conducted to ensure the calibrated PMSS model functioned as expected (i.e., produced similar seiche amplitudes and periods) for the seiche evaluation (Section 4.5.3).

4.5.3 Seiche Model Validation

The July 13-14, 1995 derecho event was evaluated to compare to the historical observations at Goderich, Ontario (Canada) and Port Huron, Michigan in Lake Huron to ensure the model accurately reproduced the recorded seiche amplitudes and periods (Figure 4.28). The model replicated the overall period of seiche oscillations. The maximum difference between positive and negative amplitudes was also similar at each location, although there was a slight shift to the positive direction (i.e., higher average SWL). Thus, it was concluded that the calibrated PMSS model was sufficient to use for the seiche evaluation without additional modifications.

4.5.4 Maximum Seiche Results

4.5.4.1 Squall Line Event Screening

Four characteristic squall line events were used in the initial screening simulations: July 19-20, 1983; July 13-14, 1995; May 31, 1998; and April 19-20, 2011. It was found that the July 13-14, 1995 and May 31, 1998 derecho events produced the highest seiche amplitudes and would be analyzed further through transpositioning and maximization. The former event had sustained winds from the northwest, while the latter had significant east-to-west winds.

4.5.4.2 Squall Line Event Transposition

Sensitivity tests were completed by shifting the squall line pressure and wind fields to find the most critical case at PBNP. The overwater and duration corrections, detailed in Section 4.4.9.5 and Section 4.4.9.6, respectively, were applied in conjunction with a linear pressure decrease of 5 mbar.

4.5.4.3 Maximum Seiche Still Water Level

The maximized, transposed May 31, 1998 derecho event generated the largest seiche amplitude (+1.0 ft [+0.3 m]) at PBNP (Figure 4.29), such that the total maximum SWL above the 100-yr recurrence monthly average high Lake level due to a seiche event was +584.1 ft-NAVD88 (+2.8 ft-Plant Datum) (Table 4.13). The maximum SWL was bounded by the maximum PMSS SWL; further, H_S during the PMSS event would be greater than during the seiche event since the seiche event occurs at PBNP after the squall line (derecho) has passed over the Lake and waves during the PMSS are generated by strong local winds. Thus, the peak

WSEL during the maximum seiche event is bounded by the peak PMSS WSEL (Section 4.4.10) and does not need to be numerically computed.

This SWL result is for a single squall line event. To amplify the initial seiche amplitude, forcing would need to be applied to the Lake at a resonant frequency to the basin's geometry. A fast Fourier transform was performed to establish the Lake's natural periods of oscillations. The dominant frequencies were found to be 40 min, 90 min, and 110 min. As discussed in Section 4.5.1, subsequent strong squall lines must be spaced at least 12 hr apart in order for the necessary atmospheric conditions to recharge. Thus, a series of squall line or derecho events occurring at the Lake's characteristic resonant frequencies are physically impossible. Seiche amplification above the +1.0 ft (+0.3 m) produced in the model simulations at PBNP is implausible.

4.6 Probable Maximum Tsunami

The potential sources of a tsunami that may cause a probable maximum tsunami (PMT) for PBNP were analyzed from observational records and current scientific literature. Queries were performed in the NGDC tsunami, earthquake, and volcano databases to determine whether any historical events were reported regionally or near PBNP (Figure 4.30) (NOAA, 2014hh). The USGS database was queried for any possible tsunamigenic landslide activities in the Great Lakes, specifically Lake Michigan (USGS, 2014a; USGS, 2014b).

No historical evidence was found of a potential tsunami occurring at or near PBNP due to earthquake (Figure 4.31), landslide, or volcanic activity. The New Madrid earthquakes of 1811-1812 in Missouri were felt near PBNP (in Orchard Lake, Michigan) but a tsunami runup was not observed in the Lake (Lockridge et al., 2002). The only historical "tsunami runup" events located in the databases were related to meteorological events; these events were not classified as true tsunami events but rather seiches (Section 4.5).

4.7 Ice-Induced Flooding and Effects

NRC (2011) states that "in the hierarchal hazard assessment framework, it may be possible to determine whether a flood caused by another flood-causing mechanism at or near the site may exceed that resulting from an ice event. If such an alternative and bounding flood is found, no further analysis for the ice-induced flooding is necessary." Accordingly, a calculation was completed to determine whether ice-induced flooding would require further hydraulic modeling analysis, or if another flood scenario is bounding.

The USACE Ice Jam Database (USACE, 2014) was queried to obtain information regarding historical ice events located in the Manitowoc-Sheboygan Watershed. No ice jams were identified. Therefore, further consideration of ice-induced flooding (including the effects of frazil ice) was not required.

4.7.1 Ice Cover

Records regarding ice cover on the Lake were obtained from the U.S. National Ice Center (USNIC) website (USNIC, 2014). These records consist of Daily Ice Analysis Charts (DIAC) and are available (digitally) from 1995 through the present.

The winter of 2013-2014 was the worst on record with regard to ice coverage on the Lake (NOAA, 2014ii). Therefore, the DIAC for 2013-2014 (through March 7, 2014) were reviewed to obtain the maximum

recorded ice thickness for the area of the Lake adjacent to PBNP: 1.0 ft (0.30 m) from March 3, 2014 through March 7, 2014.

Review of the DIAC indicates that ice thickness was greatest at the far northwest area of the Lake (Sturgeon Bay), with a maximum overall ice thickness from February 23, 2014 through March 7, 2014 of 3.9 ft (1.2 m).

4.8 Channel Migration or Diversion

PBNP is located on Lake Michigan with no major streams or rivers nearby. Therefore, channel migration or diversion is not an applicable flooding hazard.

4.9 Combined Events Flooding

The combination flooding analysis was performed in accordance with guidelines in ANSI/ANS (1992) and NRC (2011). PBNP is a "shore" location on an "enclosed body of water." For this location, combined event flooding involving surges, seiches, tsunamis, and tides might produce maximum flood levels. Because PMP flooding of streams and rivers cannot affect the site, combined events involving a riverine PMF will have no impact on PBNP. Because there are no dam failure-related flooding hazards, dam flooding combinations are precluded from analysis. Thus, the only combined event flood hazard is the storm surge-related combination:

- PMSS and seiche with wind-wave activity and
- Lesser of the 100-yr or the maximum controlled water level in the enclosed body of water.

This combination is the same as that analyzed in Section 4.4 and Section 4.5 for PMSS and seiche, respectively. Refer to those sections for the descriptions and results of the analyses.

4.10 Low Water Effects

NRC (2013a) states that "drawdown may be an issue when SSCs depend on water sources where storm surge or seiche may affect the availability of water." Accordingly, low water effects were simulated using the same calibrated numerical model as the PMSS and maximum seiche evaluations. The antecedent Lake level was the 100-yr recurrence monthly average low Lake level of +575.6 ft-NAVD88 (-5.7 ft-Plant Datum), which was set at -2.3 m-Model Datum. The two worst-case squall line events (discussed in Section 4.5) and eight synoptic events (four shifted and four transposed) were evaluated to determine which produced the minimum SWL at PBNP. This case was then modified with the overwater and duration corrections detailed in Section 4.4.9.5 and Section 4.4.9.6, respectively.

The results from the nine (i.e., eight screening and one final) low water simulations are listed in Table 4.14. The bounding case was the maximized October 29 to November 1, 2012 synoptic event from the northwest, shifted north with wind corrections applied. The minimum SWL was +572.3 ft-NAVD88 (-9.0 ft-Plant Datum), produced by a setdown of -3.3 ft during the October 29, 2012 to November 1, 2012 northwest transposed synoptic event, shifted north with the overwater and duration corrections.

4.11 Hydrostatic, Hydrodynamic, and Sediment Loading

Neither the PMSS nor maximum seiche peak produced standing water at the POIs shown on Figure 4.5. However, the peak PMSS WSEL indicated wave runup could reach the wave barrier adjacent to Door 336

on the southern side of the CWPH. The only other applicable flooding-induced loadings result from the LIP event.

4.11.1 Local Intense Precipitation Loading

The static (i.e., hydrostatic) and impact (i.e., hydrodynamic) forces were determined from the modeled WSEL and velocity time series at each POI. The hydrostatic pressure increases in proportion to the water depth due to the increasing weight that is exerted from above. From USACE (2008), the hydrostatic pressure varies from zero at the water surface to a maximum at the base of the wall, given by:

$$p_s = \gamma_w h_w \qquad \text{Equation 4.10}$$

where:

p_s = hydrostatic pressure (psf);
γ_w = specific unit weight of freshwater (=62.4 pcf); and
h_w = water depth (ft).

Once the maximum static pressure was calculated, a maximum hydrostatic force per horizontal unit length was then calculated:

$$F_s = \frac{1}{2} p_s h_w \qquad \text{Equation 4.11}$$

where:

Fs = maximum hydrostatic force per horizontal unit length (lbs/ft);
p_s = hydrostatic pressure (psf); and
h_w = water depth (ft).

The hydrodynamic impact pressure due to the velocity of LIP surface runoff was estimated using the velocity time series at each POI. From FLO-2D (2013), the hydrodynamic pressure (p_d) is represented by:

$$p_d = k p_f v^2 \qquad \text{Equation 4.12}$$

where:

p_d = hydrodynamic impact pressure (psf);
k = empirical coefficient (dimensionless);
p_f = freshwater density (=1.94 slugs/ft^3); and
v = maximum velocity (ft/s).

A maximum hydrodynamic force per horizontal unit length (F_d) was then calculated:

$$F_d = p_d h_d \qquad \text{Equation 4.13}$$

where:

F_d = maximum hydrodynamic force per horizontal unit length (lbs/ft);
p_d = hydrodynamic impact pressure (psf); and
h_d = water depth at maximum velocity (ft/s).

The maximum static and impact forces were summed to determine the maximum total force at each POI through the LIP event. The resulting static, impact, and total forces for LIP Scenario A and Scenario B are listed in Table 4.15 at each PBNP POI. The maximum total force occurred during Scenario B for most

POIs due to the excess ponding near the CPWH and TB caused by the runoff obstruction from the temporary wave barriers. For the two CWPH doors protected by the temporary wave barriers (Door 336 and Door 340), the impact forces were computed from the computational cells adjacent to the wave barriers. Since the temporary barriers and sandbags are expected to eliminate impact forces (i.e., flowing water) at the doors, the listed hydrodynamic forces are conservative.

The drainage area for PBNP consists mostly of concrete and paved surfaces which contain very few unconsolidated particles. The only area of predominantly unconsolidated material is along the beach east of the CWPH which, due to the topography, does not drain towards the power block. Thus, significant sediment accumulation at any evaluated POI is not expected.

4.11.2 Probable Maximum Storm Surge Loading

During the peak of the PMSS event, some wave runup is expected to reach the wave barrier adjacent to CWPH Door 336. A surging breaking wave force was calculated at the wave barriers and would be bounding for all PBNP POIs. The breaking wave force was computed with a relationship presented in USACE (2008):

$$F_{surge} = 0.18\gamma_w {H_b}^2 \left(1 - \frac{X_1 \tan\beta}{R_a}\right)^2 \qquad \text{Equation 4.14}$$

where:

F_{surge} = breaking wave force (lbs/ft);
γ_w = specific unit weight of freshwater (=62.4 pcf);
H_b = breaking wave height (ft);
X_1 = lateral distance from SWL to structure in runup zone (ft);
β = beach slope (degrees); and
R_a = wave runup above SWL (ft).

For a breaking wave height (H_b) of 2.4 ft, lateral distance (X_1) of 50 ft (15 m), beach slope (β) of 3.57 degrees, and total runup height (R_a) of 3.9 ft, the total breaking wave force (F_{surge}) was found to be approximately 3 lbs/ft. This loading is bounded by the total hydrostatic and hydrodynamic loading at Door 336 during the LIP Scenario A event, 278.2 lbs/ft (Table 4.15).

4.12 Debris and Waterborne Projectiles

Guidance states that debris loads on SSCs important to safety should be considered and that the methodologies for determining impact loads described in American Society of Civil Engineers (ASCE) Standard 7-10 (ASCE, 2010) are acceptable (NRC, 2013a). Accordingly, ASCE 7-10 (ASCE, 2010) was used to calculate impact loads. Per ASCE 7-10 (ASCE, 2010), impact loads are those that result from logs and other objects striking buildings, structures, or parts thereof.

Per ASCE 7-10 (ASCE, 2010), a 1,000 lb object can be considered a reasonable average for waterborne debris. This represents a reasonable weight for trees, logs, and other large woody debris that are the most common forms of damaging debris nationwide. This weight corresponds to a log approximately 30 ft in length and just under 1 ft in diameter. This reference also notes that regional or local conditions should be

considered to determine the debris object weight. ASCE 7-10 (ASCE, 2010) states that debris weight generally falls into three classes for coastal locations as follows:

1. In the Pacific Northwest, a 4,000 lb debris weight is typical due to the large trees and logs in this area;
2. In other coastal areas where piers and large pilings are available locally, debris weights may range from 1,000 to 2,000 lbs; and
3. In other coastal areas where large logs and pilings are not expected, debris will likely be derived from failed decks, steps, and building components and will likely average less than 500 lbs.

Although there are no piers located near PBNP, a debris object weight (W) of 2,000 lbs was selected conservatively to determine the maximum impact load. To account for the larger weight, a slightly larger diameter of 1.25 ft was used to calculate the resulting pressure. The 1.25-ft diameter offsets the improbable length: a 1-ft diameter, 2,000 lb log would have a length of 60 ft.

ASCE 7-10 (ASCE, 2010) presents a relationship for the magnitude of impact forces:

$$F = \frac{\pi W v C_I C_O C_D C_B R_{max}}{2g\Delta t} \qquad \text{Equation 4.15}$$

where:

F = impact force (lbs);
W = debris/projectile weight (lbs);
v = maximum flow velocity (ft/s);
g = gravitational acceleration (32.2 ft/s^2);
Δt = impact duration time (0.03 s [ASCE, 2010]);
C_I = importance coefficient (1.3 [ASCE, 2010]);
C_O = orientation coefficient (0.8 since direct impact is unlikely [ASCE, 2010]);
C_D = depth coefficient (1.0 [ASCE, 2010]);
C_B = blockage coefficient (1.0 [ASCE, 2010]); and
R_{max} = maximum response ratio for impulsive loads (1.8 [ASCE, 2010]).

Impact pressures (p_i, psf) were evaluated by dividing the impact force (F) by the cross-sectional area (A, ft^2) of the debris (i.e., $p_i = F/A$). A range of potential flow velocities was considered: 1 to 20 ft/s. Table 4.16 summarizes the debris impact force and pressure for the entire flow velocity range. The maximum waterborne projectile impact force (F=121,761 lbs) and pressure (p_i=99,220 psf) occurred for a flow velocity of 20 ft/s.

5.0 COMPARISON WITH CURRENT DESIGN BASIS

5.1 Precipitation Flooding

The CLB combined rainfall-snowmelt event for PBNP is 4.90 in. over 6 hr. The maximum WSELs produced by the CLB combined event are listed in Table 3.1. The short duration of the maximum WSELs does not adversely affect SSCs.

The site-specific LIP evaluated in the FHR for PBNP is 12.8 in. over 1 hr. Four temporal distributions (first quartile, second quartile, third quartile, and fourth quartile) of the rainfall total were evaluated to determine the sensitivity to precipitation timing. Further, two scenarios corresponding to potential site configurations were considered, as detailed in Section 4.1.7. The maximum flow depths and WSELs produced for the FHR LIP Scenario A and Scenario B events are listed in Table 4.2. In general, the third quartile and fourth quartile hyetographs resulted in the maximum flood elevations, with maximum flow depths up to +3.4 ft at the CWPH. The FHR WSELs and maximum flow depths exceed the CLB at the each POI.

5.2 Riverine Flooding

The CLB and FHR concluded that PBNP is not affected by flooding from streams, rivers, or canals.

5.3 Dam Breaches and Failures

The CLB and FHR concluded that PBNP is not affected by flooding from dam breaches or failures.

5.4 Storm Surge

The CLB maximum PMSS WSEL is +589.72 ft-NAVD88 (+8.42 ft-Plant Datum), which is a result of the historical maximum Lake level of +583.0 ft-NAVD88 (+1.7 ft-Plant Datum), +0.17 ft of wind setup, and +6.55 ft of wave runup on a vertical structure (i.e., +583.0 ft-NAVD88 + 0.17 ft + 6.55 ft = +589.72 ft-NAVD88). The flood protection level is +590.3 ft-NAVD88 (+9.0 ft-Plant Datum), providing a minimum physical margin of +0.58 ft (i.e., +590.3 ft-NAVD88 – [+589.72 ft-NAVD88] = +0.58 ft).

The FHR maximum PMSS SWL was below the grade elevation at the CWPH and TB POIs (Figure 4.5 for POI layout). As described in Section 4.4.10, the maximum PMSS SWL is a combination of the 100-yr recurrence monthly average high Lake level (+583.1 ft-NAVD88 [+1.8 ft-Plant Datum]) and a maximum storm surge of +4.5 ft. The WSEL at the maximum SWL, shown on Figure 4.25, is lower than plant grade at the CWPH and TB. Some wave runup is expected to overtop the riprap crest to a maximum temporary peak WSEL of +589.7 ft-NAVD88 (+8.4 ft-Plant Datum). Frictional losses and expansion of flow as the overtopped water volume travels landward are expected to reduce this maximum WSEL before reaching the nearest POI (CWPH Door 336 [Figure 4.5]). Thus, the FHR concluded that PBNP is not affected by flooding from the PMSS event and that available physical margin increased to at least +0.6 ft.

5.5 Seiche

The CLB proposes that a maximum seiche of 1 to 2 ft could occur. The FHR concluded that the maximum seiche to impact PBNP is 1.0 ft in amplitude. When considered with the 100-yr recurrence monthly average high Lake level (+583.1 ft-NAVD88 [+1.8 ft-Plant Datum]), the maximum seiche SWL is +584.1 ft-NAVD88 (+2.8 ft-Plant Datum). Thus, the CLB and FHR concluded that PBNP is not affected by flooding from a seiche event.

5.6 Tsunami Flooding

A tsunami was not considered a meaningful hazard to PBNP per the CLB. The FHR determined that there were no earthquakes, landslides, or volcanic eruptions that would generate a tsunami in the Lake near PBNP. Therefore, the CLB and FHR concluded that PBNP is not affected by flooding from tsunamis.

5.7 Ice-Induced Flooding

Ice-induced flooding and associated effects were not considered meaningful hazards at PBNP per the CLB. The FHR indicates that ice jams have not been recorded in the watershed surrounding PBNP. Therefore, further consideration of ice-induced flooding (including the effects of frazil ice) was not required.

5.8 Channel Migration or Diversion Flooding

The CLB and FHR Report (FHRR) concluded that PBNP is not affected by flooding from channel migration or diversion since no streams of significance flow near PBNP.

5.9 Combined Events Flooding

Combined flooding events related to storm surge and seiche flooding apply to PBNP and are addressed in Section 4.4 and Section 4.5, respectively. The relevant combined event comparisons are provided in Section 5.4 and Section 5.5 for storm surge and seiche flooding, respectively. All other combination events (e.g., riverine PMF, dam breaches and failures, tsunami) were screened and do not affect PBNP.

5.10 Low Water Effects

The CLB historical low water level was +576.5 ft-NAVD88 (-4.8 ft-Plant Datum). No additional wind setdown was considered in the CLB. The FHR considered an antecedent Lake level of +575.6 ft-NAVD88 (-5.6 ft-Plant Datum), which was the 100-yr recurrence monthly average Lake level. The maximum wind setdown was -3.31 ft, producing the minimum SWL at the intake structure of +572.3 ft-NAVD88 (-9.0 ft-Plant Datum). The FHR low water level is below the CLB historical low water level.

A decreasing Lake level will manifest itself as a decreasing pump bay level. For any given Lake level, the pump bay level will vary based on the number of circulating water pumps that are running. Current PBNP procedures require operators to monitor pump bay level and to take actions, including securing some or all circulating water pumps as needed to assure pump bay level remains above +569.8 ft-NAVD88

(-11.5 ft-Plant Datum). Remaining above that level assures operability limits of the service water system are not exceeded. If Lake level is below +572.3 ft-NAVD88 (-9.0 ft-Plant Datum), there remains sufficient margin in these existing operating procedures to assure pump bay level remains above +569.8 ft-NAVD88 (-11.5 ft-Plant Datum). Thus, there is no impact to PBNP based on the low water effects.

5.11 Hydrostatic, Hydrodynamic, and Sediment Loads

Hydrostatic, hydrodynamic, and sediment loads were not considered in the CLB. However, the CLB did include airborne tornado missile design criteria for Class I structures. The FHR combined hydrostatic and hydrodynamic loads at the POIs (Table 4.15) were bounded by the maximum tornado impact pressure by a significant margin for Class I structures. Non-Class I structures or other POIs not considered in the FHR would need to be evaluated independently to determine the effect of LIP hydrostatic and hydrodynamic loading and/or wave runup forces on the southern side of the CWPH.

5.12 Debris and Waterborne Projectiles

Flood debris and waterborne projectiles were not considered in the CLB. However, the CLB did include airborne tornado missile design criteria for Class I structures. The FHR waterborne projectile impact pressures (Table 4.16) were compared to the CLB tornado missiles, and found that sufficient margin existed for Class I structures, even at the highest range of expected flood velocities. Further, the PMSS SWL does not reach the CWPH POIs (Figure 4.5) or further inland. Thus, waterborne projectiles will not impact any POI considered in the FHR.

5.13 Summary of Comparison

The CLB-FHR comparisons discussed in Section 5.1 through Section 5.12 are summarized in Table 5.1. The reevaluated LIP maximum flow depths exceed the CLB maximum flow depths. The reevaluated PMSS (with wave runup) maximum WSELs are below maximum CLB levels.

6.0 INTERIM EVALUATION AND ACTIONS

This section identifies interim actions to be taken before the Integrated Assessment (IA) is completed. It identifies the items to be addressed in the IA and the rationale for doing so.

6.1 Local Intense Precipitation

The FHR LIP analysis is for a duration of one hour and the maximum depth of accumulated ponded water in the power block area is approximately +3.4 ft. Additional interim actions to address LIP flood heights that exceed CLB flood heights are not needed to assure PBNP's successful implementation of Flexible Coping Capability (FLEX) strategies.

Implementation of the site FLEX strategies requires equipment access via the Unit 1 and Unit 2 TB doors. If those doors are unavailable for access, the door near the station heating boilers is used as an alternate. The maximum water height at the TB doors from a LIP event is 2.6 ft and decreases rapidly, to less than one inch within three hours after the start of the LIP event (Figure 4.9). The maximum water height at the door near the heating boiler room is 2.2 ft, which decreases to approximately three inches within three hours after the start of the LIP event. FLEX strategies rely on these doors for access, but not until three hours after the start of the evaluated Beyond Design Basis event. LIP water levels will not impact access at three hours into the event.

In addition to availability of the doors discussed above, implementation of the site FLEX strategies also relies on certain installed station equipment. Equipment relied upon includes the Turbine Driven Auxiliary Feedwater (AFW) Pump, the Diesel Driven fire pump and the DC distribution system. The Turbine Driven AFW Pump is located in the AFW Pump Room. The Diesel Driven Fire Pump is located in the CWPH. Two of the four safety related batteries at the station are located in the Vital Switchgear Room along with DC distribution busses D01 and D02 and three safety related battery chargers. Thus, the three areas with equipment relied upon for FLEX are the AFW Pump Room, the Vital Switchgear Room, and the CWPH.

If the TB rollup doors should fail during the LIP event, the external flood waters would enter the TB, resulting in 2.6 ft of flood height at the doors to the AFW Pump Room and the Vital Switchgear Room. Calculation 2013-0021 Revision 1 addresses structural integrity of the doors to these rooms during a flood of up to 2 ft (NEE, 2013). That calculation concludes that these doors have a large structural margin to withstand 2 ft of water because the calculation contains several very large conservatisms (NEE, 2013). It is reasonable to conclude that the higher flood height of 2.6 ft (an increase of 30%) will not affect the conclusion of the calculation. Thus, there is reasonable assurance that these doors will remain structurally intact during and after a LIP event if the TB rollup doors are assumed to fail.

Regarding potential leakage past the doors to the AFW Pump Room and the Vital Switchgear Room, existing procedural requirements provide adequate protection during flooding at the site. Abnormal Operating Procedure (AOP) 13C Revision 38 is entered for a flood watch or warning or for actual significant water intrusion into the plant (NEE, 2015a). The AOP contains actions for operators to specifically monitor these two rooms and install sandbags to protect equipment in the two rooms (NEE, 2015a). Routine Maintenance Procedure (RMP) 9422 Revision 0 provides instruction for sandbag staging and placement (NEE, 2015b). The RMP requires an inventory of 2,400 sandbags on site, and materials on hand to fill an additional 1,000 sandbags (NEE, 2015b). These procedural actions and sandbag inventories

are sufficient to control leakage past these room doors and assure equipment availability inside these rooms during the increased flood levels of a LIP event.

If the external doors in the CWPH should fail during the LIP event, water external to the building would flow into the CWPH and out the flood relief gates to the Lake. Calculation 2009-0008 Revision 2 addresses flood scenarios by establishing an acceptable flood height inside the CWPH, and then calculating the flow rate into the CWPH from a given flood height outside the CWPH (NEE, 2014d). The calculation assumes all doors are fully open, and considers an external flood height of 2 ft (NEE, 2014d). At that flood height, the calculation concludes that flood water will be sufficiently relieved through two of the eight flood relief gates without flooding critical equipment in the CWPH (NEE, 2014d). A comparison can be made using this same method for the higher flood heights of 2.3 ft in the LIP event. In that case, the flood waters are relieved adequately through the flood relief gates and the internal flood height remains below the new Diesel Driven Fire Pump. Thus, it is concluded that during and after a LIP event the Diesel Driven Fire Pump will remain available for implementation of the FLEX strategies.

During high Lake level conditions, wave barriers 3.5 ft high are procedurally installed outside the CWPH rollup doors and sandbags are installed to seal the rollup doors. When the barriers are installed, the maximum LIP flood heights near the CWPH doors are projected to increase to 3.4 ft. It is reasonable to conclude that any leakage into the CWPH will be quickly relieved through the flood relief gates and no substantial water build up would occur inside the CWPH. It is therefore concluded that the Diesel Driven Fire Pump will remain available in a LIP event with the CWPH wave barriers in place.

In addition, further evaluations will be performed as part of the IA to assure protection of existing plant safety related equipment during a LIP event. Most of the ingress points into the plant for the higher flood levels projected from a LIP event are the same points of interest for a precipitation event flood defined in the CLB. Ingress points will be considered for specific corrective actions in the IA. Possible contributions by the yard drain system will also be considered along with preventive maintenance and inspection requirements to assure the system remains available as a drainage path. These and other specific corrective actions to protect safety-related equipment for the LIP event will be evaluated and identified in the IA report.

6.2 Riverine Flooding

No interim measures are required since this hazard does not apply to PBNP. Therefore, this hazard will not be addressed in the IA.

6.3 Dam Breaches and Failures

No interim measures are required since this hazard does not apply to PBNP. Therefore, this hazard will not be addressed in the IA.

6.4 Storm Surge

No interim measures are required for this hazard since reevaluated PMSS levels would not adversely affect critical SSCs. The reevaluated PMSS levels are bounded by the CLB at the TB and CWPH POIs. Therefore, this hazard will not be addressed in the IA.

6.5 Seiche

No interim measures are required for this hazard since maximum reevaluated seiche levels are bounded by the reevaluated PMSS. Therefore, this hazard will not be addressed in the IA.

6.6 Tsunami

No interim measures are required since tsunami flooding does not apply to PBNP. Therefore, this hazard will not be addressed in the IA.

6.7 Ice-Induced Flooding

No interim measures are required since ice-induced flooding does not apply to PBNP. Therefore, this hazard will not be addressed in the IA.

6.8 Channel Migration or Diversion Flooding

No interim measures are required since channel migration or diversion flooding does not apply to PBNP. Therefore, this hazard will not be addressed in the IA.

6.9 Combined Events Flooding

Combined flooding event comparisons related to storm surge and seiche flooding apply to PBNP and are addressed in Section 5.4 and Section 5.5, respectively. As discussed in Section 6.4 and Section 6.5, no interim measures are required for the storm surge or seiche hazards, respectively, and combined events will not be addressed in the IA.

6.10 Low Water Effects

No interim measures are required since the existing site procedures bound the low water level effects.

6.11 Hydrostatic, Hydrodynamic, and Sediment Loads

The loading from hydrostatic, hydrodynamic, and sediment loads on potentially impacted structures is bounded by design loading from tornado missiles for Class I structures at or above the minimum POI elevation evaluated. Therefore, this hazard will not be addressed in the IA for Class I structures. Other structures may be reevaluated as necessary. No interim actions are required.

6.12 Debris and Waterborne Projectiles

The loading from debris and waterborne projectiles on potentially impacted structures is bounded by design loading from tornado missiles for Class I structures at or above the minimum POI elevation evaluated. Therefore, this hazard will not be addressed in the IA for Class I structures. Other structures may be reevaluated as necessary. No interim actions are required.

7.0 ADDITIONAL ACTIONS

There are no additional actions identified as of the date of this submittal.

8.0 REFERENCES

Alkyon (2003), Alkyon Hydraulic Consultancy and Research (Alkyon), "Calibration of SWAN 40.20 for Field Cases Petten, Slotermeer, and Westerschelde," Revision 4, December 2003.

ANSI/ANS (1992), American National Standards Institute/American Nuclear Society (ANSI/ANS), "American National Standard for Determining Design Basis Flooding at Power Reactor Sites," ANSI/ANS-2.8-1992, La Grange Park, Illinois, July 28, 1992.

ASCE (2010), American Society of Civil Engineers (ASCE), Standard 7-10, "Minimum Design Loads for Buildings and Other Structures," Chapter C5, 2010.

Assel (2014), Assel, R., "NOAA Atlas, an Electronic Atlas of Great Lakes Ice Cover Winters: 1973 – 2002," Available at http://www.glerl.noaa.gov/data/ice/atlas/, Accessed on March 7, 2014.

Battjes and Janssen (1978), Battjes, J.A. and J.P.F.M. Janssen, "Energy loss and Set-up due to Breaking of Random Waves," Proceedings of 16th International Conference on Coastal Engineering, American Society of Civil Engineers, pp. 569-587, New York, 1978.

Bechtel (1970), Bechtel Corporation (Bechtel), "Westinghouse Electric Corporation, Wisconsin Michigan Power Company, Point Beach Atomic Power Station, Design Criteria for Nuclear Power Plants against Tornadoes," B-TOP-3, March 12, 1970.

Booij et al. (1999), Booij, N, L.H. Holthuijsen, and R. Ris, "A Third-generation Wave Model for Coastal Regions, Part I, Model Description and Validation," Volume 104 (C4), pp. 7649-7666, 1999.

Deltares (2011), Deltares, "Delft3D Computer Program," Version 4.00.04.757, 2600 MH Delft, The Netherlands, 2011.

Deltares (2014a), Deltares, "Delft3D-FLOW User Manual," Version 3.15, Revision 33641, 2600 MH Delft, The Netherlands, Available at http://oss.deltares.nl/documents/183920/185723/Delft3D-FLOW_User_Manual.pdf, Accessed on December 1, 2014.

Deltares (2014b), Deltares, "Delft3D-FLOW User Manual," Version 3.05, Revision 34160, 2600 MH Delft, The Netherlands, Available at http://content.oss.deltares.nl/delft3d/manuals/Delft3D-WAVE_User_Manual.pdf, Accessed on December 1, 2014.

ESRI (2012), Environmental Systems Research Institute (ESRI), "ArcGIS Desktop Computer Program," Version 10.1, ESRI, Redlands, California, 2012.

FLO-2D (2013), FLO-2D Software, Inc. (FLO-2D), "FLO-2D Reference Manual," 2013.

FLO-2D (2014), FLO-2D Software, Inc. (FLO-2D), "FLO-2D PRO Model," Build 14.08.09, 2014.

Hansen et al. (1982), Hansen, E.M., L.C. Schreiner, and J.F. Miller, National Weather Service, National Oceanic and Atmospheric Administration, U.S. Department of Commerce, "Application of Probable Maximum Precipitation Estimates, United States East of 105th Meridian," Hydrometeorological Report (HMR) No. 52, Silver Spring, Maryland, 1982.

Hasselmann et al. (1973), Hasselmann, K., T.P. Barnett, E. Bouws, H. Carlson, D.E. Cartwright, K. Enke, J.A. Ewing, H. Gienapp, D.E. Hasselmann, P. Kruseman, A. Meerburg, P. Muller, D.J. Olbers, K. Richter, W. Sell, and H. Walden, "Measurements of Wind-Wave Growth and Swell Decay during the Joint North Sea Wave Project (JONSWAP)," Deutsches Hydrographisches Institut, Hamburg, Germany, 1973.

Hasselmann et al. (1985), Hasselmann, S., K. Hasselmann, J.H. Allender, and T.P. Barnett, "Computations and Parameterizations of the Nonlinear Energy Transfer in a Gravity-Wave Spectrum, Part II: Parameterizations of the Nonlinear Energy Transfer for Application in Wave Models," Journal of Physical Oceanography, Volume 15 (11), pp. 1375-1391, 1985.

Herbert (1987), Herbert, D., "An Estimate of the Effective Horizontal Eddy Viscosity in the Gulf Stream due to Internal Waves," Journal of Physical Oceanography, Volume 17 (10), pp. 1837-1841, 1987.

Jensen et al. (2012), Jensen, R.E., M.A. Cialone, R.S. Chapman, B.A. Ebersole, M. Anderson, and L. Thomas, "Lake Michigan Storm: Wave and Water Level Modeling," U.S. Army Corps of Engineers ERDC TR-12-X, 2012.

Liu (1965), Liu, P., "Some Features of Wind Waves in Lake Michigan," U.S. Lake Survey, 1965.

Lockridge et al. (2002), Lockridge, P.A., L.S. Whiteside, and J.F. Lander, "Tsunamis and Tsunami-Like Waves of the Eastern United States," Science of Tsunami Hazards, Volume 20 (3), pp. 120-157.

Nash and Sutcliffe (1970), Nash, J.E. and J.V. Sutcliffe, "River Flow Forecasting through Conceptual Models Part I – A Discussion of Principles," Journal of Hydrology," Volume 10 (3), pp. 282-290, 1970.

NEE (2010), NextEra Energy (NEE), Point Beach Nuclear Plant, "Final Safety Analysis Report," Chapter 5, Section 5.1, 2010, as updated.

NEE (2012a), NextEra Energy (NEE), Point Beach Nuclear Plant, "NextEra Energy Point Beach, LLC's 60-Day Response to NRC Letter, Request for Information Pursuant to Title 10 of the Code of Federal Regulations 50.54(f) Regarding Recommendations 2.1, 2.3, and 9.3, of the Near-Term Task Force Review of Insights from the Fukushima Dai-ichi Accident; dated March 12, 2012," NRC 2012-0027, May 10, 2012.

NEE (2012b), NextEra Energy (NEE), Point Beach Nuclear Plant, "Flooding Walkdown Report in Response to the 50.54(f) Information Request Regarding Near-Term Task Force Recommendation 2.3: Flooding for the Point Beach Nuclear Plant," NEE05-PR-001, Revision 0, November 14, 2012, ADAMS Accession Number ML12326A713.

NEE (2012c), NextEra Energy (NEE), Point Beach Nuclear Plant, "Final Safety Analysis Report," Chapter 2, 2012, as updated.

NEE (2013), NextEra Energy (NEE), Point Beach Nuclear Plant, "Analysis of Hydrostatic Pressure on Flood Doors," Calculation 2013-0021, Revision 0, December 3, 2013.

NEE (2014a), NextEra Energy (NEE), Point Beach Nuclear Plant, "PBNP Topographic and Bathymetric Survey Data," Engineering Evaluation No. 2013-0002, Revision 1.

NEE (2014b), NextEra Energy (NEE), Point Beach Nuclear Plant, "Final Safety Analysis Report," Chapter 2, 2014, as updated.

NEE (2014c), NextEra Energy (NEE), Point Beach Nuclear Plant, "Final Safety Analysis Report," Appendix A.7, 2014, as updated.

NEE (2014d), NextEra Energy (NEE), Point Beach Nuclear Plant, "Circulating Water Pump House Internal/External Flooding," Calculation 2009-0008, Revision 2, October 2, 2014.

NEE (2015a), NextEra Energy (NEE), Point Beach Nuclear Plant, "Point Beach Nuclear Plant Abnormal Operating Procedure, Severe Weather Conditions," AOP-13C, Revision 38, January 2015.

NEE (2015b), NextEra Energy (NEE), Point Beach Nuclear Plant, "Routine Maintenance Procedure 9422, Circulating Water Pumphouse and Turbine Hall Barrier Placement," RMP 9422, Revision 1, January 30, 2015.

NEI (2012), National Energy Institute (NEI), "Guidelines for Performing Verification of Plant Flood Protection Features," NEI 12-07, Revision 0-A, dated May, 2012, endorsed by NRC on May 31, 2012.

NOAA (1986), National Oceanic and Atmospheric Administration (NOAA), National Ocean Service, U.S. Department of Commerce, "The National Geodetic Survey Gravity Network," National Oceanic and Atmospheric Administration Technical Report NOS 121 NGS 39, Rockville, Maryland, December 1986.

NOAA (1999a), National Oceanic and Atmospheric Administration (NOAA), U.S. Department of Commerce, "Bathymetry of Lake Michigan," National Geophysical Data Center Website, Available at http://www.ngdc.gov/mgg/greatlakes/michigan.html, Accessed on December 1, 2014.

NOAA (1999b), National Oceanic and Atmospheric Administration (NOAA), U.S. Department of Commerce, "Bathymetry of Lake Huron," National Geophysical Data Center Website, Available at http://www.ngdc.gov/mgg/greatlakes/huron.html, Accessed on December 1, 2014.

NOAA (2013), National Oceanic and Atmospheric Administration (NOAA), U.S. Department of Commerce, "Tidal Datums – NOAA Tides & Currents," Revised October 15, 2013, Available at http://tidesandcurrents.noaa.gov/datum_options.html, Accessed on November 4, 2014.

NOAA (2014a), National Oceanic and Atmospheric Administration (NOAA), U.S. Department of Commerce, "National Geophysical Data Center Digital Elevation Model Frequently Asked Questions," National Geophysical Data Center Website," Available at http://www.ngdc.noaa.gov/mgg/global/dem_faq.html, Accessed on December 1, 2014.

NOAA (2014b), National Oceanic and Atmospheric Administration (NOAA), U.S. Department of Commerce, "Station 9087044, Calumet Harbor, Illinois," Available at http://tidesandcurrents.noaa.gov/waterlevels.html? id=9087044, Accessed on June 6, 2014.

NOAA (2014c), National Oceanic and Atmospheric Administration (NOAA), U.S. Department of Commerce, "Station 9087068, Kewaunee, Wisconsin," Available at http://tidesandcurrents.noaa.gov/waterlevels.html? id=9087068, Accessed on June 6, 2014.

NOAA (2014d), National Oceanic and Atmospheric Administration (NOAA), U.S. Department of Commerce, "Station 9087088, Menominee, Michigan" Available at http://tidesandcurrents.noaa.gov/waterlevels.html? id=9087088, Accessed on June 6, 2014.

NOAA (2014e), National Oceanic and Atmospheric Administration (NOAA), U.S. Department of Commerce, "Station 9087096, Port Inland, Michigan" Available at http://tidesandcurrents.noaa.gov/waterlevels.html? id=9087096, Accessed on June 6, 2014.

NOAA (2014f), National Oceanic and Atmospheric Administration (NOAA), U.S. Department of Commerce, "Station 9087079, Green Bay, Wisconsin" Available at http://tidesandcurrents.noaa.gov/waterlevels.html? id=9087079, Accessed on June 6, 2014.

NOAA (2014g), National Oceanic and Atmospheric Administration (NOAA), U.S. Department of Commerce, "Station 9087023, Ludington, Michigan" Available at http://tidesandcurrents.noaa.gov/waterlevels.html? id=9087023, Accessed on June 6, 2014.

NOAA (2014h), National Oceanic and Atmospheric Administration (NOAA), U.S. Department of Commerce, "Station 9087057, Milwaukee, Wisconsin" Available at http://tidesandcurrents.noaa.gov/waterlevels.html? id=9087057, Accessed on June 6, 2014.

NOAA (2014i), National Oceanic and Atmospheric Administration (NOAA), U.S. Department of Commerce, "Station 9087072, Sturgeon Bay Canal, Wisconsin" Available at http://tidesandcurrents.noaa.gov/waterlevels.html? id=9087072, Accessed on June 6, 2014.

NOAA (2014j), National Oceanic and Atmospheric Administration (NOAA), U.S. Department of Commerce, "Station 9087031, Holland, Michigan" Available at http://tidesandcurrents.noaa.gov/waterlevels.html? id=9087031, Accessed on June 6, 2014.

NOAA (2014k), National Oceanic and Atmospheric Administration (NOAA), U.S. Department of Commerce, "Station 9087064, Manitowoc, Wisconsin" Available at http://tidesandcurrents.noaa.gov/waterlevels.html? id=9087064, Accessed on June 6, 2014.

NOAA (2014l), National Oceanic and Atmospheric Administration (NOAA), U.S. Department of Commerce, "Station 9087028, Muskegon, Michigan" Available at http://tidesandcurrents.noaa.gov/waterlevels.html? id=9087028, Accessed on June 6, 2014.

NOAA (2014m), National Oceanic and Atmospheric Administration (NOAA), U.S. Department of Commerce, "Station 9075080, Mackinaw City, Michigan" Available at http://tidesandcurrents.noaa.gov/waterlevels.html? id=9075080, Accessed on June 6, 2014.

NOAA (2014n), National Oceanic and Atmospheric Administration (NOAA), U.S. Department of Commerce, "Station 9075065, Alpena, Michigan" Available at http://tidesandcurrents.noaa.gov/waterlevels.html? id=9075065, Accessed on June 6, 2014.

NOAA (2014o), National Oceanic and Atmospheric Administration (NOAA), U.S. Department of Commerce, "Station 9075035, Essexville, Michigan" Available at http://tidesandcurrents.noaa.gov/waterlevels.html? id=9075035, Accessed on June 6, 2014.

NOAA (2014p), National Oceanic and Atmospheric Administration (NOAA), U.S. Department of Commerce, "Station 9075014, Harbor Beach, Michigan" Available at http://tidesandcurrents.noaa.gov/waterlevels.html? id=9075014, Accessed on June 6, 2014.

NOAA (2014q), National Oceanic and Atmospheric Administration (NOAA), U.S. Department of Commerce, "Station 9075002, Lakeport, Michigan" Available at http://tidesandcurrents.noaa.gov/waterlevels.html? id=9075002, Accessed on June 6, 2014.

NOAA (2014r), National Oceanic and Atmospheric Administration (NOAA), U.S. Department of Commerce, "Station 9014098, Fort Gratiot, Michigan" Available at http://tidesandcurrents.noaa.gov/waterlevels.html? id=9014098, Accessed on June 6, 2014.

NOAA (2014s), National Oceanic and Atmospheric Administration (NOAA), U.S. Department of Commerce, "Station PNLM4," Available at http://www.ndbc.noaa.gov/station_page.php?station=PNLM4, Accessed on June 9, 2014.

NOAA (2014t), National Oceanic and Atmospheric Administration (NOAA), U.S. Department of Commerce, "Station 45022," Available at http://www.ndbc.noaa.gov/station_page.php?station=45022, Accessed on June 9, 2014.

NOAA (2014u), National Oceanic and Atmospheric Administration (NOAA), U.S. Department of Commerce, "Station 45002," Available at http://www.ndbc.noaa.gov/station_page.php?station=45002, Accessed on June 9, 2014.

NOAA (2014v), National Oceanic and Atmospheric Administration (NOAA), U.S. Department of Commerce, "Station CBRW3," Available at http://www.ndbc.noaa.gov/station_page.php?station=CBRW3, Accessed on June 9, 2014.

NOAA (2014w), National Oceanic and Atmospheric Administration (NOAA), U.S. Department of Commerce, "Station 45014," Available at http://www.ndbc.noaa.gov/station_page.php?station=45014, Accessed on June 9, 2014.

NOAA (2014x), National Oceanic and Atmospheric Administration (NOAA), U.S. Department of Commerce, "Station GBLW3," Available at http://www.ndbc.noaa.gov/station_page.php?station=GBLW3, Accessed on June 9, 2014.

NOAA (2014y), National Oceanic and Atmospheric Administration (NOAA), U.S. Department of Commerce, "Station 45024," Available at http://www.ndbc.noaa.gov/station_page.php?station=45024, Accessed on June 9, 2014.

NOAA (2014z), National Oceanic and Atmospheric Administration (NOAA), U.S. Department of Commerce, "Station 45161," Available at http://www.ndbc.noaa.gov/station_page.php?station=45161, Accessed on June 9, 2014.

NOAA (2014aa), National Oceanic and Atmospheric Administration (NOAA), U.S. Department of Commerce, "Station 45013," Available at http://www.ndbc.noaa.gov/station_page.php?station=45013, Accessed on June 9, 2014.

NOAA (2014bb), National Oceanic and Atmospheric Administration (NOAA), U.S. Department of Commerce, "Station 45007," Available at http://www.ndbc.noaa.gov/station_page.php?station=45007, Accessed on June 9, 2014.

NOAA (2014cc), National Oceanic and Atmospheric Administration (NOAA), U.S. Department of Commerce, "Station 45170," Available at http://www.ndbc.noaa.gov/station_page.php?station=45170, Accessed on June 9, 2014.

NOAA (2014dd), National Oceanic and Atmospheric Administration (NOAA), U.S. Department of Commerce, "Station BHRI3," Available at http://www.ndbc.noaa.gov/station_page.php?station=BHRI3, Accessed on June 9, 2014.

NOAA (2014ee), National Oceanic and Atmospheric Administration (NOAA), U.S. Department of Commerce, "Station 45003," Available at http://www.ndbc.noaa.gov/station_page.php?station=45003, Accessed on June 9, 2014.

NOAA (2014ff), National Oceanic and Atmospheric Administration (NOAA), U.S. Department of Commerce, "Station MACM4," Available at http://www.ndbc.noaa.gov/station_page.php?station=MACM4, Accessed on June 9, 2014.

NOAA (2014gg), National Oceanic and Atmospheric Administration (NOAA), U.S. Department of Commerce, "Station 45008," Available at http://www.ndbc.noaa.gov/station_page.php?station=45008, Accessed on June 9, 2014.

NOAA (2014hh), National Oceanic and Atmospheric Administration (NOAA), U.S. Department of Commerce, "Natural Hazards Data, Images and Education," Available at http://www.ngdc.noaa.gov/hazard/hazards.shtml, Accessed on February 28, 2014.

NOAA (2014ii), National Oceanic and Atmospheric Administration (NOAA), National Climatic Data Center, U.S. Department of Commerce, "National Climatic Data Center," Available at http://ncdc.noaa.gov/sotc/national/2014/2/supplemental/page-6, Accessed on March 7, 2014.

NOAA (2014jj), National Oceanic and Atmospheric Administration (NOAA), Earth System Research Laboratory, Physical Science Division, "20th Century Reanalysis (V2) Data Composites," Available at http://www.esrl.noaa.gov/psd/data/composites/subdaily_20thc/, Accessed on June 30, 2014.

NOAA (2014kk), National Oceanic and Atmospheric Administration (NOAA), Earth System Research Laboratory, Physical Science Division, "6-Hourly NCEP/NCAR Reanalysis Data Composites," Available at http://www.esrl.noaa.gov/psd/data/composites/hour/, Accessed on June 30, 2014.

NOAA (2014ll), National Oceanic and Atmospheric Administration (NOAA), Earth System Research Laboratory, Physical Science Division, "3-Hourly NCEP North American Regional Reanalysis (NARR) Composites," Available at http://www.esrl.noaa.gov/psd/cgi-bin/data/narr/plothour.pl., Accessed on June 30, 2014.

NRC (1977), U.S. Nuclear Regulatory Commission (NRC), "Design Basis Floods for Nuclear Power Plants," Regulatory Guide 1.59, Revision 2, Washington D.C., August 1977, with errata dated June 30, 1980.

NRC (1978), U.S. Nuclear Regulatory Commission (NRC), "Standard Format and Content of Safety Analysis Reports for Nuclear Power Plants," Regulatory Guide 1.70, Revision 3, Washington, D.C., 1978.

NRC (2007), U.S. Nuclear Regulatory Commission (NRC), "Standard Review Plan for the Review of Safety Analysis Reports for Nuclear Power Plants: LWR Edition," NUREG-0800, Washington, D.C., March 2007.

NRC (2009), U.S. Nuclear Regulatory Commission (NRC), "Tsunami Hazard Assessment at Nuclear Power Plant Sites in the United States of America Final Report," NUREG/CR-6966 PNNL-17397, Washington, D.C., March 2009.

NRC (2011), U.S. Nuclear Regulatory Commission (NRC), "Design-Basis Flood Estimation for Site Characterization at Nuclear Power Plants in the United States of America," NUREG/CR-7046, Washington, D.C., November 2011.

NRC (2012), U.S. Nuclear Regulatory Commission (NRC), "Request for Information Pursuant to Title 10 of the Code of Federal Regulations 50.54(f) Regarding Recommendations 2.1, 2.3, and 9.3, of the Near-term Task Force Review of Insights from the Fukushima Dai-ichi Accident," Washington, D.C., March 12, 2012.

NRC (2013a), U.S. Nuclear Regulatory Commission (NRC), "Guidance for Performing a Tsunami, Surge, or Seiche Hazard Assessment," JLD-ISG-2012-06, Revision 0, Washington, D.C., January 4, 2013.

NRC (2013b), U.S. Nuclear Regulatory Commission (NRC) "Guidance for Assessment of Flooding Hazards Due to Dam Failure," JLD-ISG-2013-01, Revision 0, July 29, 2013.

Riedel et al. (1956), Reidel, J.T., J.F. Appleby, and R.W. Schloemer, Weather Bureau, U.S. Department of Commerce, "Seasonal Variation of the Probable Maximum Precipitation East of the 105th Meridian for Areas from 10 to 1000 Square Miles and Durations of 6, 12, 24, and 48 Hours," Hydrometeorological Report (HMR) No. 33, Washington, D.C., 1956.

S&L (1967), Sargent and Lundy Engineers (S&L), "Point Beach Nuclear Plant, Wisconsin Michigan Power Company, Maximum Deep Water Waves & Beach Run-up at Point Beach," January 14, 1967.

Schreiner and Riedel (1978), Schreiner, L.C. and J.T. Riedel, National Weather Service (NWS), National Oceanic and Atmospheric Administration (NOAA), U.S. Department of Commerce, "Probable Maximum Precipitation Estimates, United States East of the 105th Meridian," Hydrometeorological Report (HMR) No. 51, Washington, D.C., 1978.

Schwab and Morton (1984), Schwab, D. and J. Morton, "Estimation of Overlake Wind Speed from Overland Wind Speed: A Comparison of Three Methods." Journal of Great Lakes Resources, 10, pp. 68-72.

SCO (2012), Wisconsin State Cartographer's Office (SCO), "Wisconsin Coordinate Reference Systems," Second Edition, Madison, Wisconsin, 2012.

Street et al. (1996), Street, R.L., G.Z. Watters, and J.K. Vennard, "Elementary Fluid Mechanics," 7th Edition, John Wiley & Sons, 784 p., 1996.

USACE (1991), U.S. Army Corps of Engineers (USACE), North Central Division, "Great Lakes Levels, International Great Lakes Datum," Update Letter No. 76, November 4, 1991.

USACE (2008), U.S. Army Corps of Engineers (USACE), "Coastal Engineering Manual," EM 1110-2-1100.

USACE (2012), U.S. Army Corps of Engineers (USACE), "Statistical Analysis and Storm Sampling Approach for Lakes Michigan and St. Clair, Great Lakes Coastal Flood Study," 2012 Federal Interagency Initiative.

USACE (2014), U.S. Army Corps of Engineers (USACE), "National Ice Jam Database, Bulletin and Survey," Available at http://icejams.crrel.usace.army.mil/, Accessed on March 7, 2014.

USGS (2011), U.S. Geological Survey (USGS), "1/3-Arc Second National Elevation Dataset," National Elevation Dataset grid n45w088_1, United States Geological Survey National View Website," Available at http://viewer.nationalmap.gov/viewer, Accessed on December 1, 2014.

USGS (2014a), U.S. Geological Survey (USGS), "Landslide Hazards Program," Available at http://landslides.usgs.gov, Accessed on March 4, 2014.

USGS (2014b), U.S. Geological Survey (USGS), "Landslide Monitoring," Available at http://landslides.usgs.gov/monitoring, Accessed on March 4, 2014.

USNIC (2014), U.S. National Ice Center (USNIC), "National Ice Center," Available at http://www.natice.noaa.gov/products/great_lakes.html, Accessed on March 7, 2014.

Walstra and Koster (2006), Walstra, D.J.R. and L. Koster, Delft Hydraulics, "Benchmarking Database for Delft3D," November 2006.

Wang et al. (2012), Wang, J., R. Assel, S. Waltersheid, A. Clites, and X. Bai, "Great Lakes Ice Climatology Update: Winter 2006-2011 Description of the Digital Ice Cover Dataset," National Oceanic and Atmospheric Administration Technical Memorandum GLERL-155.

WMO (2009), World Meteorological Organization (WMO), "Manual for Estimation of Probable Maximum Precipitation," Operational Hydrology Report No. 1045, Geneva, 2009.

Wuest and Lorke (2003), Wuest, A. and A. Lorke, "Small-scale Hydrodynamics in Lakes," Annual Review of Fluid Mechanics 35, pp. 373-412.

Table 2.1 – Vertical Datum Conversions

Datum Output (Conversion to)	Datum Input (Conversion from)			
	ft-IGLD55	ft-IGLD85	ft-NAVD88	ft-Plant Datum
ft-IGLD55	0.0	-0.7	-1.1	+580.2
ft-IGLD85	+0.7	0.0	-0.4	+580.9
ft-NAVD88	+1.1	+0.4	0.0	+581.3
ft-Plant Datum	-580.2	-580.9	-581.3	0.0

Sample Conversions: 600.0 ft-NAVD88 = 18.7 ft-Plant Datum (i.e., 600.0 ft – 581.3 ft = 18.7 ft)
599.6 ft-IGLD85 = 600.0 ft-NAVD88 (i.e., 599.6 ft + 0.4 ft = 600.0 ft)

References: NEE, 2010; NEE, 2012c

Table 3.1 – CLB Precipitation Flood Event Maximum WSELs at POIs

Building	POI (Door Location)	Maximum Flow Depth (ft)[5]	Maximum WSEL	
			(ft-Plant Datum)	(ft-NAVD88)
Turbine Building	1	N/A	+8.1	+589.4
	2	0.4	+8.1	+589.4
	4	0.2	+8.1	+589.4
	11	0.3	+8.2	+589.5
	13	0.1	+8.2	+589.5
Diesel Generator	600	N/A	+26.9	+608.2
	601	0.1	+27.2	+608.5
	602	N/A	+27.6	+608.9
	603	N/A	+27.3	+608.6
	604	0.2	+27.6	+608.9
Unit 1 & Unit 2	151	0.2	+26.1	+607.4
	152	0.3	+26.2	+607.5
	154	0.4	+26.3	+607.6
	209	N/A	+25.9	+607.2
	210	0.1	+26.1	+607.4
	231	1.0	+26.6	+607.9
	232	1.0	+26.6	+607.9
Service Building	310	0.1	+25.7	+607.0
	311	N/A	+25.7	+607.0
	312	N/A	+25.8	+607.1
	313	0.1	+25.9	+607.2
	314	0.1	+25.9	+607.2
CWPH	336	0.7	+7.6	+588.9
	338	0.7	+7.7	+589.0
	339	0.8	+7.8	+589.1
	340	0.6	+7.6	+588.9

References: NEE, 2014b

[5] N/A for maximum flow depth indicates a maximum flow depth <0.1 ft, not necessarily 0.0 ft.

Table 3.2 – CLB Wave Runup

Type of Surface[6]	Vertical Height of Runup (ft)	Wind Setup (ft)	Maximum Lake Level (ft-Plant Datum)	Total WSEL (ft-Plant Datum)
1:1½ Riprap Slope	+5.38	+0.17	+1.7	+7.25
Vertical Structure	+6.55	+0.17	+1.7	+8.42

References: NEE, 2014b

[6] Slopes are reported as vertical (V) to horizontal (H), V:H.

Table 4.1 – Site-Specific Subhourly PBNP LIP Precipitation Depths

Time (min)	Precipitation Depths (in)
60	12.8
30	9.9
15	6.9
5	4.4

References: None

Table 4.2 – Site-Specific LIP Scenario A and Scenario B Maximum Flow Depths and WSELs at POIs

Building	POI (Door Location)	Scenario A			Scenario B		
		Maximum Flow Depth (ft)	Maximum WSEL		Maximum Flow Depth, (ft)	Maximum WSEL	
			(ft-Plant Datum)	(ft-NAVD88)		(ft-Plant Datum)	(ft-NAVD88)
Turbine Building	1	1.9	+9.9	+591.2	2.5	+10.5	+591.8
	2	1.9	+9.9	+591.2	2.5	+10.5	+591.8
	4	1.9	+9.9	+591.2	2.5	+10.5	+591.8
	11	2.1	+10.1	+591.4	2.6	+10.6	+591.9
	13	2.1	+10.1	+591.4	2.6	+10.6	+591.9
Diesel Generator	600	0.2	+26.4	+607.7	0.2	+26.4	+607.7
	601	0.1	+28.0	+609.3	0.1	+28.0	+609.3
	602	0.5	+28.0	+609.3	0.5	+28.0	+609.3
	603	0.3	+27.8	+609.1	0.3	+27.8	+609.1
	604	0.7	+28.0	+609.3	0.7	+28.0	+609.3
Unit 1 & Unit 2	151	1.9	+27.7	+609.0	1.9	+27.7	+609.0
	152	2.1	+28.0	+609.3	2.1	+28.0	+609.3
	154	2.3	+28.2	+609.5	2.3	+28.2	+609.5
	159	2.4	+28.3	+609.6	2.4	+28.3	+609.6
	167	2.2	+28.2	+609.5	2.2	+28.2	+609.5
	209	1.0	+27.1	+608.4	1.0	+27.0	+608.3
	210	1.9	+27.7	+609.0	1.9	+27.8	+609.1
	231	2.3	+28.2	+609.5	2.3	+28.2	+609.5
	232	2.5	+28.2	+609.5	2.5	+28.2	+609.5
Service Building	310	1.0	+26.4	+607.7	1.0	+26.4	+607.7
	311	0.9	+26.7	+608.0	0.9	+26.7	+608.0
	312	0.9	+26.8	+608.1	0.9	+26.8	+608.1
	313	1.2	+27.0	+608.3	1.2	+27.0	+608.3
	314	1.1	+27.1	+608.4	1.1	+27.0	+608.3
CWPH	336	2.1	+9.2	+590.5	2.5	+9.8	+591.1
	338	2.8	+9.8	+591.1	3.4	+10.5	+591.8
	339	2.8	+10.0	+591.3	3.3	+10.5	+591.8
	340	2.3	+9.6	+590.9	2.6	+9.9	+591.2
G5 Building	G501	2.1	+27.9	+609.2	2.1	+27.9	+609.2
	G502	2.1	+27.9	+609.2	2.1	+27.9	+609.2
	G503	2.2	+28.0	+609.3	2.2	+28.0	+609.3
	G504	2.0	+27.9	+609.2	2.0	+27.9	+609.2
	G505	1.8	+27.7	+609.0	1.8	+27.7	+609.0

References: None

Table 4.3 – Summary of Lake Level Frequency Analysis Results

	100-Year Recurrence Monthly Average High Lake Level at PBNP		100-Year Recurrence Monthly Average Low Lake Level at PBNP	
	(ft-NAVD88)	(ft-Plant Datum)	(ft-NAVD88)	(ft-Plant Datum)
Kewaunee, WI[7]	+583.1	+1.8	+575.6	-5.7
Milwaukee, WI[8]	+583.1	+1.8	+575.9	-5.4

References: ESRI, 2012; NOAA, 2014c; NOAA, 2014h

[7] Kewaunee station is approximately 12.7 miles from PBNP, measured using ArcGIS (ESRI, 2012).

[8] Milwaukee station is approximately 90.1 miles from PBNP, measured using ArcGIS (ESRI, 2012).

Table 4.4 – Potential PMWS Scenarios

Scenario	Event (Date – Approach Direction)
1	January 18-21, 1907 – Southwest
2	January 18-21, 1907 – West
3	March 21-22, 1913 – Southwest
4	March 21-22, 1913 – West
5	November 7-10, 1913 – North
6	November 7-10, 1913 – Northwest
7	October 19-21, 1916 – Northeast
8	October 20-24, 1929 – North
9	October 10-11, 1949 – South
10	December 24-26, 1965 – Northwest
11	January 10-12, 1975 – Northwest
12	January 10-12, 1975 – South
13	January 10-12, 1975 – Southeast
14	January 25-28, 1978 – North
15	January 25-28, 1978 – Southwest
16	April 3-4, 1982 – Northeast
17	April 3-4, 1982 – Northwest
18	January 23-24, 1982 – East
19	January 23-24, 1982 – Southeast
20	January 4-5, 1982 – Northeast
21	December 1-2, 1985 – Northeast
22	March 4-5, 1985 – East
23	December 15-17, 1987 – East
24	December 15-17, 1987 – Southeast
25	September 22-24, 1989 – North
26	September 22-24, 1989 – Northeast
27	December 3-4, 1990 – East
28	December 3-4, 1990 – Northwest
29	November 9-12, 1998 – South
30	November 9-12, 1998 – Southeast
31	November 9-12, 1998 – Southwest
32	March 9-11, 2002 – Northwest
33	March 9-11, 2002 – West
34	November 11-14, 2003 – Northwest
35	November 11-14, 2003 – South
36	November 11-14, 2003 – Southwest
37	December 27-29, 2008 – South
38	December 27-29, 2008 – Southwest
39	December 27-29, 2008 – West
40	October 27-28, 2010 – Northwest
41	October 27-28, 2010 – Southwest
42	October 27-28, 2010 – West
43	October 29-November 1, 2012 – North
44	October 29-November 1, 2012 – Northeast
45	October 29-November 1, 2012 – Northwest

References: None

Table 4.5 – NOAA Tide and Water Level Stations Considered for Calibration and Validation

Station ID	Latitude	Longitude	1985 Event	1990 Event	2010 Event
9087044	41.73	-87.54	60 minute	60 minute	6 minute
9087068	44.46	-87.50	60 minute	unused data[9]	6 minute
9087088	45.10	-87.59	no data	no data	6 minute
9087096	45.97	-85.87	60 minute	60 minute	6 minute
9087079	44.54	-88.01	60 minute	60 minute	6 minute
9087023	43.95	-86.44	60 minute	60 minute	6 minute
9087057	43.00	-87.89	60 minute	60 minute	6 minute
9087072	44.80	-87.31	60 minute	60 minute	6 minute
9087031	42.77	-86.20	60 minute	60 minute	6 minute
9087064	44.09	-87.65	no data	no data	no data
9087028	43.23	-86.34	no data	no data	no data
9075080	45.78	-84.73	60 minute	60 minute	6-minute
9075065	45.06	-83.43	no data	no data	6-minute
9075035	43.64	-83.85	60 minute	60 minute	6 minute
9075014	43.85	-82.64	60 minute	60 minute	6 minute
9075002	43.14	-82.49	60 minute	60 minute	6 minute
9014098	43.01	-82.42	60 minute	60 minute	6 minute

References: NOAA, 2014b through NOAA, 2014r

[9] "unused data" indicated that greater than 50% of the water level observations during the event were rejected by NOAA (i.e., data flag = '999').

Table 4.6 – NOAA Buoy Stations Considered for Calibration and Validation

Station ID	Depth (m)	Latitude	Longitude	1985 Event	1990 Event	2010 Event
PNLM4	-	45.97	-85.87	No	No	Yes
45022	2.98	45.40	-85.09	No	No	Yes
45002	173	45.34	-86.41	No	unused data[10]	Yes
CBRW3	-	45.20	-87.36	No	No	Yes
45014	13	44.80	-87.76	No	No	No
GBLW3	-	44.65	-87.90	No	No	unused data[6]
45024	-	43.98	-86.56	No	No	No
45161	25	43.18	-86.36	No	No	No
45013	20	43.10	-87.85	No	No	No
45007	160	42.67	-87.03	unused data[6]	No	Yes
45170	19	41.76	-86.97	No	No	No
BHRI3	-	41.65	-87.15	No	No	unused data[6]
45003	134.7	45.36	-82.90	No	No	Yes
MACM4	-	45.78	-84.72	No	No	unused data[6]
45008	54.3	44.28	-82.42	unused data[6]	No	Yes

References: NOAA, 2014s through NOAA, 2014gg

[10] "unused data" indicated that greater than 50% of the water level observations during the event were rejected by the following rejection criteria:

- All data with data flag = '999' were removed from consideration.
- All wave direction values ≥ 360 degrees were removed from consideration.
- All Hs ≥ 10 m were removed from consideration.
- All periods of repeating Hs were removed from consideration.
- All peak wave period values (T) ≥ 10 s were removed from consideration.

Table 4.7 – Delft3D-FLOW Storm Surge Calibration Simulations

Calibration Simulation	Wind Drag Formulation	Manning's n Coefficient (dimensionless)	Air density (kg/m^3)	RMSE (m)[11]	NSE (dimensionless)	Notes
1	Deltares (2014a)	0.02	1	0.092	0.613	-
2	Jensen et al. (2012)	0.02	1	0.100	0.538	-
3	Liu (1965)	0.02	1	0.089	0.634	-
4	Wuest and Lorke (2003)	0.02	1	0.098	0.559	-
5	Liu (1965)	0.01	1	0.100	0.543	-
6	Liu (1965)	0.03	1	0.086	0.661	-
7	Liu (1965)	0.04	1	0.086	0.663	-
9	**Liu (1965)**	**0.04**	**1.28**	**0.096**	**0.559**	**Extended time series**

References: Liu, 1965; Wuest and Lorke, 2013; Jensen et al., 2012; Deltares, 2014a

[11] RMSE and NSE are calculated for water surface elevation simulated and observed data across all available sites.

Table 4.8 – Delft3D Final Calibrated Parameter Values

Parameter	Calibrated Value
Wave scheme	Stationary
Wind drag coefficient	Liu (1965)
Manning's roughness	0.04
C_{JON}	0.067
γ (Depth-induced breaking)	0.55

References: Liu, 1965

Table 4.9 – Summary of Parameters for Delft3D-FLOW Model

Grid Parmeters	Lake Michigan Flow Grid 1	Lake Huron Flow Grid 2	Strait of Mackinac	Flow Grid 2	Reference
Grid Type	Rectangular	Rectangular	Rectangular	Rectangular	-
Grid Cell Size	2 km	2 km	0.66 km	0.285 km	-
Grid Cells M Direction	129	196	43	176	-
Grid Cells N Direction	268	183	94	183	-
Reference Datum	Model datum	Model datum	Model datum	Model datum	-
Coordinate System	Cartesian GCS North American 1927 NAD 1927 Albers projection	Cartesian GCS North American 1927 NAD 1927 Albers projection	Cartesian GCS North American 1927 NAD 1927 Albers projection	Cartesian GCS North American 1927 NAD 1927 Albers projection	-
Number of Layers	1	1	1	1	-
Thin Dams	None Specified	None Specified	None Specified	None Specified	-
Dry Points	None Specified	None Specified	None Specified	None Specified	-
Time Step	0.25 min	0.25 min	0.25 min	0.25 min	-
Physical Processes Modeled	Wind and Pressure Forcing; Online Wave Interactions	Wind and Pressure Forcing; Online Wave Interactions	Wind and Pressure Forcing; Online Wave Interactions	Wind and Pressure Forcing; Online Wave Interactions	Deltares (2014a)
Initial Condition Water Level	Uniform at 0 m	Uniform at 0 m	Uniform at 0 m	Uniform at 0 m	-
Open Boundary Conditions	N/A	N/A	N/A	N/A	-
Boundary Conditions Type	N/A	N/A	N/A	N/A	-
Number of Boundary Conditions	0	0	0	0	-
Open Boundary Condition Pressure	N/A	N/A	N/A	N/A	-
Open Boundary Condition Reflection Coefficient	N/A	N/A	N/A	N/A	-

Grid Parmeters	Lake Michigan Flow Grid 1	Lake Huron Flow Grid 2	Strait of Mackinac	Flow Grid 2	Reference
Gravitational Acceleration	9.81 m/s^2	9.81 m/s^2	9.81 m/s^2	9.81 m/s^2	NOAA (1986)
Water Density	1000 kg/m^3	1000 kg/m^3	1000 kg/m^3	1000 kg/m^3	Street et al. (1996)
Air Density	1.28 kg/m^3	1.28 kg/m^3	1.28 kg/m^3	1.28 kg/m^3	Street et al. (1996)
Wind Drag Coefficient Breakpoints	A – 0.00063 at 0 m/s B – 0.0025 at 25 m/s C – 0.0025 at 100 m/s	A – 0.00063 at 0 m/s B – 0.0025 at 25 m/s C – 0.0025 at 100 m/s	A – 0.00063 at 0 m/s B – 0.0025 at 25 m/s C – 0.0025 at 100 m/s	A – 0.00063 at 0 m/s B – 0.0025 at 25 m/s C – 0.0025 at 100 m/s	Deltares (2014a)
Bottom Roughness	Spatially varied Manning's n (0.02 uniform)	Spatially varied Manning's n (0.02 uniform)	Spatially varied Manning's n (0.02 uniform)	Spatially varied Manning's n (0.02 uniform)	-
Stress Formulation due to Wave Forces	Fredsoe	Fredsoe	Fredsoe	Fredsoe	Deltares (2014a)
Wall Roughness Slip Condition	Free Slip	Free Slip	Free Slip	Free Slip	Deltares (2014a)
Eddy Viscosity / Diffusivity	Uniform at 1 m^2/s	Uniform at 1 m^2/s	Uniform at 1 m^2/s	Uniform at 1 m^2/s	Deltares (2014a)
Wind	Space Varying Wind and Pressure	Space Varying Wind and Pressure	Space Varying Wind and Pressure	Space Varying Wind and Pressure	-
Drying and Flooding Check at	Grid Cell Centers and Faces	Grid Cell Centers and Faces	Grid Cell Centers and Faces	Grid Cell Centers and Faces	-
Depth Specified at	Grid Cell Corners	Grid Cell Corners	Grid Cell Corners	Grid Cell Corners	-
Depth at Grid Cell Centers	Maximum	Maximum	Maximum	Maximum	-
Depth at Grid Cell Faces	Mean	Mean	Mean	Mean	-
Advection Scheme for Momentum	Cyclic	Cyclic	Cyclic	Cyclic	-
Threshold Depth	0.1 m	0.1 m	0.1 m	0.1 m	-
Marginal Depth	None	None	None	None	-
Smoothing Time	60 min	60 min	60 min	60 min	-

Grid Parmeters	Lake Michigan Flow Grid 1	Lake Huron Flow Grid 2	Strait of Mackinac	Flow Grid 2	Reference
Threshold Depth for Critical Flow Limiter	N/A	N/A	N/A	N/A	-

References: NOAA, 1986; Street et al., 1996; Deltares, 2014a

Table 4.10 – Summary of Parameter for Delft3D-WAVE Model

Grid Parmeters	Wave Grid 1	Reference
Grid Type	Rectangular	-
Grid Cell Size	2 km	-
Grid Cells M Direction	335	-
Grid Cells N Direction	286	-
Reference Datum	Model Datum	-
Coordinate System	Cartesian GCS North American 1927 NAD 1927 Albers projection	
Spec. Res. N Directions	36	-
Lowest Freq.	0.01 Hz	-
Highest Freq.	1 Hz	-
N bins	24	-
Boundary Hs	N/A	-
Boundary – Peak period	N/A	-
Boundary (nautical)	N/A	-
Boundary - Directional Spreading	N/A	-
Gravity	9.81 m/s^2	NOAA (1986)
Water density	1000 kg/m^3	Street et al. (1996)
North w.r.t. x-axis	90 (deg)	-
Minimum depth	0.05 (m)	-
Generation Mode	3rd generation	Deltares (2014b)
Depth-induced breaking alpha	1	Deltares (2014b)
Depth-induced breaking gamma	0.73	Deltares (2014b)
Non-linear triad interactions alpha	0.1	Deltares (2014b)
Non-linear triad interactions beta	2.2	Deltares (2014b)
Bottom friction type	JONSWAP	Deltares (2014b)
JONSWAP Coefficient	0.067 m^2 / s^3	Deltares (2014b)
Wind Growth	Activated	Deltares (2014b)
Whitecapping	Komen et al.	Deltares (2014b)
Wave Propagation – Refraction	Activated	Deltares (2014b)
Wave Propagation – Frequency Shift	Activated	Deltares (2014b)
Directional space scheme	0.5	-
Frequency space scheme	0.5	-
Relative Change Hs-Tm01	0.1	-
Percentage wet criteria	98%	-
Relative Change Hs	0.1	-
Relative Change TM01	0.1	-
N Iterations	15	-

References: NOAA, 1986; Street et al., 1996; Deltares, 2014b

Table 4.11 – Peak WSEL from Synoptic Screening Events

Scenario	Approach	h (ft)	Hs (ft)	T (s)	R (ft)	WSEL (ft-Plant Datum)	WSEL (ft-NAVD88)
1	1	11.0	2.9	4.6	1.4	+3.5	+584.8
1	2	9.4	2.7	4.5	1.2	+3.2	+584.5
2	1	11.0	2.1	3.4	0.9	+2.9	+584.2
2	2	9.4	2.0	3.3	0.8	+2.7	+584.0
3	1	11.3	4.3	6.0	2.5	+4.8	+586.1
3	2	9.7	3.8	5.9	2.0	+4.3	+585.6
4	1	11.3	4.3	5.9	2.5	+4.9	+586.2
4	2	10.0	4.4	6.0	2.6	+5.2	+586.5
5	1	11.1	2.7	4.4	1.4	+3.6	+584.9
5	2	9.5	2.6	4.4	1.2	+3.3	+584.6
6	1	10.9	1.5	3.6	0.7	+2.6	+583.9
6	2	8.8	3.0	5.1	1.1	+2.6	+583.9
7	1	10.9	2.3	3.9	1.0	+3.0	+584.3
7	2	9.3	2.6	3.6	1.0	+3.0	+584.3
8	1	10.7	4.3	5.1	1.6	+3.3	+584.6
8	2	9.1	4.3	5.2	1.7	+3.4	+584.7
9	1	11.7	3.9	5.9	3.0	+5.7	+587.0
9	2	10.1	4.0	6.3	2.8	+5.5	+586.8
10	1	10.9	4.3	5.4	1.8	+3.7	+585.0
10	2	9.3	4.3	5.4	1.9	+3.8	+585.1
11	1	10.5	3.9	5.1	1.4	+3.0	+584.3
11	2	8.9	3.9	5.1	1.5	+3.0	+584.3
12	1	11.8	4.1	5.8	3.1	+6.0	+587.3
12	2	10.2	4.0	6.0	2.8	+5.5	+586.8
13	**1**	**11.6**	**4.3**	7.1	**3.3**	**+6.0**	**+587.3**
13	**2**	**10.2**	**4.1**	8.2	**3.4**	**+6.3**	**+587.6**
14	1	10.8	3.9	7.9	2.1	+3.9	+585.2
14	2	9.2	3.7	7.8	2.0	+3.8	+585.1
15	1	10.8	3.9	7.9	2.1	+3.9	+585.2
15	2	9.2	3.7	7.8	2.0	+3.8	+585.1
16	1	11.0	4.0	7.0	2.1	+4.1	+585.4
16	2	9.4	3.7	7.0	2.0	+4.0	+585.3
17	1	10.7	3.6	4.4	1.3	+3.1	+584.4
17	2	9.1	3.4	4.7	1.4	+3.1	+584.4
18	1	10.8	4.1	4.6	1.5	+3.3	+584.6
18	2	9.3	5.0	6.4	1.5	+3.3	+584.6
19	1	11.1	4.8	5.5	2.1	+4.2	+585.5
19	2	9.5	4.7	5.5	2.2	+4.3	+585.6
20	1	11.4	4.5	5.1	2.4	+4.8	+586.1
20	2	9.9	4.3	5.3	2.3	+4.8	+586.1
21	1	10.9	4.4	7.1	2.2	+4.1	+585.4
21	2	9.3	3.9	7.0	1.9	+3.9	+585.2
22	1	11.0	5.0	5.5	1.5	+3.4	+584.7

Scenario	Approach	h (ft)	Hs (ft)	T (s)	R (ft)	WSEL (ft-Plant Datum)	WSEL (ft-NAVD88)
22	2	9.4	4.8	5.5	1.7	+3.7	+585.0
23	1	11.4	4.3	5.5	2.3	+4.7	+586.0
23	2	9.8	4.4	5.6	2.3	+4.7	+586.0
24	1	11.3	4.7	5.3	2.5	+4.7	+586.0
24	2	9.7	4.4	5.4	2.2	+4.6	+585.9
25	1	11.0	3.8	5.9	2.0	+4.1	+585.4
25	2	9.2	3.6	7.1	1.9	+3.7	+585.0
26	1	11.0	4.7	6.7	1.9	+3.9	+585.2
26	2	9.4	4.7	6.8	2.1	+4.0	+585.3
27	1	10.8	4.6	5.1	1.6	+3.4	+584.7
27	2	9.2	4.3	5.1	1.7	+3.5	+584.8
28	1	11.1	4.5	5.9	2.4	+4.5	+585.8
28	2	9.5	4.0	5.9	1.9	+4.1	+585.4
29	1	12.7	7.1	8.6	1.4	+5.1	+586.4
29	2	11.1	6.2	8.5	1.5	+5.2	+586.5
30	1	11.0	1.2	3.2	0.5	+2.5	+583.8
30	2	9.4	1.3	3.2	0.5	+2.5	+583.8
31	1	12.7	7.1	8.6	1.4	+5.0	+586.3
31	2	11.1	6.2	8.5	1.5	+5.2	+586.5
32	1	11.0	3.8	5.7	2.0	+4.0	+585.3
32	2	9.4	3.4	5.4	1.5	+3.5	+584.8
33	1	11.3	4.7	5.7	2.5	+4.7	+586.0
33	2	9.6	4.2	5.8	2.1	+4.4	+585.7
34	1	11.0	2.0	3.8	0.9	+2.9	+584.2
34	2	9.4	1.9	3.8	0.8	+2.8	+584.1
35	1	11.0	2.5	4.8	1.3	+3.3	+584.6
35	2	9.4	2.3	4.6	1.0	+3.0	+584.3
36	1	11.5	4.1	5.8	2.6	+5.1	+586.4
36	2	9.8	3.7	5.6	2.1	+4.6	+585.9
37	1	11.3	4.7	6.2	2.7	+5.0	+586.3
37	2	9.8	4.6	6.7	2.6	+4.9	+586.2
38	1	11.2	2.8	5.1	1.6	+3.8	+585.1
38	2	9.5	2.6	4.9	1.3	+3.5	+584.8
39	1	11.4	2.8	4.4	1.7	+4.1	+585.4
39	2	9.7	2.6	4.3	1.4	+3.7	+585.0
40	1	10.7	2.0	3.2	0.6	+2.4	+583.7
40	2	9.1	2.0	3.2	0.6	+2.4	+583.7
41	1	11.8	4.0	5.3	3.0	+5.9	+587.2
41	2	10.2	4.1	5.8	2.7	+5.5	+586.8
42	1	11.0	0.9	1.5	0.2	+2.2	+583.5
42	2	9.4	0.9	1.6	0.2	+2.2	+583.5
43	1	10.7	4.3	5.2	1.6	+3.3	+584.6
43	2	9.1	4.2	5.2	1.7	+3.4	+584.7
44	1	11.4	4.2	4.8	2.3	+4.7	+586.0
44	2	9.9	4.4	5.4	2.4	+4.9	+586.2

Scenario	Approach	h (ft)	Hs (ft)	T (s)	R (ft)	WSEL (ft-Plant Datum)	WSEL (ft-NAVD88)
45	1	10.7	3.1	4.6	1.2	+2.8	+584.1
45	2	9.1	3.1	4.5	1.2	+2.9	+584.2

References: None

Table 4.12 – PMSS Results at PBNP

Scenario	Water Depth (ft)	Hs (ft)	T (s)	PMSS SWL[12]		Wave Runup (ft) [13]	Peak WSEL at Beach Riprap	
				(ft-Plant Datum)	(ft-NAVD88)		(ft-Plant Datum)	(ft-NAVD88)
PMSS	3.7	2.4	11.0	+4.5	+585.8	+3.9	+8.4	+589.7

References: None

[12] SWL is presented at the timestep of maximum WSEL, this is not necessarily the peak SWL.

[13] Runup is calculated using the empirical USACE (2008) formulae for runup on a gently sloping, impermeable surface.

Table 4.13 – Peak Seiche SWL from Squall Line Events

Squall Line Event	Antecedent Lake Level,[14]		Maximum Seiche Amplitude, (ft)	Total Maximum SWL,	
	(ft-NAVD88)	(ft-Plant Datum)		(ft-NAVD88)	(ft-Plant Datum)
Maximized May 31, 1998 Derecho Event	+583.1	+1.8	+1.0	+584.1	+2.8

References: None

[14] Antecedent Lake level for the maximum seiche simulations was the 100-year recurrence monthly average high Lake level, +583.1 ft-NAVD88 (+1.8 ft-Plant Datum).

Table 4.14 – Low Water SWL from Synoptic and Squall Line Events

Event	Antecedent Lake Level,[15]		Maximum Wind Setdown, (ft)	Minimum SWL,	
	(ft-NAVD88)	(ft-Plant Datum)		(ft-NAVD88)	(ft-Plant Datum)
Jan. 25-28, 1978 N Transposed Synoptic	+575.6	-5.7	-1.0	+574.6	-6.7
Jan. 25-28, 1978 SW Transposed Synoptic	+575.6	-5.7	-0.3	+575.3	-6.0
Oct. 27-28, 2010 NW Transposed Synoptic	+575.6	-5.7	-1.2	+574.4	-6.9
Oct. 29-Nov. 1, 2012 NW Transposed Synoptic	+575.6	-5.7	-1.3	+574.3	-7.0
Oct. 27-28, 2010 NW Transposed Synoptic, Shifted E	+575.6	-5.7	-1.1	+574.5	-6.8
Oct. 27-28, 2010 NW Transposed Synoptic, Shifted N	+575.6	-5.7	-1.3	+574.3	-7.0
Oct. 29-Nov. 1, 2012 NW Transposed Synoptic, Shifted E	+575.6	-5.7	-1.3	+574.3	-7.0
Oct. 29-Nov. 1, 2012 NW Transposed Synoptic, Shifted N	+575.6	-5.7	-1.3	+574.3	-7.0
Jul. 13-14, 1995 Shifted Squall Line	+575.6	-5.7	-0.3	+575.3	-6.0
May 31, 1998 Shifted Squall Line	+575.6	-5.7	-0.9	+574.7	-6.6
Oct. 29-Nov. 1, 2012 NW Transposed Synoptic, Shifted N with Wind Corrections	**+575.6**	**-5.7**	**-3.3**	**+572.3**	**-9.0**

References: None

[15] Antecedent Lake level for the low-water simulations was the 100-year recurrence monthly average low Lake level, +575.6 ft-NAVD88 (-5.7 ft-Plant Datum).

Table 4.15 – Hydrostatic and Hydrodynamic Loads during LIP Event

	Door	Scenario A			Scenario B		
		Static Force, (lbs/ft)	Impact Force, (lbs/ft)	Total Force, (lbs/ft)	Static Force, (lbs/ft)	Impact Force, (lbs/ft)	Total Force, (lbs/ft)
Turbine Building	**1**	112.6	1.0	113.7	195.0	3.5	**198.5**
	2	112.6	1.9	114.5	195.0	6.7	**201.7**
	4	112.6	0.7	113.3	195.0	3.5	**198.5**
	11	137.6	2.7	140.2	210.9	7.4	**218.3**
	13	137.6	3.2	140.8	210.9	7.0	**217.9**
Diesel Generator	**600**	1.2	0.1	**1.3**	1.2	0.1	**1.3**
	601	0.3	0.0	0.3	0.3	0.0	**0.3**
	602	7.8	0.5	**8.3**	7.8	0.4	8.2
	603	2.8	0.7	**3.5**	2.8	0.7	**3.5**
	604	15.3	0.1	**15.4**	15.3	0.1	**15.4**
Unit 1 & Unit 2	**151**	112.6	1.3	113.9	112.6	1.4	**114.0**
	152	137.6	6.6	144.2	137.6	8.3	**145.9**
	154	165.0	6.0	**171.0**	165.0	3.4	168.4
	159	179.7	6.6	**186.3**	179.7	4.5	184.2
	167	151.0	5.4	**156.4**	151.0	3.5	154.5
	209	31.2	1.1	**32.3**	31.2	1.1	**32.3**
	210	112.6	0.7	113.4	112.6	1.0	**113.7**
	231	165.0	5.6	170.6	165.0	5.8	**170.9**
	232	195.0	8.2	203.2	195.0	8.7	**203.7**
Service Building	**310**	31.2	2.4	33.6	31.2	4.3	**35.5**
	311	25.3	27.5	**52.8**	25.3	26.7	52.0
	312	25.3	24.3	**49.6**	25.3	23.2	48.4
	313	44.9	11.2	**56.1**	44.9	9.1	54.1
	314	37.8	2.2	**39.9**	37.8	2.1	**39.9**
CWPH	**336**[16]	137.6	140.6	**278.2**	195.0	70.3	265.3
	338	244.6	22.3	266.9	360.7	69.9	**430.5**
	339	244.6	21.2	265.8	339.8	29.4	**369.1**
	340[12]	165.0	102.7	*267.7*	210.9	205.2	**416.2**
G5 Building	**G501**	137.6	2.2	139.8	137.6	2.9	**140.5**
	G502	137.6	1.1	138.7	137.6	1.2	**138.8**
	G503	151.0	0.4	151.4	151.0	0.7	**151.8**
	G504	124.8	6.7	**131.5**	124.8	4.1	128.9
	G505	101.1	38.2	**139.3**	101.1	31.2	132.3

References: None

[16] For Scenario B, the cells adjacent to Door 336 and Door 340 were manually elevated to account for temporary wave barriers. Loading values were taken from the closest, unaltered model cells; accordingly, the Scenario B total forces apply only to the barriers at these locations. The Scenario B hydrostatic force component still applies to Door 336 and Door 340. Thus, the bounding total force at Door 340 is for Scenario A (267.7 lbs/ft).

Table 4.16 – Waterborne Projectile Debris Impact Forces and Pressures

Velocity (ft/s)	Waterborne Projectile Impact Force (lb)	Waterborne Projectile Impact Pressure (psf)
1	6,088	4,961
2	12,176	9,922
3	18,264	14,883
4	24,352	19,844
5	30,440	24,805
6	36,528	29,766
7	42,616	34,727
8	48,704	39,688
9	54,792	44,649
10	60,881	49,610
11	66,969	54,571
12	73,057	59,532
13	79,145	64,493
14	85,233	69,454
15	91,321	74,415
16	97,409	79,376
17	103,497	84,337
18	109,585	89,298
19	115,673	94,259
20	121,761	99,220

References: None

Table 5.1 – Comparison of CLB and FHR Flooding Levels by Mechanism and Component

Mechanism		Current License Basis (CLB)	Flood Hazard Reevaluation (FHR)
Precipitation	PMP/LIP	4.9 in. over 6 hr[17]	12.8 in. over 1 hr
	PMP/LIP Maximum Flow Depths	Up to 0.8 ft at CWPH (See Table 3.1)	Up to 3.4 ft at CWPH (See Table 4.2)
Riverine		N/A	N/A
Dam Breaches and Failures		N/A	N/A
PMSS	Antecedent Lake Level	+583.0 ft-NAVD88 (+1.7 ft-Plant Datum)	+583.1 ft-NAVD88 (+1.8 ft-Plant Datum)
	Maximum Storm Surge	5.14 ft[18]	4.5 ft
	Maximum Wave Runup	6.55 ft on vertical structure 5.38 ft on 1:1.5 riprap slope[19]	N/A on vertical structure[20] 3.9 ft on 1:2 riprap slope
	Peak WSEL	+589.72 ft-NAVD88 (+8.42 ft-Plant Datum)[21]	+589.7 ft-NAVD88 (+8.4 ft-Plant Datum)[22]
Seiche	Antecedent Lake Level	N/A	+583.1 ft-NAVD88 (+1.8 ft-Plant Datum)
	Maximum Seiche Amplitude	1 to 2 ft	1.0 ft
	Peak SWL	N/A	+584.1 ft-NAVD88 (+2.8 ft-Plant Datum)
Tsunami		N/A	N/A
Ice-Induced Effects		N/A	N/A

[17] This volume of water is the sum of the water content of snow in late March with a 50-year recurrence frequency and the volume from a six-hour rainfall with a 50-year recurrence frequency (NEE, 2014b).

[18] Storm surge of +4.14 ft added to the maximum recorded Lake Michigan water level, +583.0 ft-NAVD88 (+1.7 ft-Plant Datum) and a +1.0 ft increase for velocities equal or greater than 70 knots (NEE, 2014b).

[19] Slopes are reported as vertical (V) to horizontal (H), V:H.

[20] There is no standing water at PBNP vertical structures during the PMSS event; therefore, there is no wave runup directly on a vertical structure (Section 4.4.10).

[21] Maximum flood elevation equals the maximum recorded Lake Michigan water level, +583.0 ft-NAVD88 (+1.7 ft-Plant Datum), +0.17 ft of wind tide setup, and +6.55 ft of wave runup on a vertical structure (NEE, 2014b).

[22] Maximum combined storm surge and wave runup above the 100-year recurrence monthly average high Lake level at the crest of the riprap slope. Peak WSEL does not necessarily occur at maximum storm surge or maximum wave runup (NEE, 2014b).

Mechanism		Current License Basis (CLB)	Flood Hazard Reevaluation (FHR)
Low-water	Antecedent Lake Level	+576.5 ft-NAVD88 (-4.8 ft-Plant Datum)	+575.6 ft-NAVD88 (-5.7 ft-Plant Datum)
	Maximum Wind Setdown	N/A	-3.3 ft
	Minimum SWL	+576.5 ft-NAVD88 (-4.8 ft-Plant Datum)	+572.3 ft-NAVD88 (-9.0 ft-Plant Datum)

References: NEE, 2014b

NextEra Energy (NEE)
Point Beach Nuclear Plant (PBNP)
Flooding Hazards Reevaluation Report (FHRR)

ENERCON

Figure 2.1
PBNP Site Location

References: ESRI, 2012

NextEra Energy (NEE) **Point Beach Nuclear Plant (PBNP)** **Flooding Hazards Reevaluation Report (FHRR)**	ENERCON
	Figure 4.1 PBNP Site Features
References: ESRI, 2012; NEE, 2014b	FPL-076-FHRPR-002 REV. 2

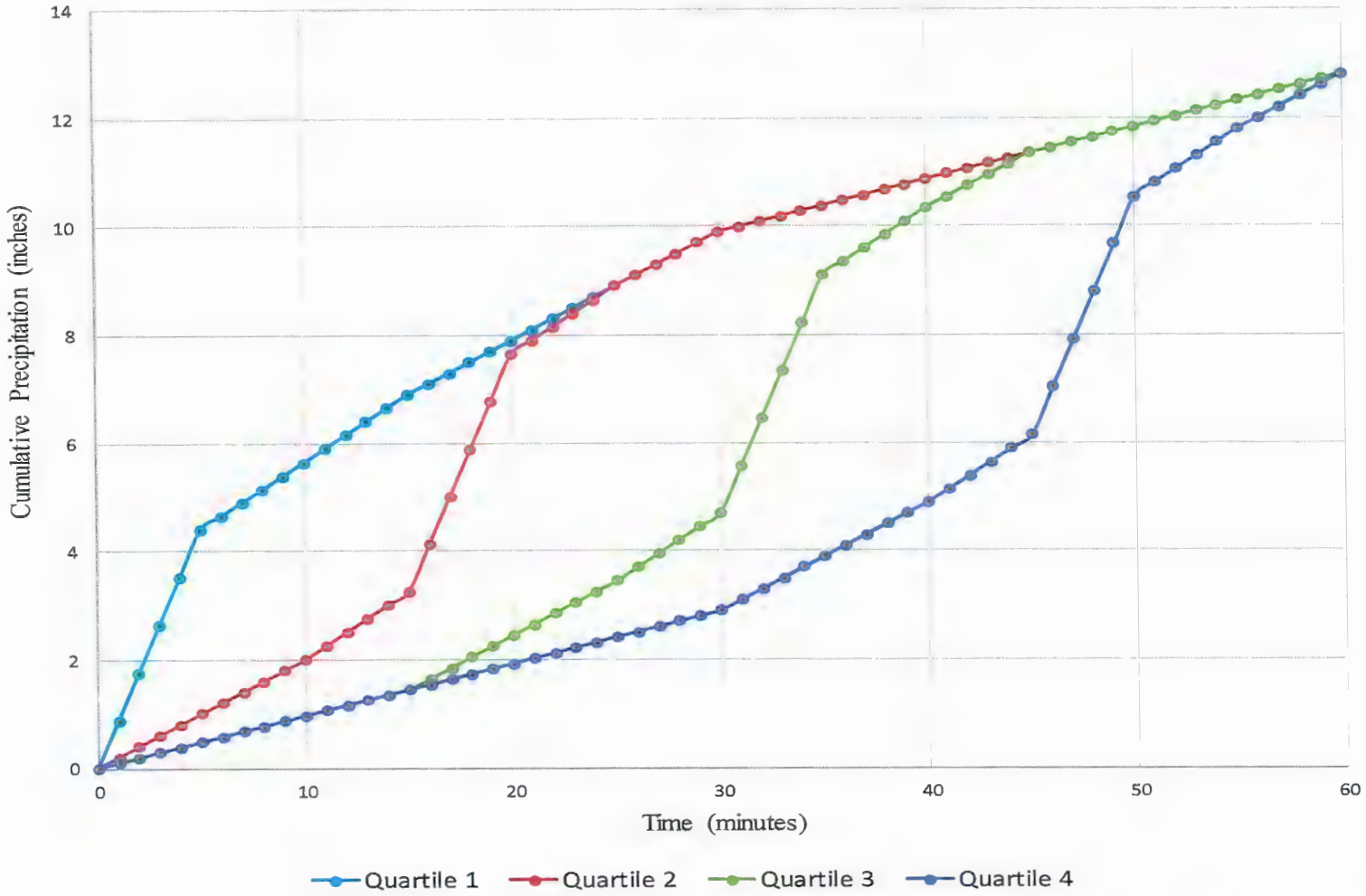

NextEra Energy (NEE) **Point Beach Nuclear Plant (PBNP)** **Flooding Hazards Reevaluation Report (FHRR)**	ENERCON **Figure 4.2** PBNP LIP Hyetographs
References:	FPL-076-FHRPR-002 REV. 2

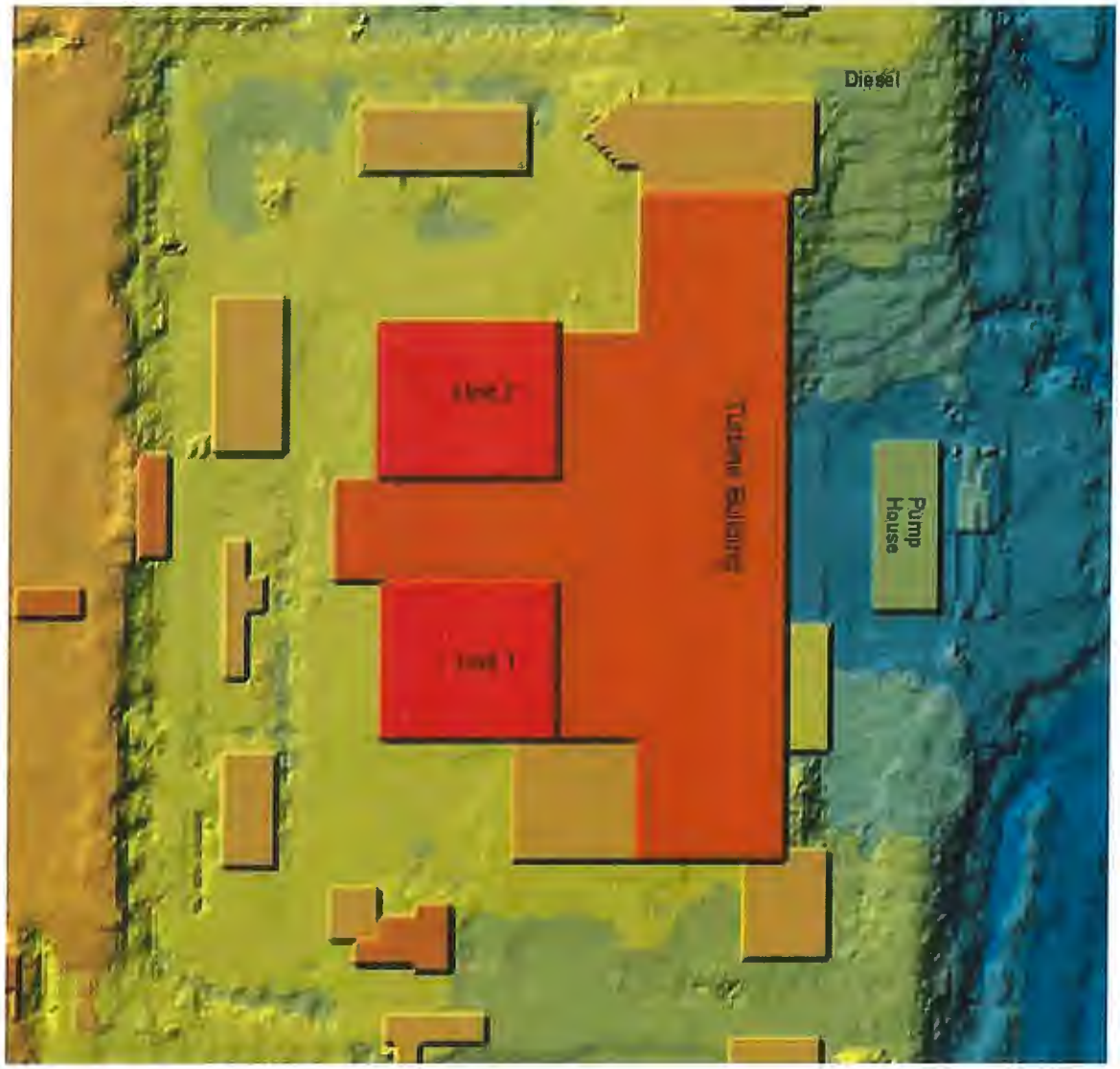

NextEra Energy (NEE)
Point Beach Nuclear Plant (PBNP)
Flooding Hazards Reevaluation Report (FHRR)

ENERCON

Figure 4.3
PBNP DTM Elevations

References:

NextEra Energy (NEE) Point Beach Nuclear Plant (PBNP) Flooding Hazards Reevaluation Report (FHRR)	ENERCON **Figure 4.4** PBNP Manning's Roughness Coefficient Spatial Distribution
References:	FPL-076-FHRPR-002 REV. 2

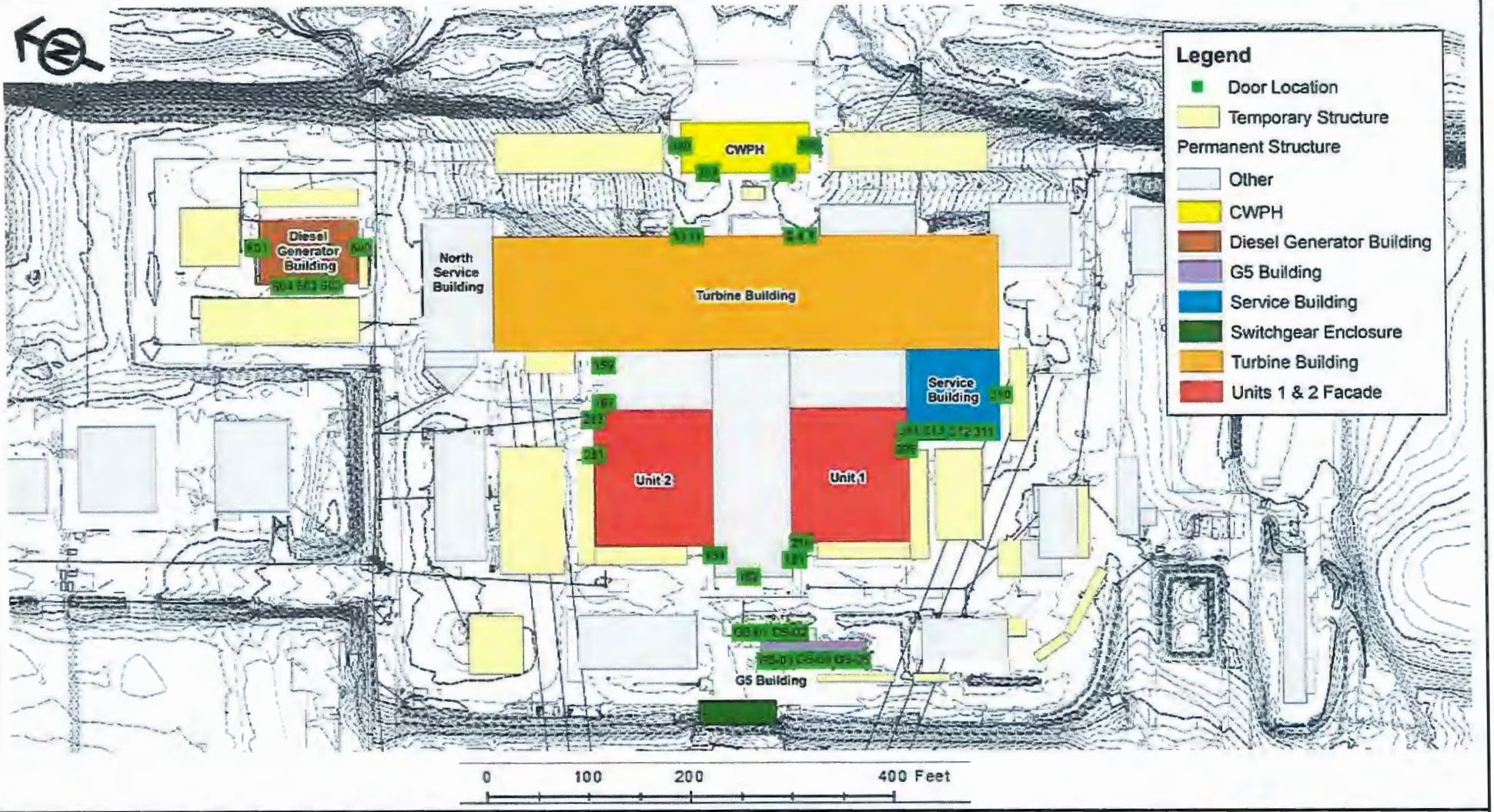

NextEra Energy (NEE)
Point Beach Nuclear Plant (PBNP)
Flooding Hazards Reevaluation Report (FHRR)

ENERCON

Figure 4.5
PBNP Door Locations

References:

FPL-076-FHRPR-002 REV. 2

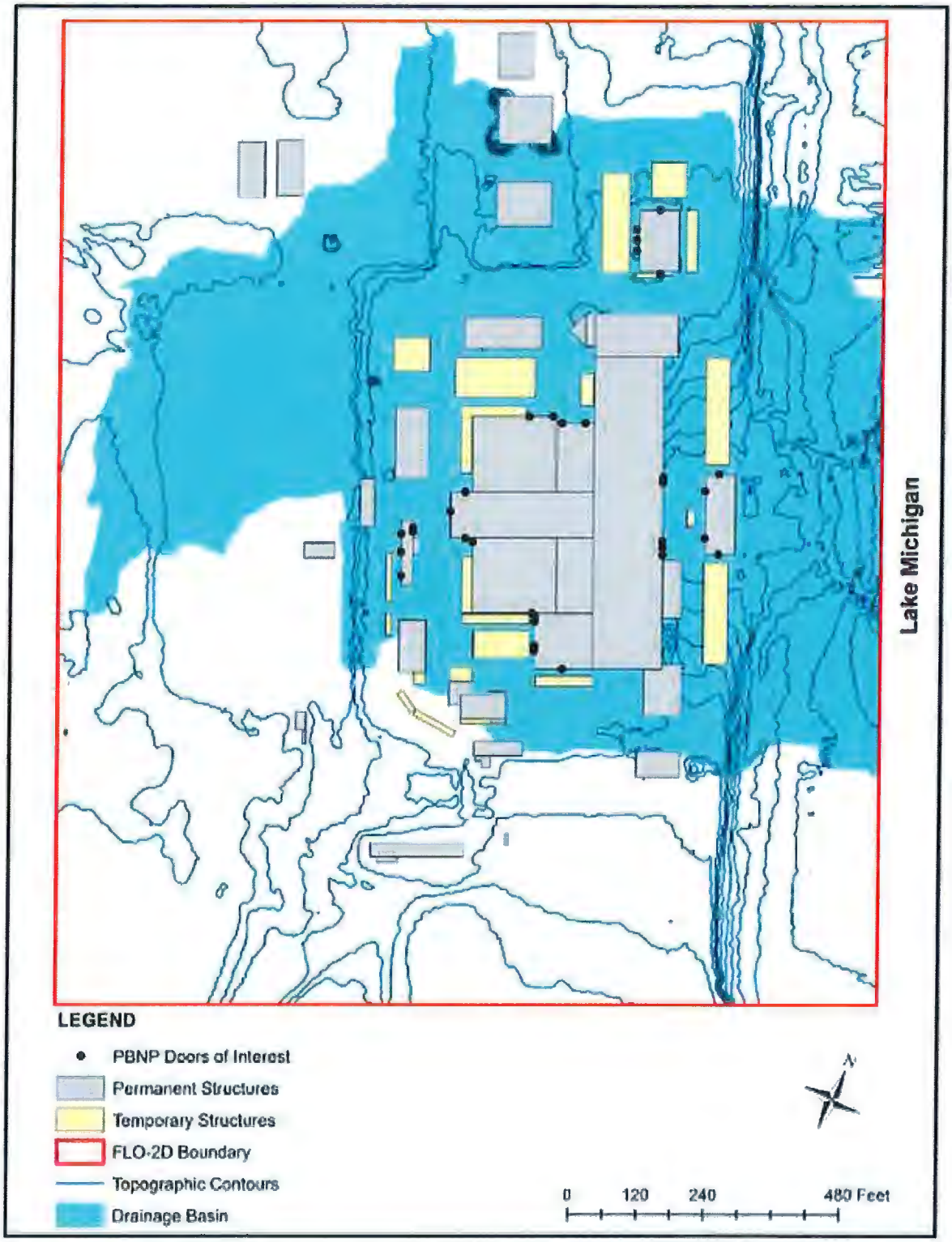

NextEra Energy (NEE)
Point Beach Nuclear Plant (PBNP)
Flooding Hazards Reevaluation Report (FHRR)

ENERCON

Figure 4.6
Direct Drainage Area at PBNP

References:

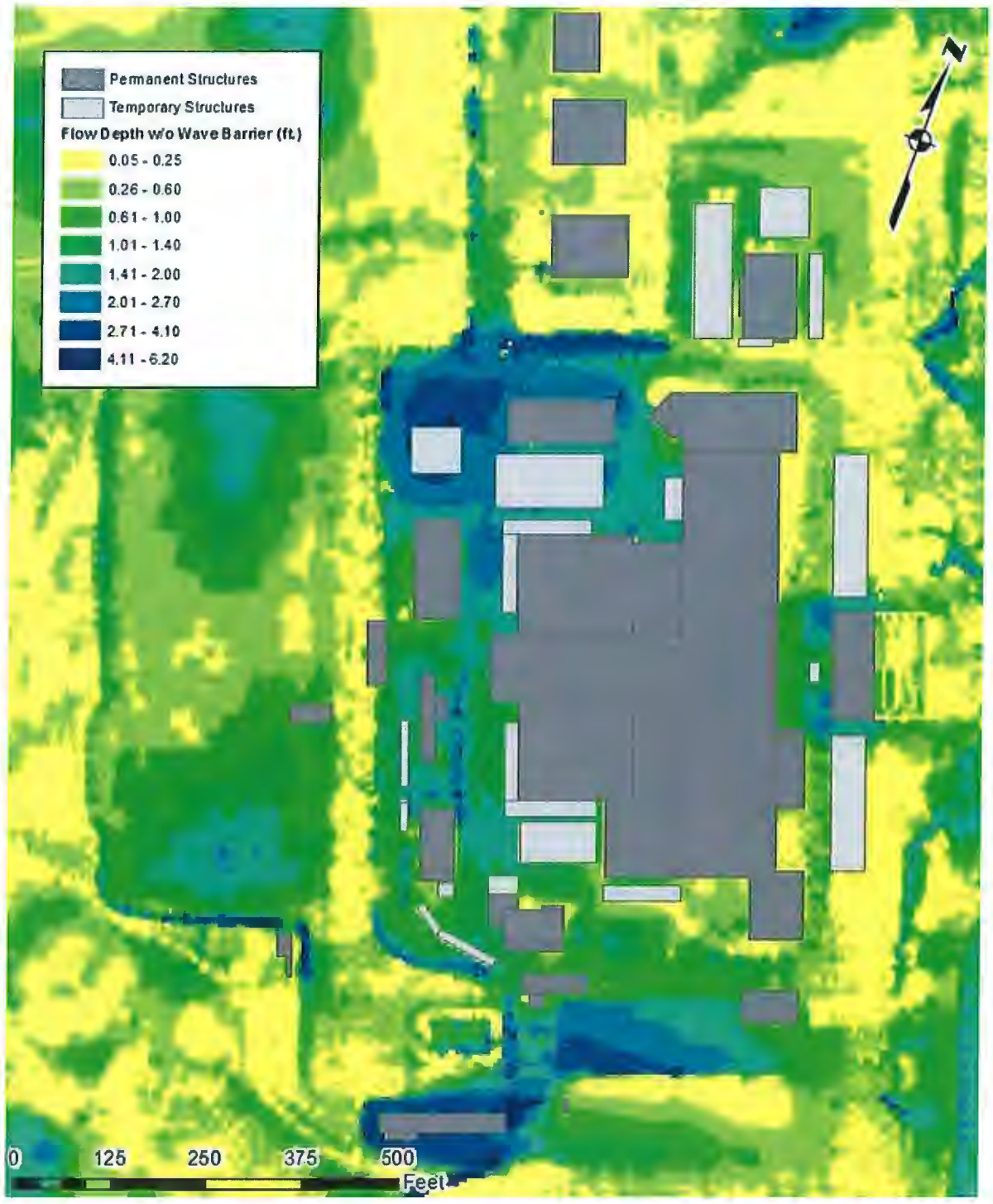

NextEra Energy (NEE)
Point Beach Nuclear Plant (PBNP)
Flooding Hazards Reevaluation Report (FHRR)

ENERCON

Figure 4.7
LIP Maximum Flow Depths – Scenario A

References:

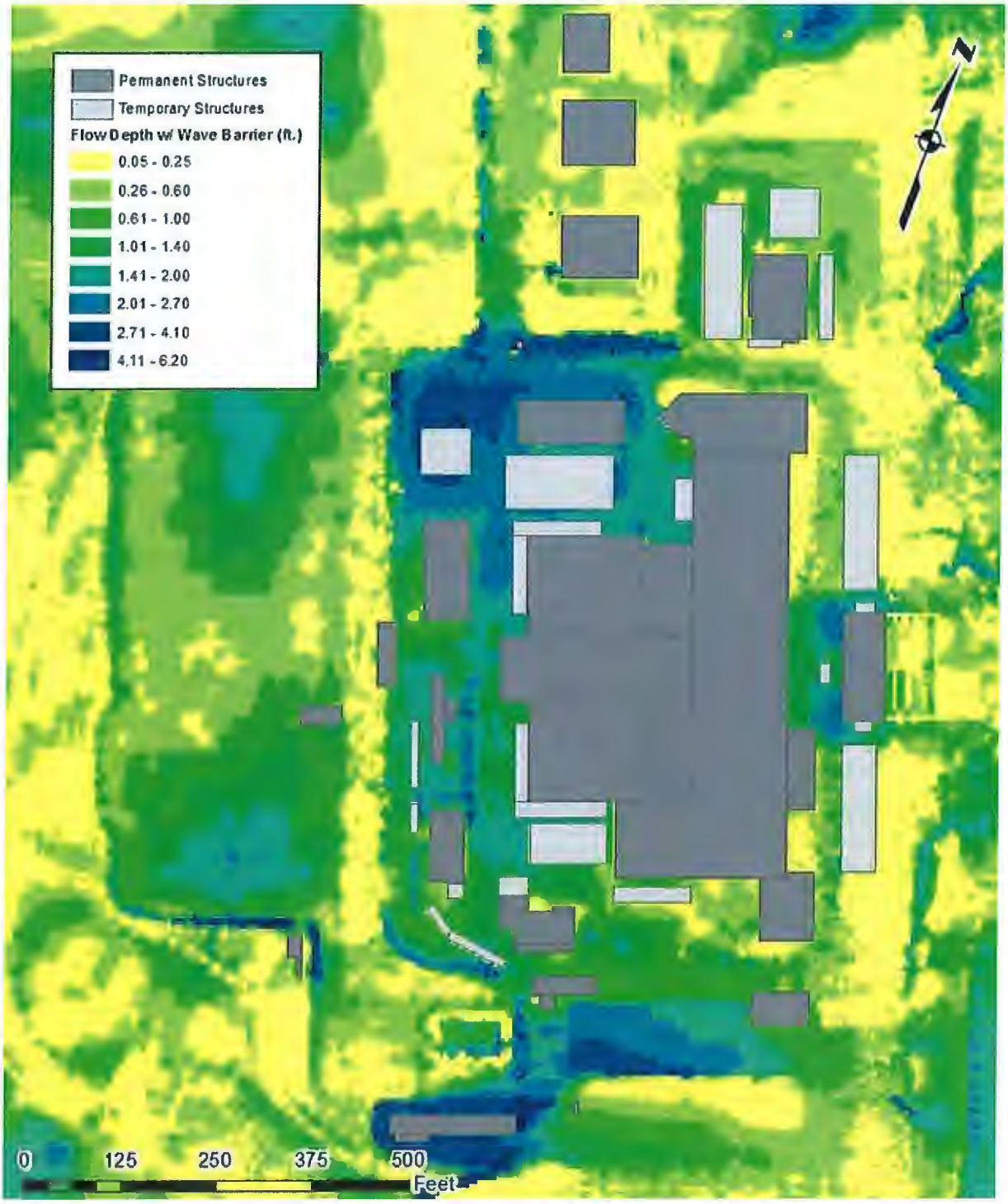

ENERCON

Figure 4.8
LIP Maximum Flow Depths – Scenario B

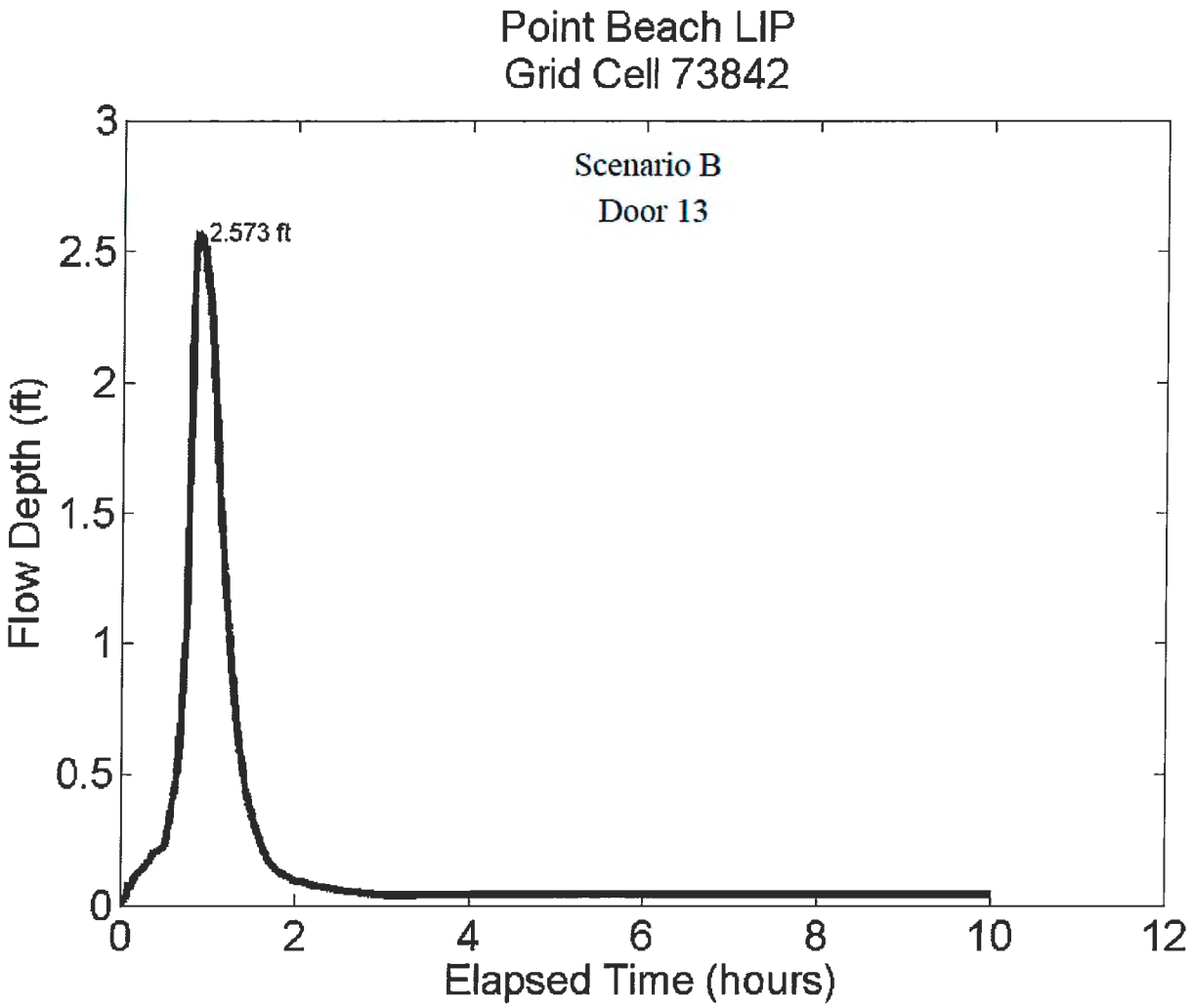
Point Beach LIP
Grid Cell 73842
Scenario B
Door 13
2.573 ft
Flow Depth (ft)
Elapsed Time (hours)
0
0.5
1
1.5
2
2.5
3
0
2
4
6
8
10
12

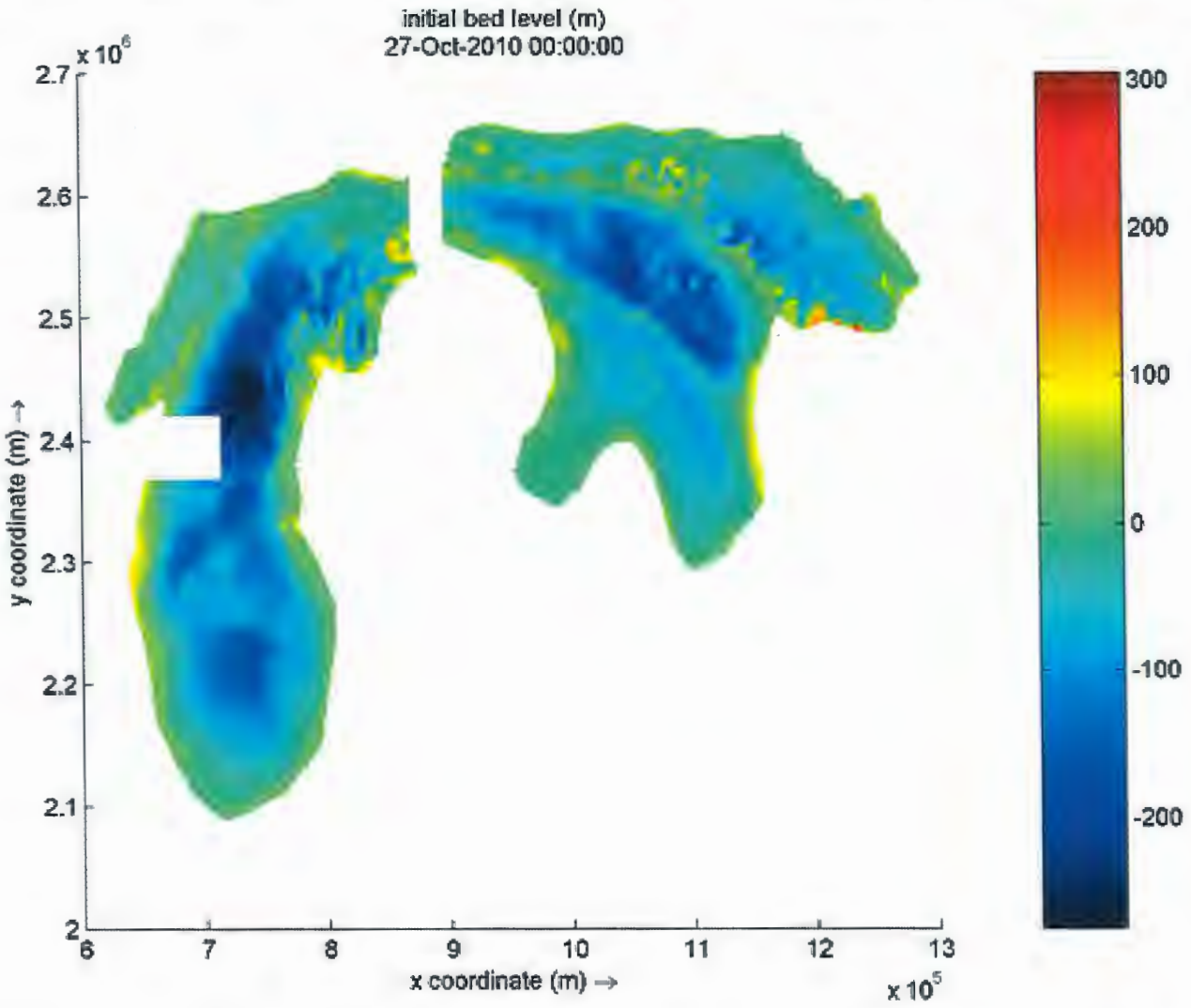

NextEra Energy (NEE)
Point Beach Nuclear Plant (PBNP)
Flooding Hazards Reevaluation Report (FHRR)

ENERCON

Figure 4.10
Delft3D-FLOW Representation of Lake Michigan and Lake Huron

References:

FPL-076-FHRPR-002 REV. 2

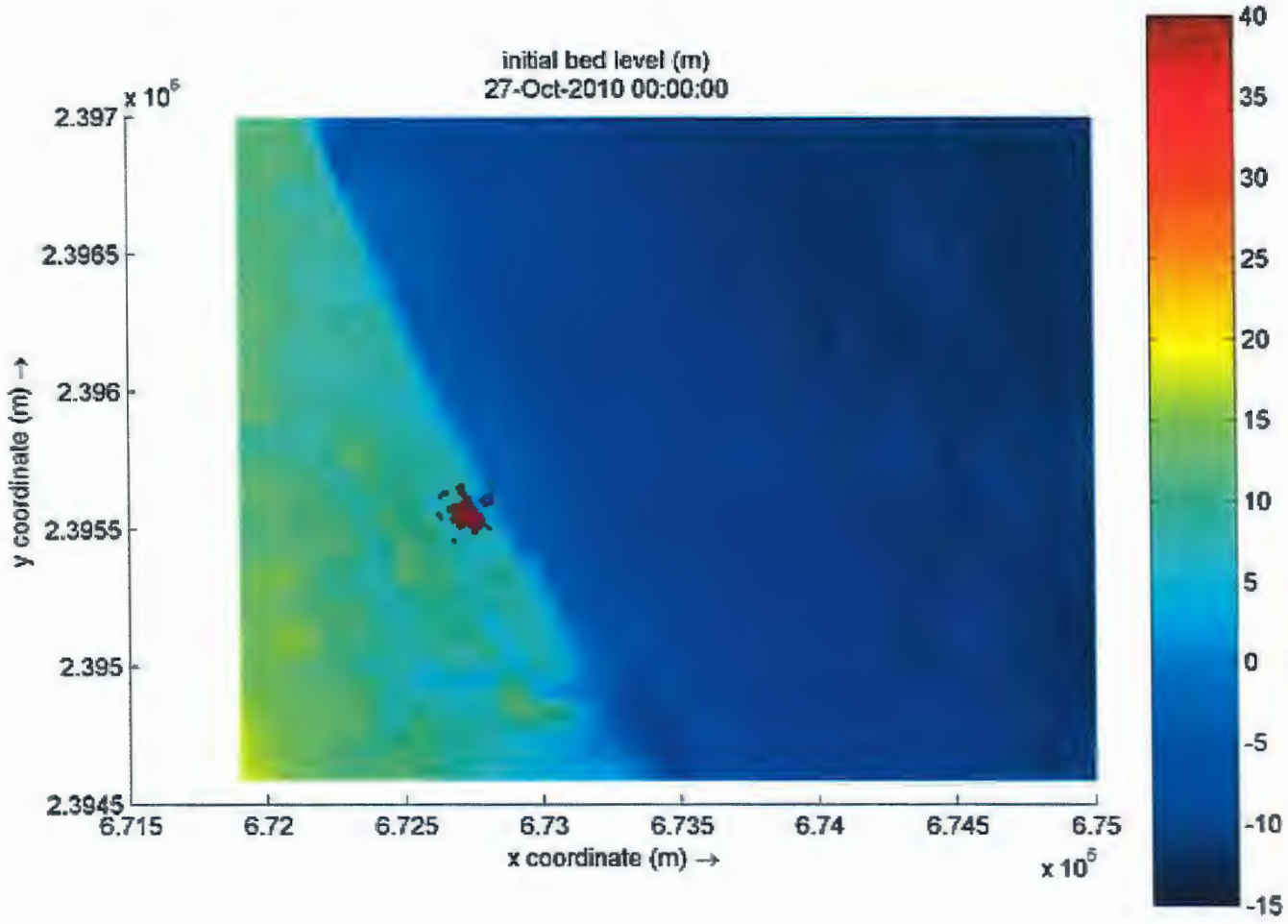

NextEra Energy (NEE) Point Beach Nuclear Plant (PBNP) Flooding Hazards Reevaluation Report (FHRR)	ENERCON **Figure 4.11** Delft3D-FLOW Representation of PBNP Nearshore
References:	FPL-076-FHRPR-002 REV. 2

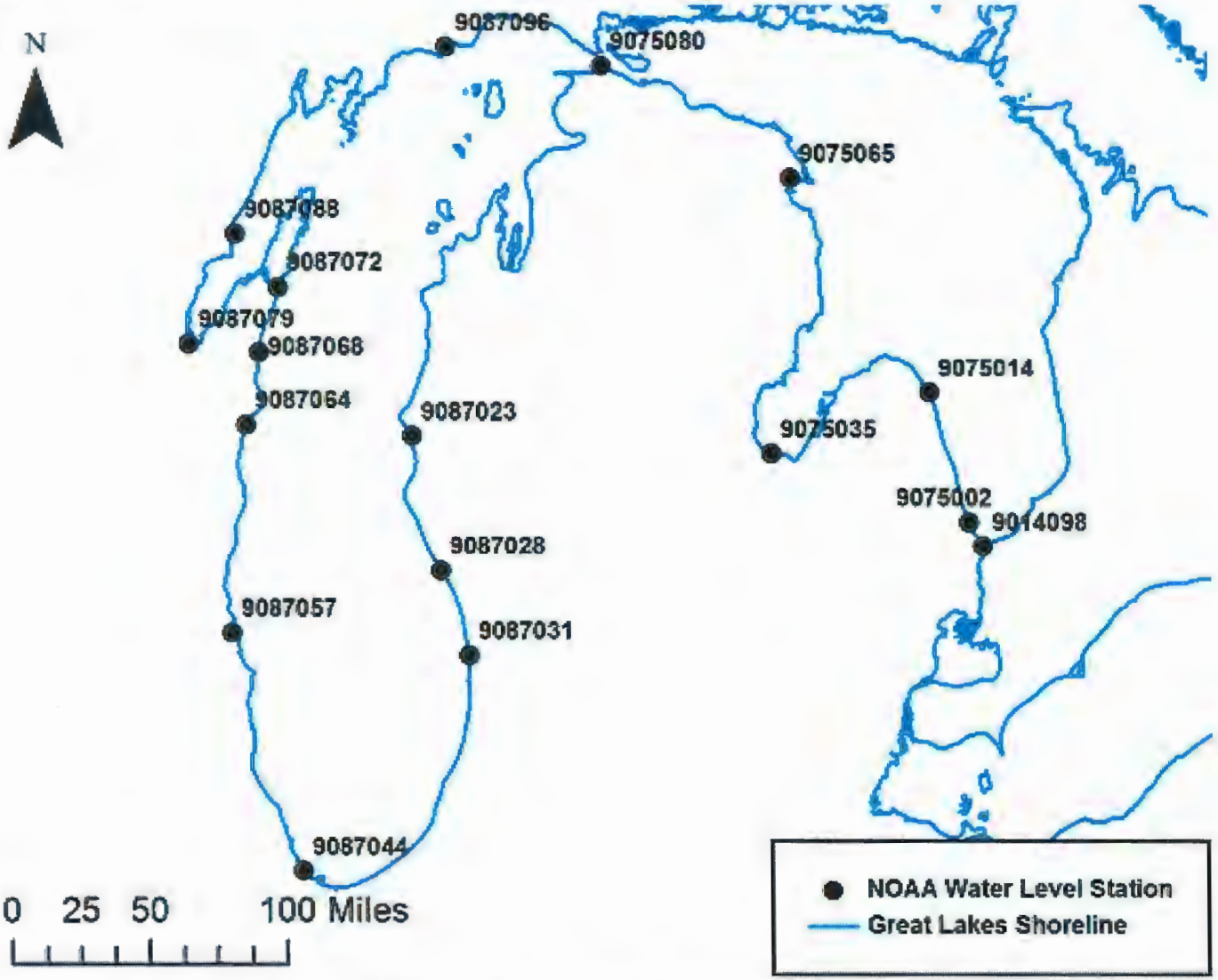

NextEra Energy (NEE)
Point Beach Nuclear Plant (PBNP)
Flooding Hazards Reevaluation Report (FHRR)

ENERCON

Figure 4.12
NOAA Water Level Stations Considered for Calibration and Validation

References: NOAA, 2014b through NOAA, 2014r

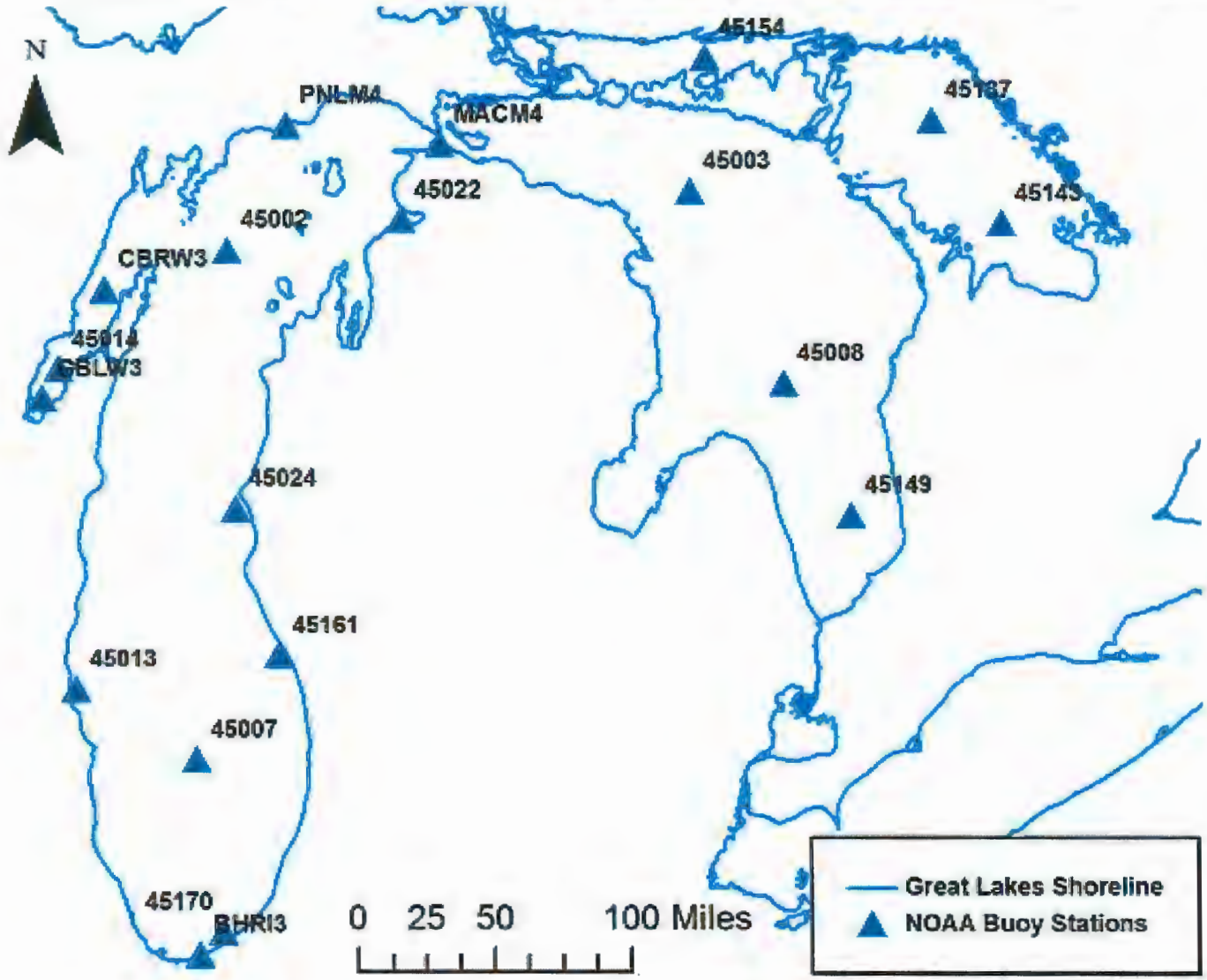

NextEra Energy (NEE)
Point Beach Nuclear Plant (PBNP)
Flooding Hazards Reevaluation Report (FHRR)

ENERCON

Figure 4.13
NOAA Buoy Stations Considered for Calibration and Validation

References: NOAA, 2014s through NOAA, 2014gg

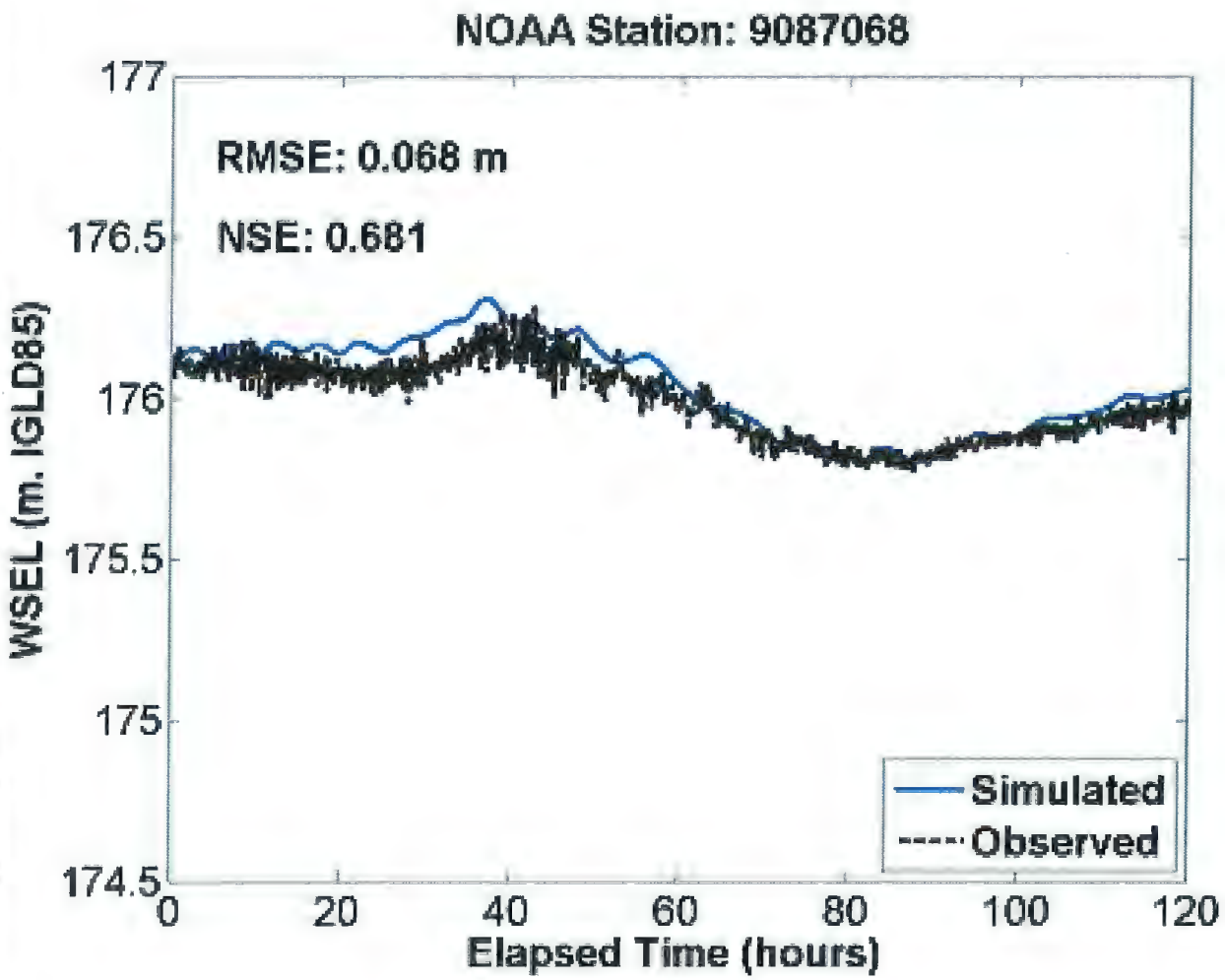

NextEra Energy (NEE) Point Beach Nuclear Plant (PBNP) Flooding Hazards Reevaluation Report (FHRR)	ENERCON
	Figure 4.14 NOAA Station 9087068 Final Calibration Near PBNP
References: NOAA, 2014c	FPL-076-FHRPR-002 REV. 2

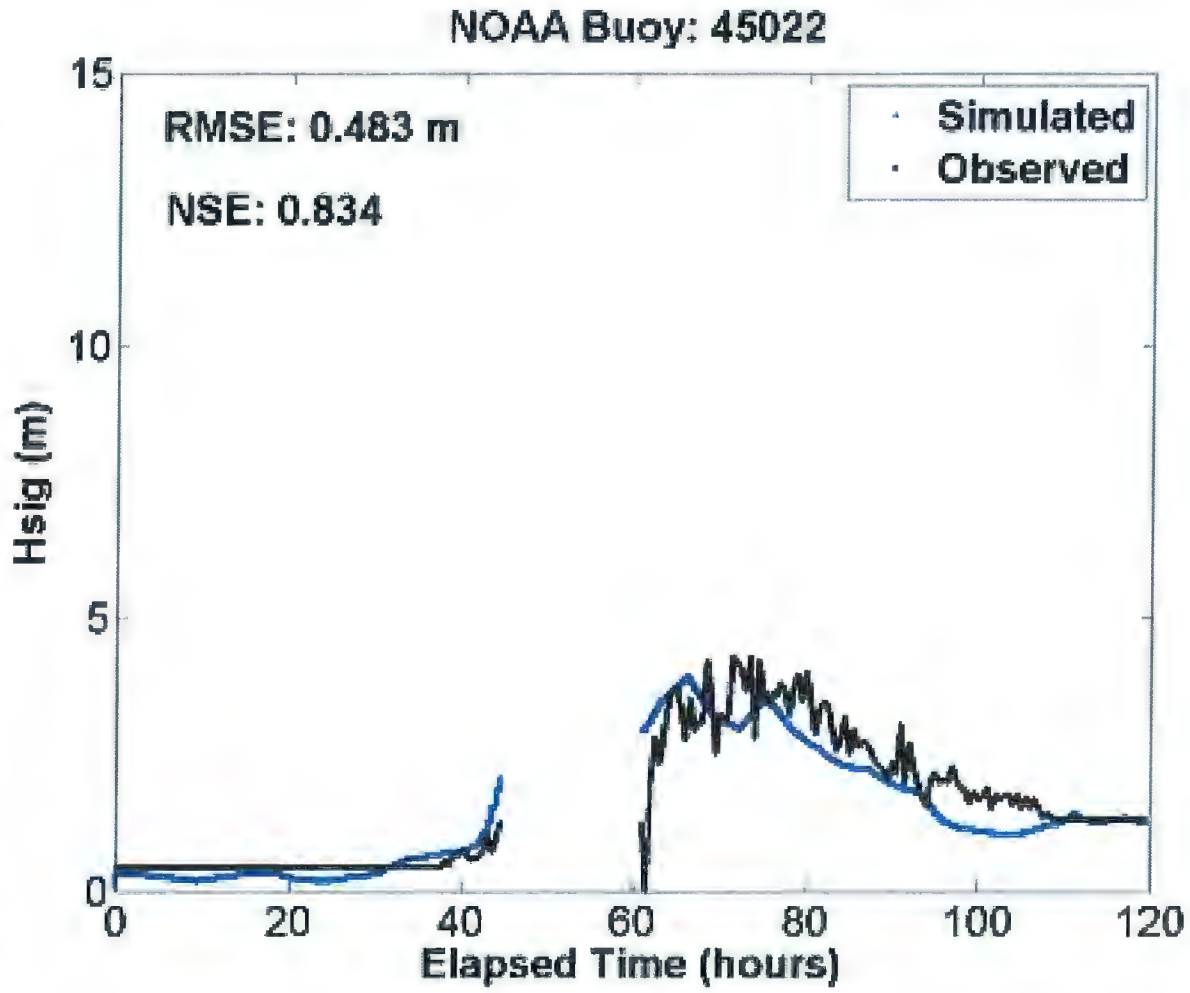

NextEra Energy (NEE) Point Beach Nuclear Plant (PBNP) Flooding Hazards Reevaluation Report (FHRR)	ENERCON
	Figure 4.15 NOAA Buoy 45022 Final Calibration in Shallow Water
References: NOAA, 2014t	FPL-076-FHRPR-002 REV. 2

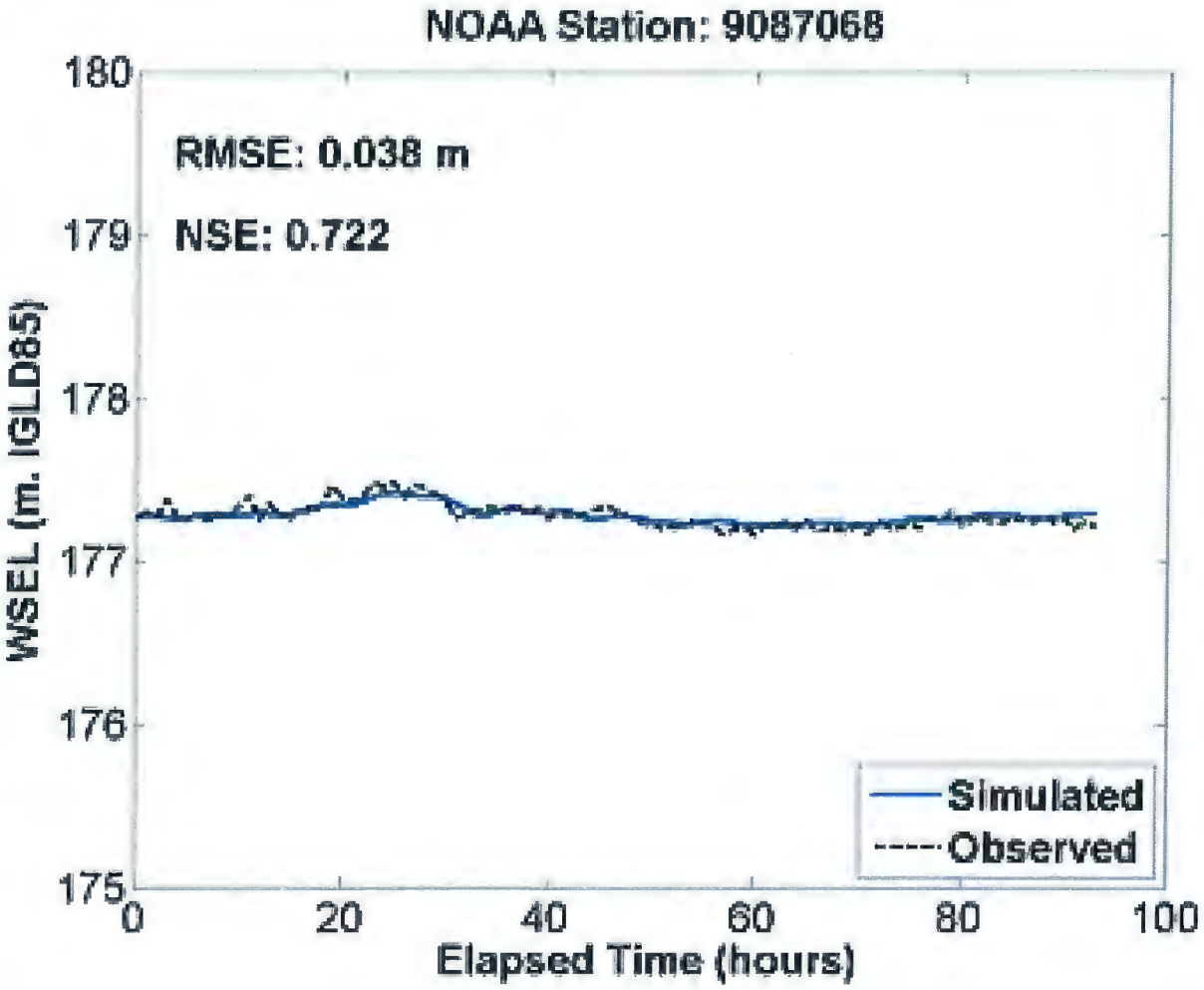
NOAA Station: 9087068
RMSE: 0.038 m
NSE: 0.722
WSEL (m. IGLD85)
Elapsed Time (hours)
Simulated
Observed
180
179
178
177
176
175
0
20
40
60
80
100

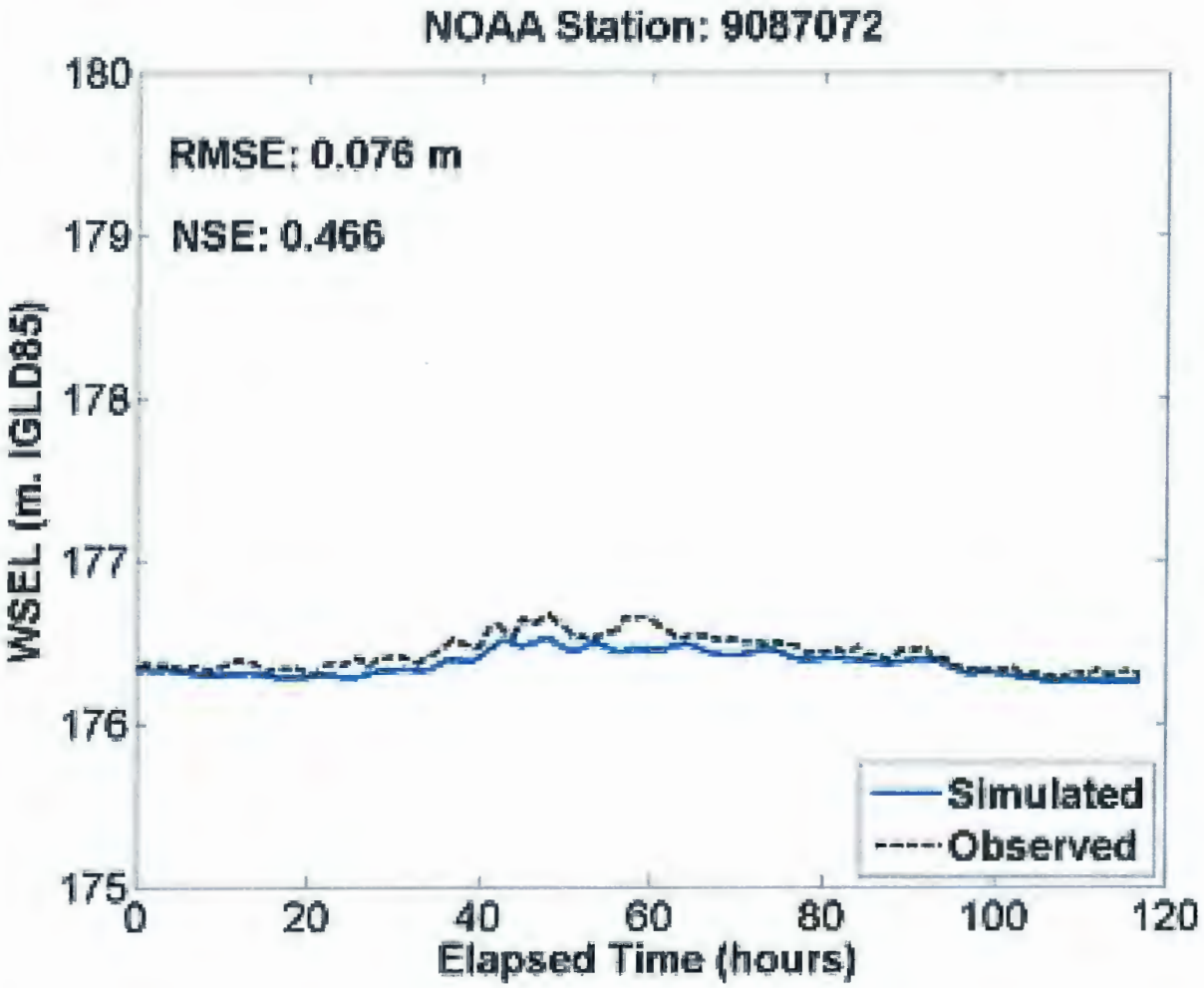
NOAA Station: 9087072
RMSE: 0.076 m
NSE: 0.466
WSEL (m. IGLD85)
180
179
178
177
176
175
0
20
40
60
80
100
120
Elapsed Time (hours)
Simulated
Observed

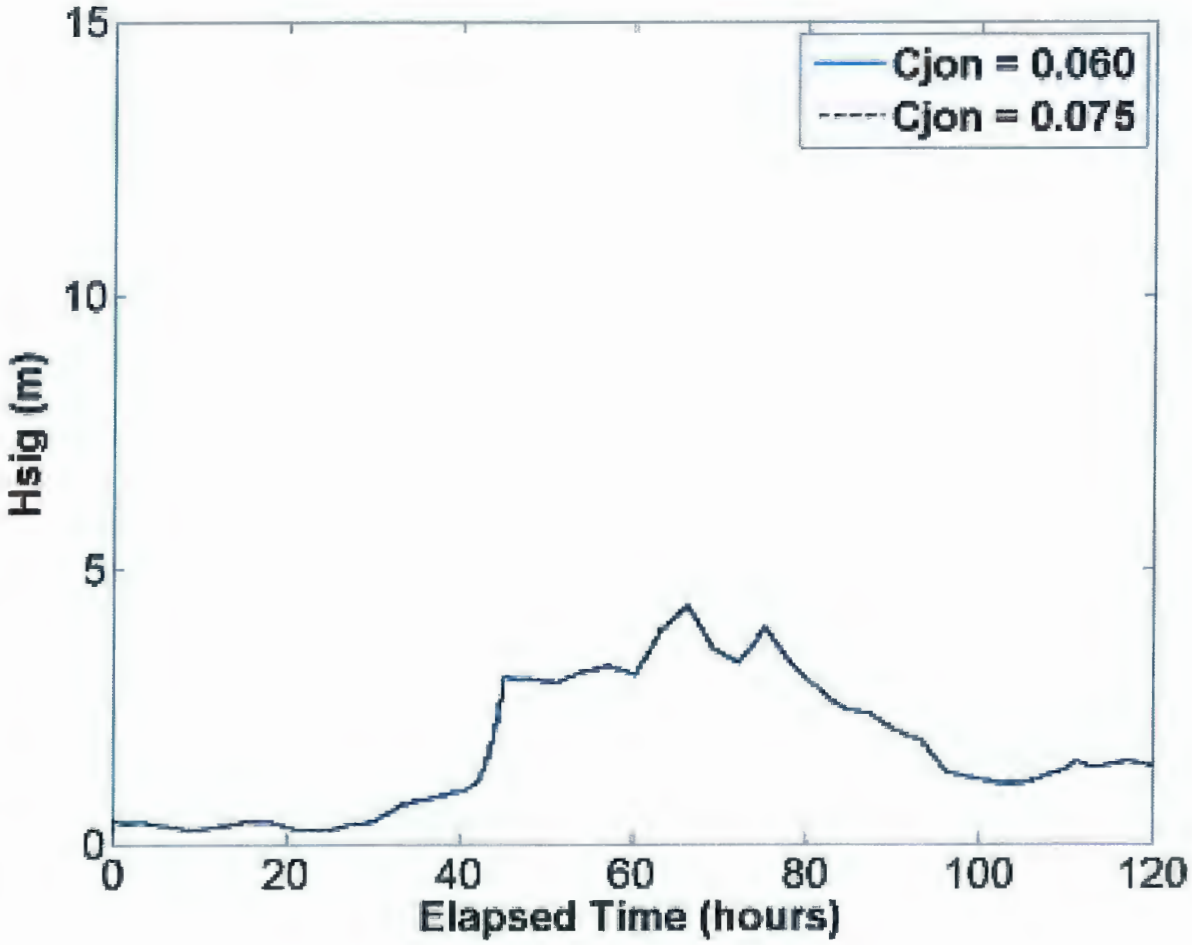
Cjon = 0.060
Cjon = 0.075
Hsig (m)
Elapsed Time (hours)
0
5
10
15
0
20
40
60
80
100
120

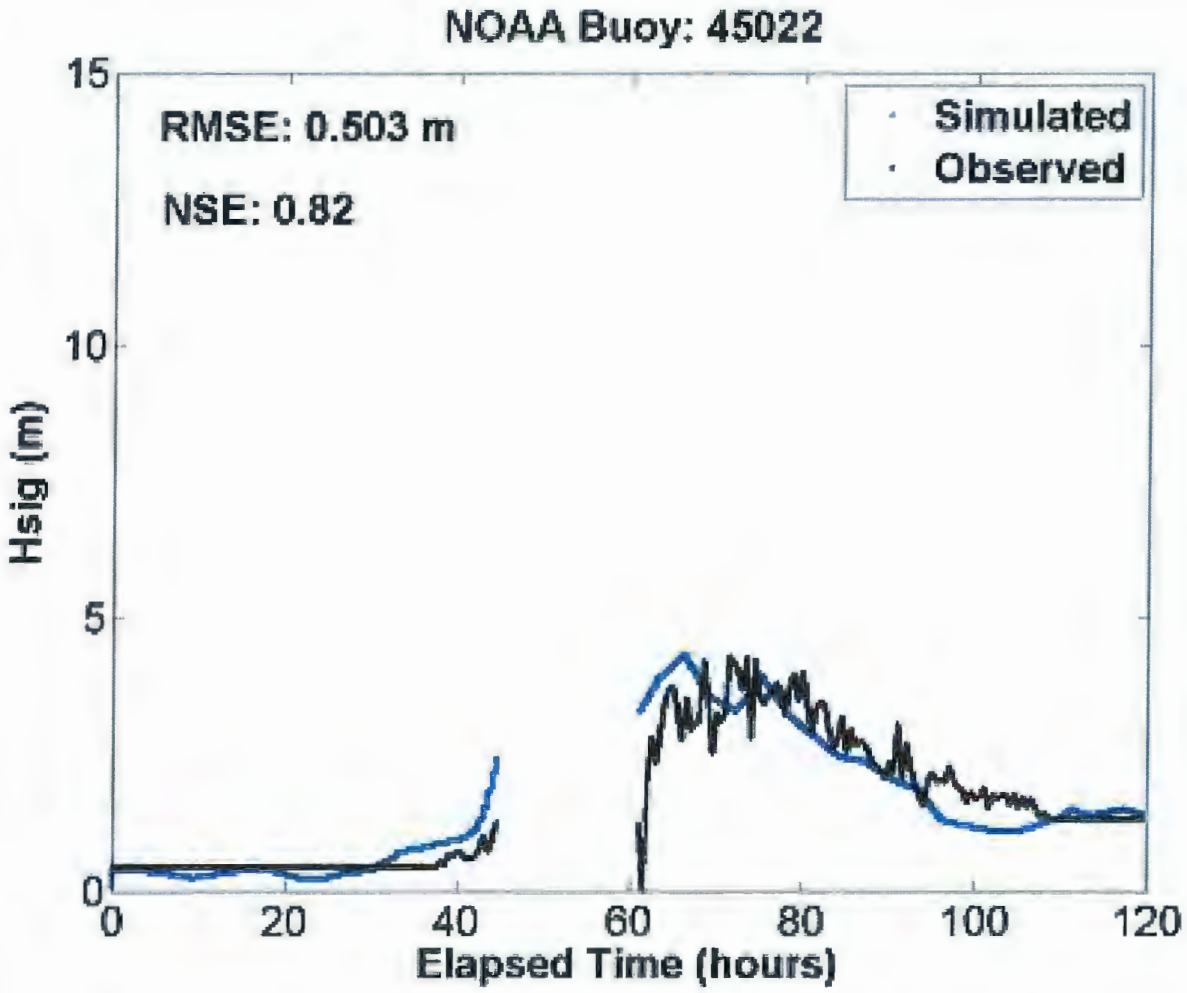

NextEra Energy (NEE) Point Beach Nuclear Plant (PBNP) Flooding Hazards Reevaluation Report (FHRR)	ENERCON
	Figure 4.19 Depth-Induced Breaking Sensitivity (γ = 0.73) for NOAA Buoy 45022
References: NOAA, 2014t	FPL-076-FHRPR-002 REV. 2

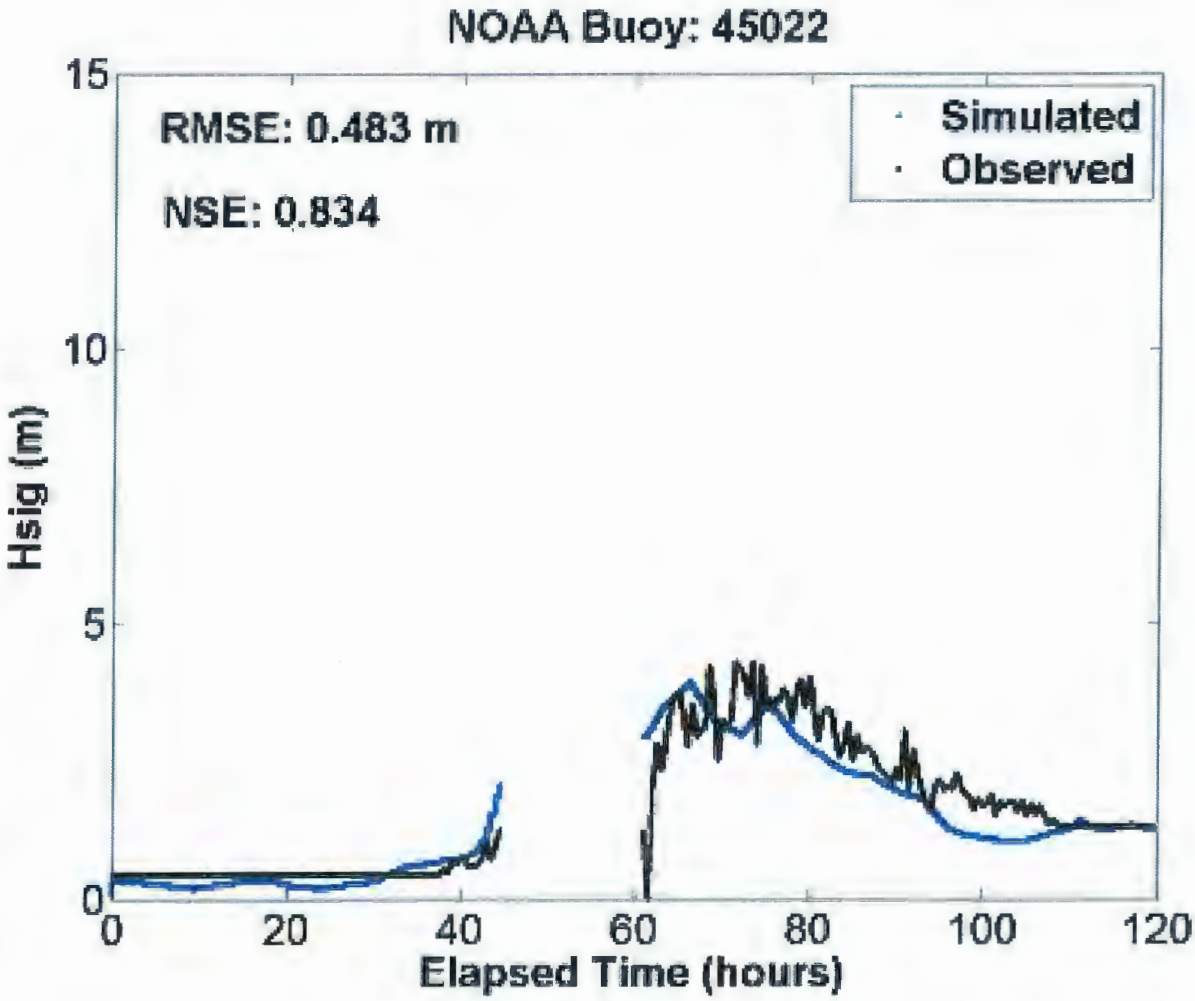

NextEra Energy (NEE) Point Beach Nuclear Plant (PBNP) Flooding Hazards Reevaluation Report (FHRR)	ENERCON
	Figure 4.20 Depth-Induced Breaking Sensitivity (γ = 0.55) for NOAA Buoy 45022
References: NOAA, 2014t	FPL-076-FHRPR-002 REV. 2

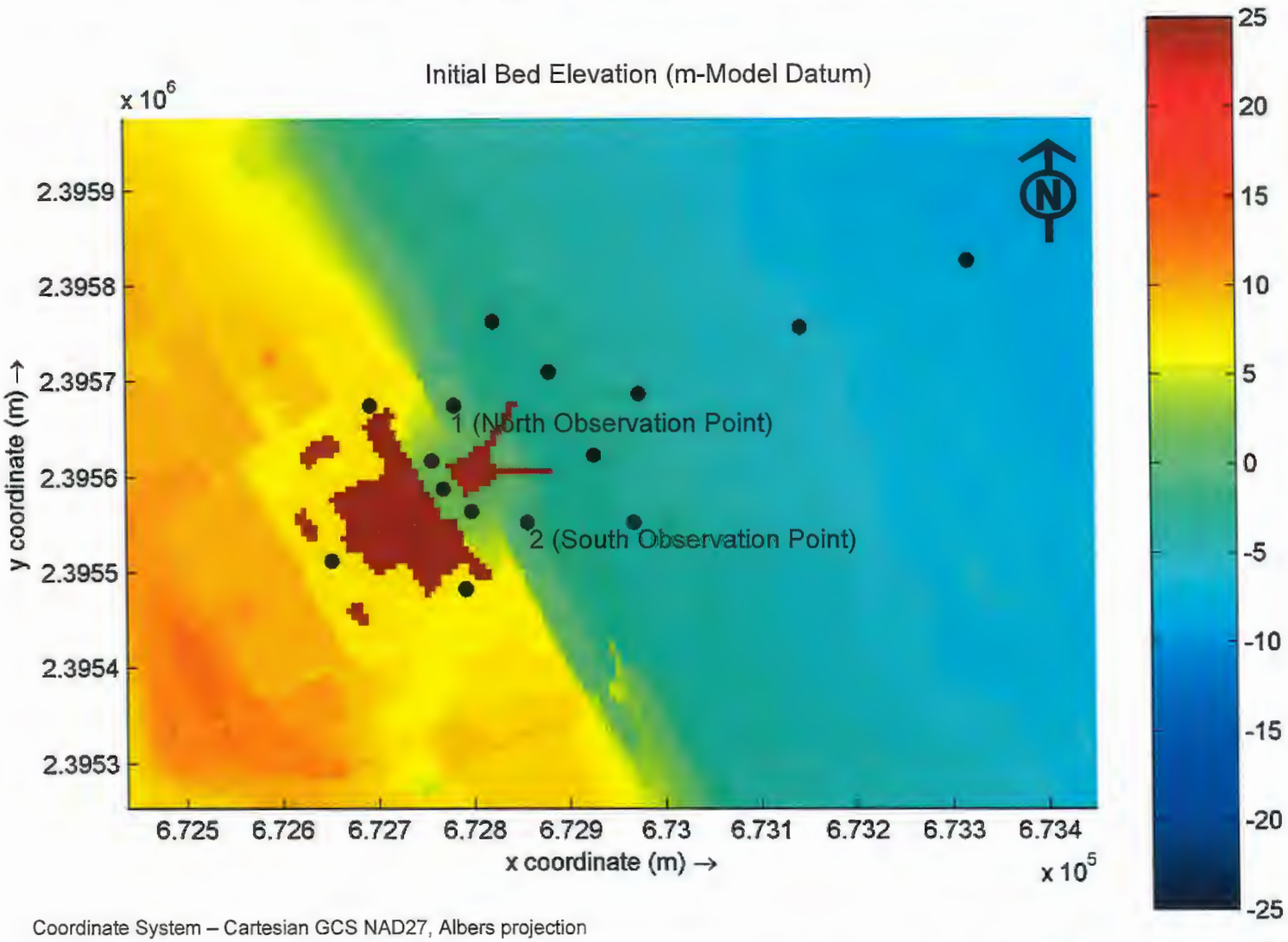

Coordinate System – Cartesian GCS NAD27, Albers projection

NextEra Energy (NEE) **Point Beach Nuclear Plant (PBNP)** **Flooding Hazards Reevaluation Report (FHRR)**	ENERCON **Figure 4.21** Nearshore Grid 4 Showing Observation Point Locations
References:	FPL-076-FHRPR-002 REV. 2

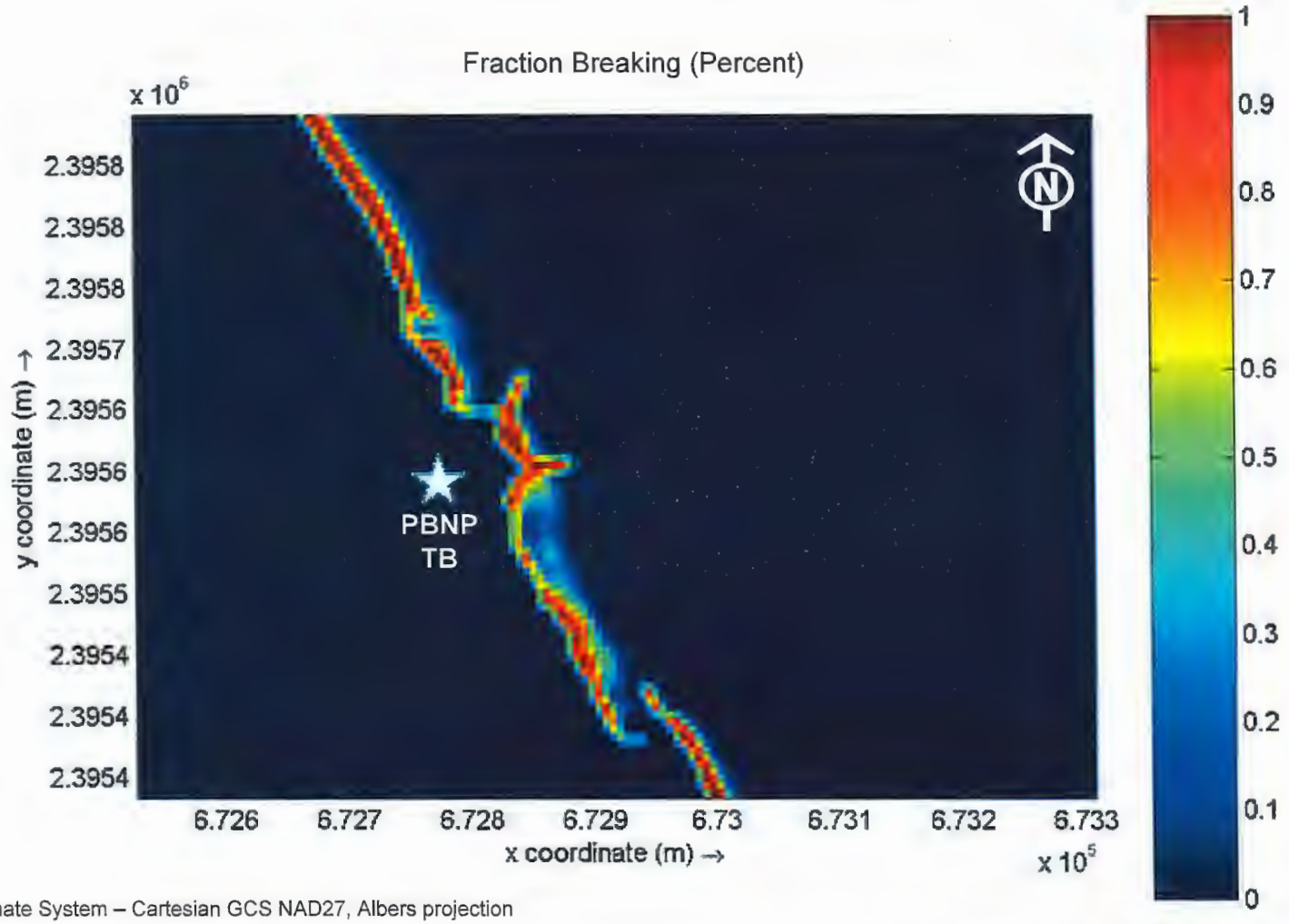

Coordinate System – Cartesian GCS NAD27, Albers projection

NextEra Energy (NEE)
Point Beach Nuclear Plant (PBNP)
Flooding Hazards Reevaluation Report (FHRR)

ENERCON

Figure 4.22
Wave Breaking Locations for PMWS (Scenario 13) with Adjusted Wind Fields

References:

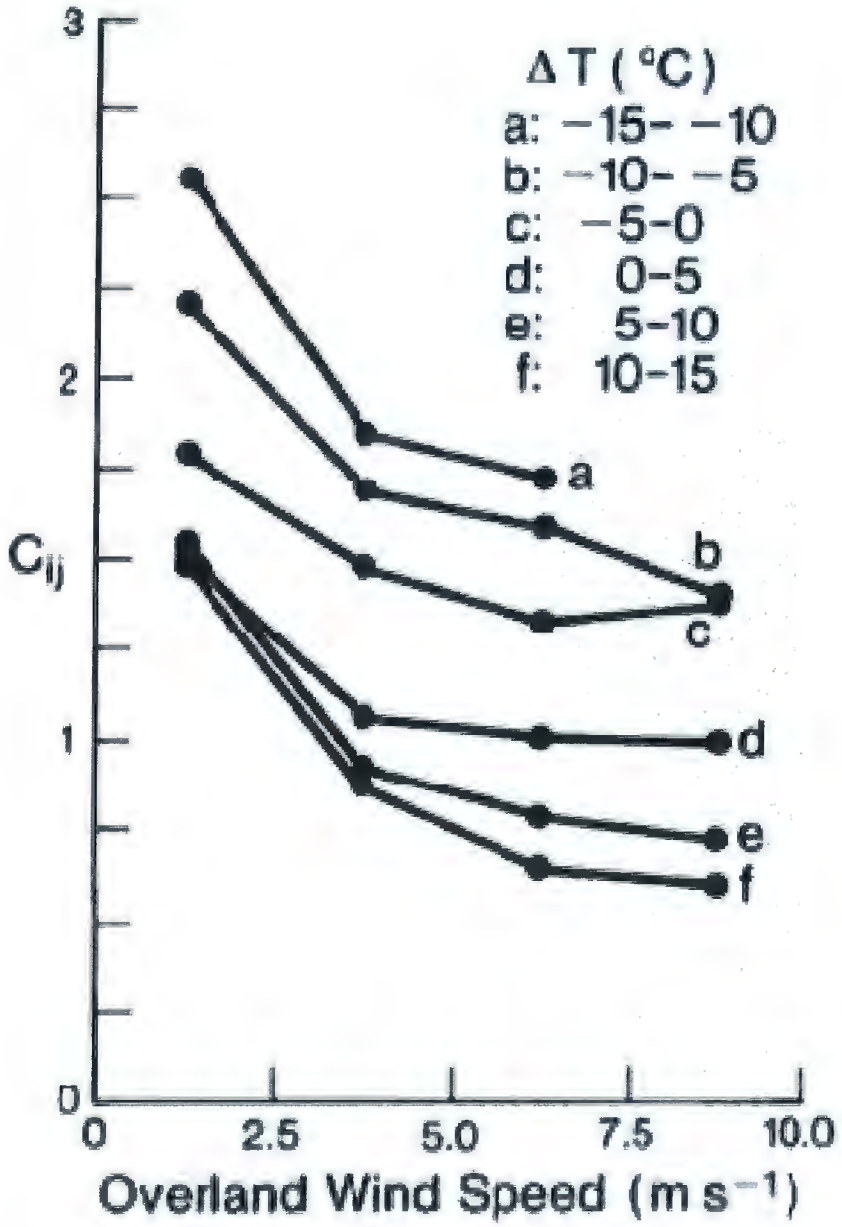

NextEra Energy (NEE) Point Beach Nuclear Plant (PBNP) Flooding Hazards Reevaluation Report (FHRR)	ENERCON **Figure 4.23** Coefficient for Calculation of Overwater Wind Speed
References: Schwab and Morton, 1984	FPL-076-FHRPR-002 REV. 2

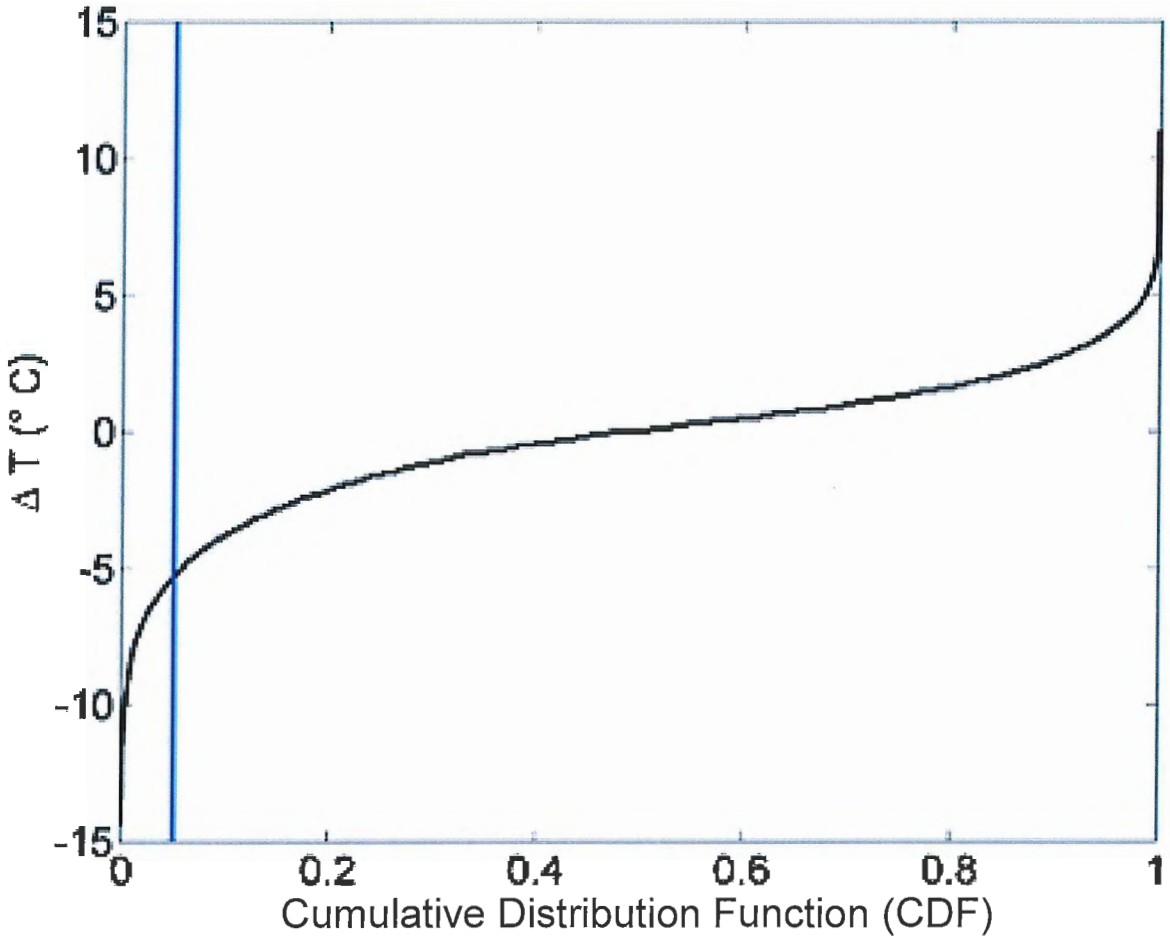
15
10
5
0
-5
-10
-15
ΔT (° C)
0
0.2
0.4
0.6
0.8
1
Cumulative Distribution Function (CDF)

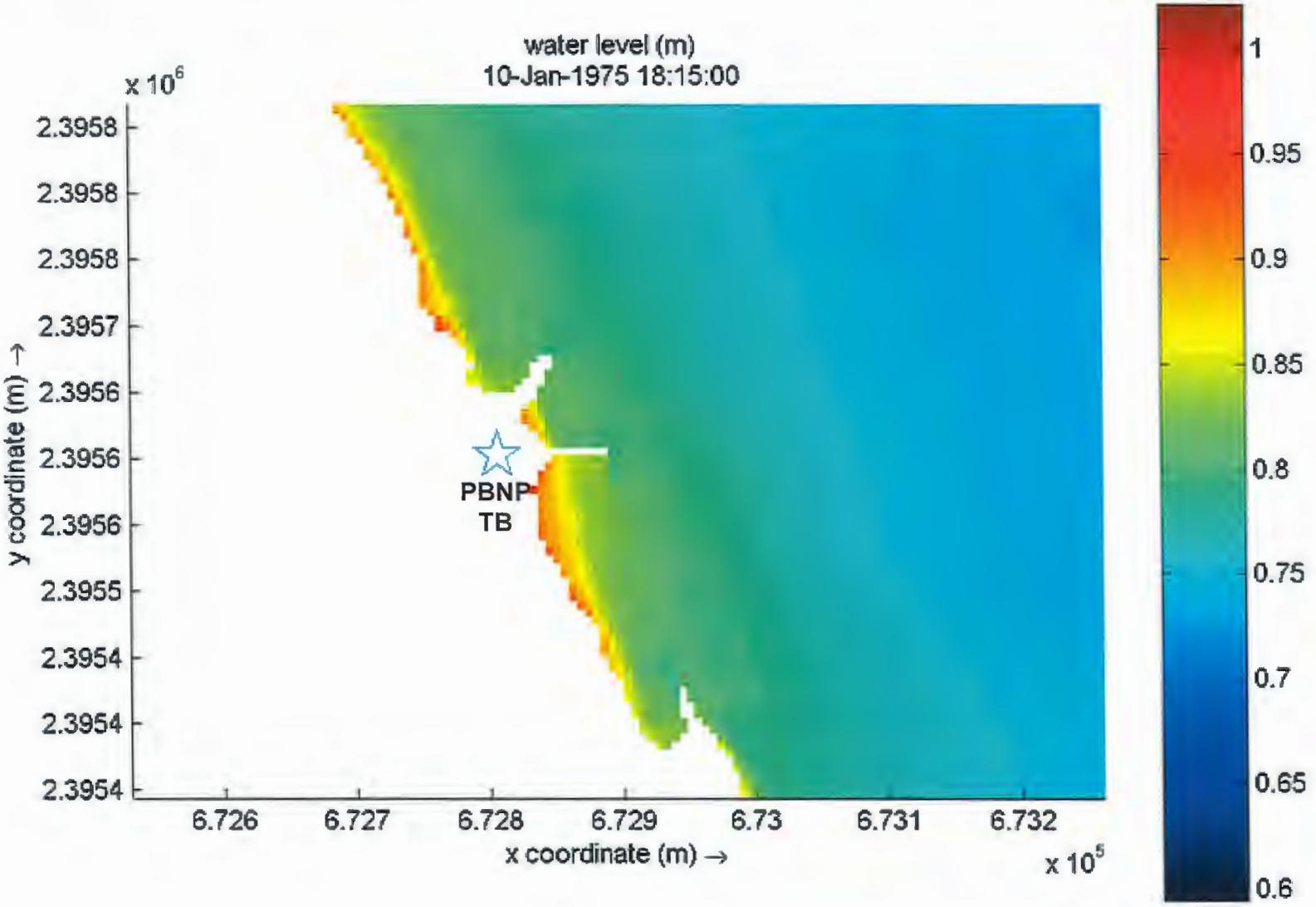

NextEra Energy (NEE)
Point Beach Nuclear Plant (PBNP)
Flooding Hazards Reevaluation Report (FHRR)

ENERCON

Figure 4.25
Peak PMSS SWL at PBNP

References:

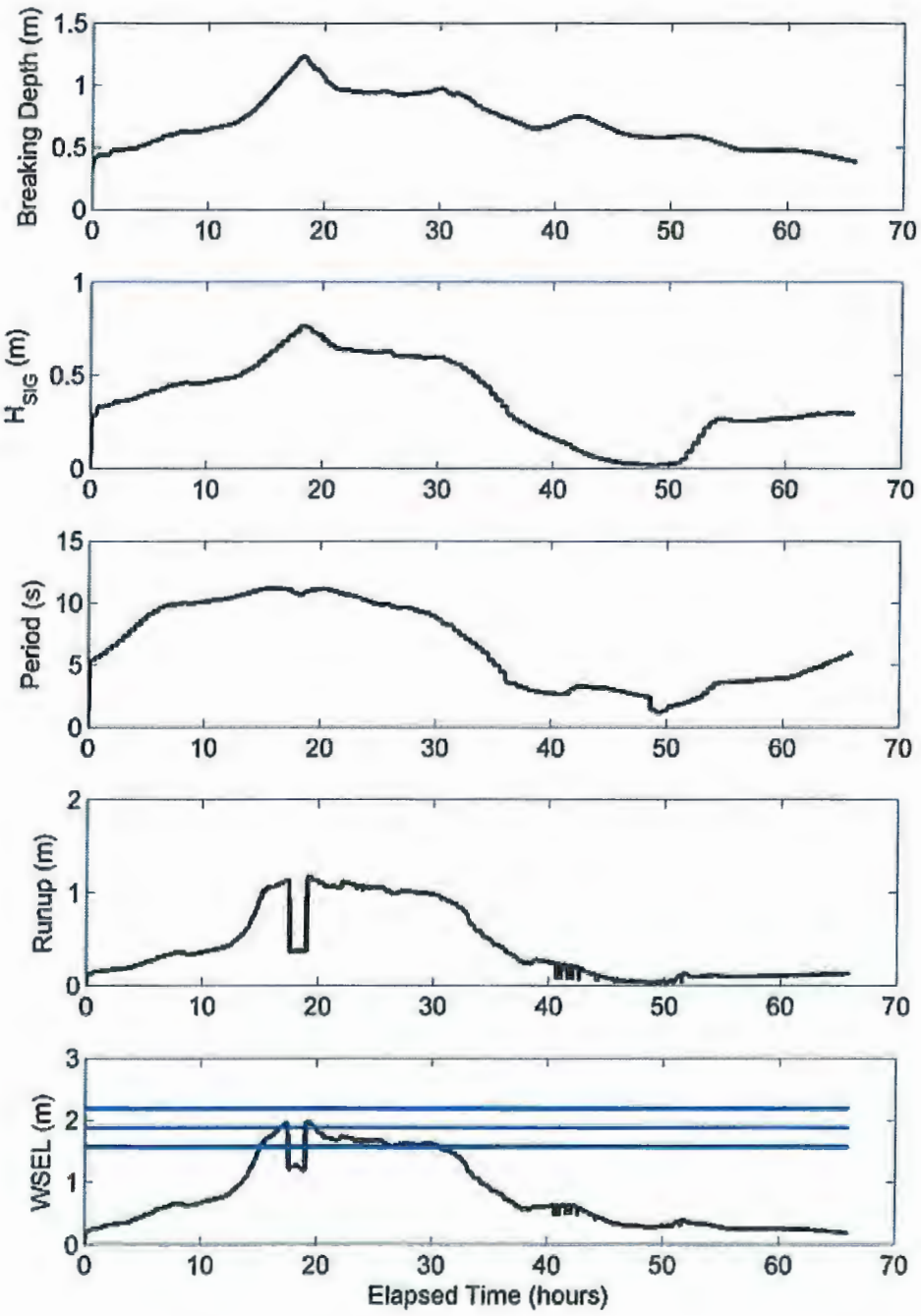

NextEra Energy (NEE)
Point Beach Nuclear Plant (PBNP)
Flooding Hazards Reevaluation Report (FHRR)

ENERCON

Figure 4.26
PMSS Results and Wave Runup on a Gently Sloping Impermeable Surface – South Approach

References:

NextEra Energy (NEE)
Point Beach Nuclear Plant (PBNP)
Flooding Hazards Reevaluation Report (FHRR)

ENERCON

Figure 4.27
Peak PMSS SWL Inundation Map at PBNP

References: ESRI, 2012; NEE, 2014b

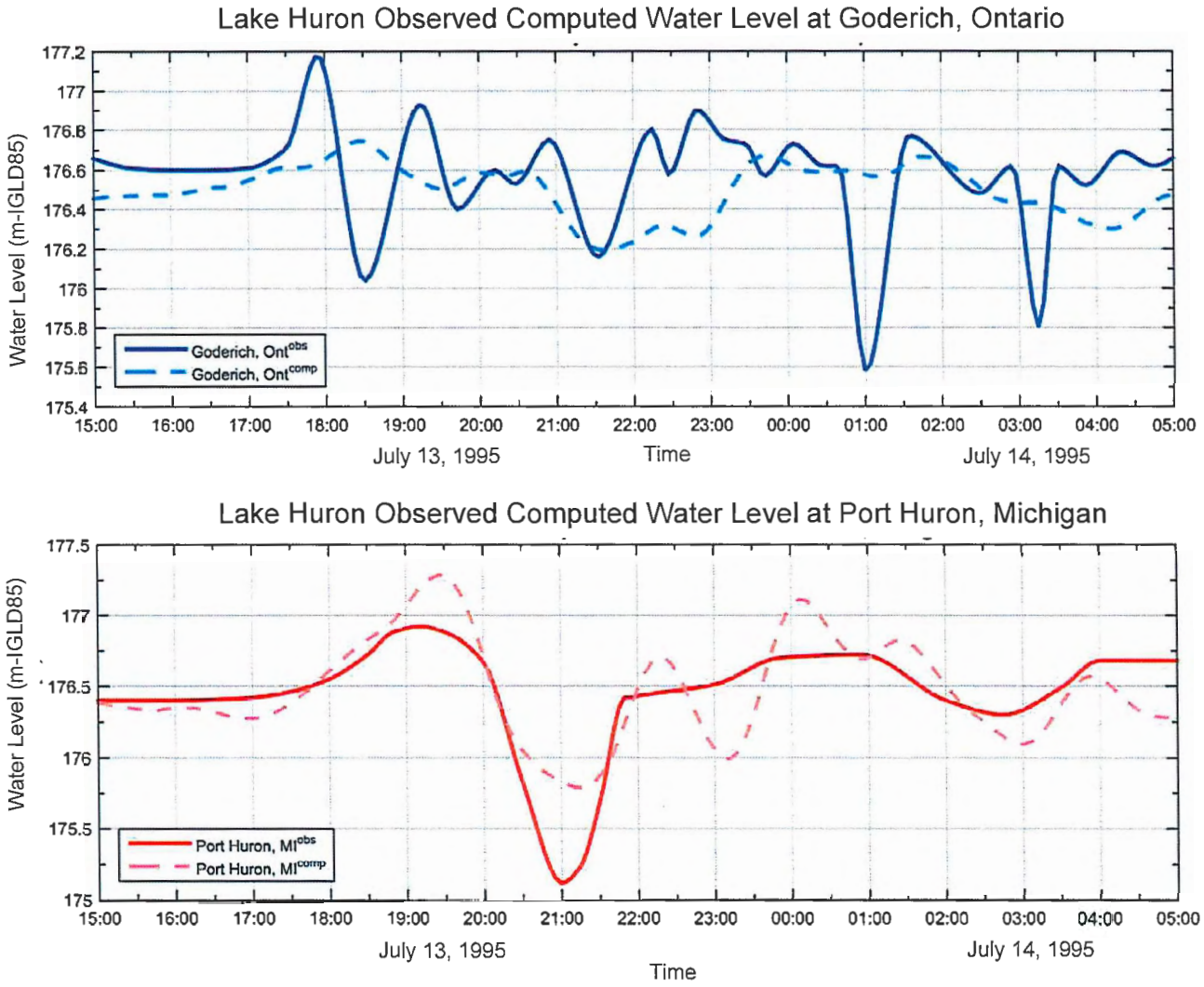

NextEra Energy (NEE)
Point Beach Nuclear Plant (PBNP)
Flooding Hazards Reevaluation Report (FHRR)

ENERCON

Figure 4.28
Lake Huron Observed Versus Modeled Values for July 13, 1995 Derecho Event

References:

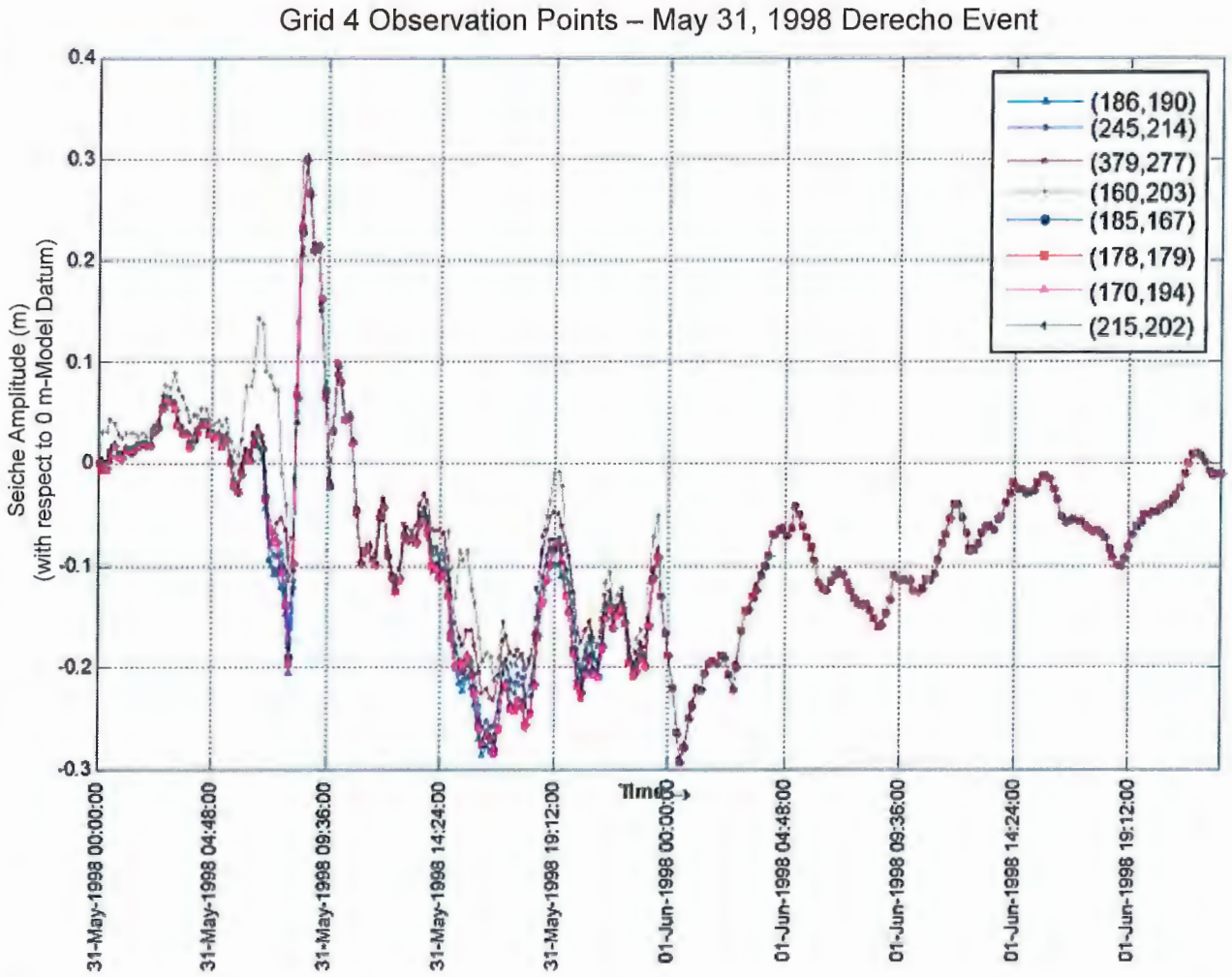

NextEra Energy (NEE) **Point Beach Nuclear Plant (PBNP)** **Flooding Hazards Reevaluation Report (FHRR)**	ENERCON **Figure 4.29** Modeled Seiche Amplitudes near PBNP for Maximized May 31, 1998 Derecho Event
References:	FPL-076-FHRPR-002 REV. 2

NextEra Energy (NEE)
Point Beach Nuclear Plant (PBNP)
Flooding Hazards Reevaluation Report (FHRR)

ENERCON

Figure 4.30
Historical Tsunami Runup and Events near PBNP

References: NOAA, 2014hh

FPL-076-FHRPR-002 REV. 2

Legend

- Significant Earthquakes
- Strong Motion Location
- Point Beach Nuclear Plant

NextEra Energy (NEE)
Point Beach Nuclear Plant (PBNP)
Flooding Hazards Reevaluation Report (FHRR)

ENERCON

Figure 4.31
Historical Earthquake Events near PBNP

References: NOAA, 2014hh

FPL-076-FHRPR-002 REV. 2